SYNTHESIS AND WEAR BEHAVIOR OF ALUMINUM 6061 ALLOY REINFORCED WITH CARBON NANOTUBES

BY

ABDULLAH KHALIL

A Thesis Presented to the
DEANSHIP OF GRADUATE STUDIES

KING FAHD UNIVERSITY OF PETROLEUM & MINERALS

DHAHRAN, SAUDI ARABIA

In Partial Fulfillment of the
Requirements for the Degree of

MASTER OF SCIENCE

In

MECHANICAL ENGINEERING

MAY 2012

KING FAHD UNIVERSITY OF PETROLEUM AND MINERALS

DHAHRAN 31261, SAUDI ARABIA

DEANSHIP OF GRADUATE STUDIES

This thesis, written by **ABDULLAH KHALIL** under the direction of his thesis advisor and approved by his thesis committee, has been presented to and accepted by the Dean of Graduate Studies, in partial fulfillment of the requirements for the degree of

MASTER OF SCIENCE IN MECHANICAL ENGINEERING

Thesis Committee

Dr. Amro M. Al Qutub (Advisor)

Dr. Saheb Nouari (Member)

Dr. Nesar Merah (Member)

Dr. Amro M. Al Qutub

Department Chairman

Dr. Salam A. Zummo

Dean of Graduate Studies

13/5/12

Date

Dedicated to all the loving and caring

Mothers

"The hand that rocks the cradle is the hand that rules the world"

(Wallace, 1865)

ACKNOWLEDGEMENT

I would like to express my deepest gratitude to Dr. Amro Al Qutub, Chairman, Department of Mechanical Engineering, KFUPM, who supervised this work. His confidence and support during different stages, especially in using the tribometer, paved the way towards successful and timely completion of this thesis.

It has been great fortune to have valuable guidance and tutelage of Dr. Saheb Nouari, Assistant Professor, Department of Mechanical Engineering, KFUPM, who played vital role in handling different technical aspects throughout the project. I will never forget his kind support and extremely humble attitude which I might not find anywhere else.

I am very thankful to Dr. Nesar Merah, Professor, Department of Mechanical Engineering, KFUPM for his valuable suggestions and guidance.

Technical support and assistance from Dr. Abbas Saeed Hakeem, Research Scientist, Center of Excellence in Nanotechnology, KFUPM, in using Spark Plasma Sintering Equipment is highly acknowledged.

Equal thanks to technical staff members in material science laboratories and workshop for their help and assistance in using different laboratory equipments.

Financial support for this work from King Abdul Aziz City for Science and Technology (KACST) through research project number ARP-28-122 is highly acknowledged.

And most of all, I find no words to thank my family members from whom I stole some most precious moments of life for pursuing my MSc abroad. Their prayers and matchless support served as a driving force for me throughout my studies.

TABLE OF CONTENTS

LIST OF FIGURES

LIST OF TABLES

ABSTRACT (ENGLISH)

NAME: ABDULLAH KHALIL

TITLE: SYNTHESIS AND WEAR BEHAVIOR OF ALUMINUM 6061 ALLOY REINFORCED WITH CARBON NANOTUBES

MAJOR: MECHANICAL ENGINEERING

DATE: MAY 2012

In the present work, Al6061 alloy was uniformly reinforced with 0.5, 0.75, 1 and 2 wt. % Carbon Nanotubes (CNTs) using two way dispersion method. For consolidation, Spark Plasma Sintering (SPS) was used which resulted in very high densification for the matrix as well as composite. Results showed that addition of CNTs lead to increased hardness of the material and maximum hardness was found for 1 wt. % CNTs. So this composition was selected for detailed wear analysis. Pin-on-disk wear tests were conducted for the monolithic Al6061 and the composite at a constant speed of 0.5 m/s with varying load from 5 N to 30 N under dry sliding conditions using AISI 4140 steel disk as a counterface. The composite displayed lower wear rate and friction coefficient at lower levels of applied stress (0.175 to 0.525 MPa). Under higher stresses (0.700 to 1.050 MPa), the increased brittleness and porosity of the composite caused severe fracturing and delamination resulting in excessive wear rate and friction coefficient for the composite as compared to monolithic Al6061. The transition from mild to severe wear regime in composite occurred also at lower stress as compared to monolith. Analysis of the worn surfaces revealed abrasion as the dominant wear mechanism for both the materials at lower stresses. At higher stress levels, adhesion was found to be dominant in monolithic Al6061 whereas in composite, excessive sub-surface fracturing and delamination was mainly observed.

ABSTRACT (ARABIC)

ملخص الرسالة

الاسم: عبدالله خليل

عنوان: تحضير سبائك ألمنيوم ٦٠٦١ مدعومة بأنابيب الكربون النانوية ودراسة مقاومتها للبلاء

التخصص: الهندسة الميكانيكية

تاريخ: مايو ٢٠١٢

في هذا العمل، تم تدعيم سبيكة الألمنيوم ٦٠٦١ بأنابيب الكربون النانوية بنسب مئوية وزنية قدرها ٠،٥ ، ٠،٧٥ ، ١ و ٢ ٪ باستخدام طريقتين لتشتيت الطور الداعم. ثم تم التلبيد عن طريق إستعمال شرارة البلازما مما نتج عنه كثافة عالية جدا بالنسبة للسبيكة وكذلك المادة المركبة. وأظهرت النتائج أن إضافة أنابيب الكربون النانوية أدى إلى زيادة الصلابة و كانت الزيادة القصوى عند إضافة نسبة ١ ٪ وزنا من أنابيب الكربون النانوية . لذلك تم اختيار هذه النسبة لدراسة و تحليل مقاومة هذه المواد ضد البلاء و الإحتكاك. وأجريت اختبارات البلاء بإستعمال طريقة الدبوس على القرص وبسرعة ثابتة قدرها ٠،٥ متر/ثانية مع زيادة الحمل من ٥ إلى ٣٠ نيوتن تحت ظروف انزلاق جافة كما أستعمل الحديد الصلب ٤١٤٠ كقرص. المادة المركبة و المدعومة أظهرت أحسن مقاومة للبلاء و أقل معامل إحتكاك عند مستويات إجهاد بين ٠،١٧٥ و٠،٥٢٥ ميجاباسكال مقارنة بسبيكة الألمنيوم ٦٠٦١ الغير مدعومة. لكن عند الإجهاد العالي بين ٠،٧٠٠ و ١،٠٥٠ ميجاباسكال وجد أن سبيكة الألمنيوم ٦٠٦١ الغير مدعومة أظهرت أحسن مقاومة للبلاء و أقل معامل إحتكاك مقارنة بالمادة المركبة و المدعومة و هذا راجع إلى زيادة هشاشة المادة المركبة و وجود بعض الفجوات. الانتقال من نظام بلاء معتدل إلى نظام بلاء حاد حدث في المادة المركبة و المدعومة عند مستويات إجهاد صغيرة مقارنة بالسبيكة الغير مدعومة. تحليل و توصيف الأسطح البالية كشف أن الكشط هو الآلية المهيمنة في بلاء كل من المادة المركبة و السبيكة الغير مدعومة عند الضغوط المنخفضة. لكن عند الضغوط المرتفعة لوحظ أن آلية البلاء التلاحمي هي المهيمنة في السبيكة الغير مدعومة بينما آلية البلاء الإنفصالي كانت هي المهيمنة في المادة المركبة و المدعومة.

CHAPTER 1

INTRODUCTION

1.1 Wear in Mechanical Systems

Almost every mechanical system involves some sort of contact and relative motion between two or more different components made up of similar or different material. Such contact and relative motion always results in the deformation and/or removal of material from the asperities in contact due to the mechanical action of the counter surface. This phenomenon is termed as 'wear'. Depending upon the forces, intensity of motion and the mechanical properties of the contacting asperities, the magnitude of wear may vary from microscopic range-being negligible to macroscopic range-being critical, depending upon the application and performance requirements.

Research and development towards wear of engineering materials has been accelerated during past two decades. The driving force for this research and development is the considerable cost which incurs in the form of maintenance and replacement of worn out components during the service life cycle of a mechanical system.

The wear of any material is dependent upon several factors which may be 'extrinsic' or 'intrinsic' to the system. The extrinsic factors may be the type of operating environment (vacuum, air, corrosive or humid), operating temperature (high or low) or operating conditions (load, speed etc.). The intrinsic factors are the properties which the material

itself possesses. In most of the situations, we have a very little control over the extrinsic factors. For instance, the pistons reciprocating against the cylinder block in an automobile engine have to reciprocate at a specified speed under high temperature and under the influence of reactive gases to maintain the required efficiency. However, one has a control over the intrinsic factors i.e. by tailoring the mechanical and chemical properties of the piston material, its wear resistance can be improved under the specified operating conditions. Most of the research work in this area is, therefore, focused towards improving the material itself; either by different types of treatments and coatings or by incorporating certain percentage of a different material to form a composite. The later approach has been more attractive and effective as the former approach involves strengthening the material only from the exterior which may not remain effective with the passage of time. In contrast, the later approach involves strengthening the material as a whole on the continuum level so that the properties remain unaffected with the passage of time.

As far as metals are concerned, aluminum is one of the most important materials which find plenty of applications. Ranging from domestic utensils to the frames of high performance aircrafts, aluminum and its alloys have a very broad spectrum of applications. It is due to their high strength to weight ratio and excellent corrosion resistance that aluminum and its alloys justify themselves as the ideal materials in countless engineering applications. However, some of the properties of aluminum and its alloys like high coefficient of thermal expansion, low melting point, low hardness and consequently poor wear resistance limit their use in many applications. Among these drawbacks, the wear resistance of aluminum has gained much significance during the

past twenty to thirty years. Along with low weight and structural rigidity, the improved wear resistance is one of the important desirable characteristic required from aluminum and its alloys.

1.2 Wear Mechanisms

The mechanism by which any mechanical component undergoes wear is dependent upon the relative properties of the materials in contact and the environmental conditions. However, for same materials and environment, the wear mechanism may switch with varying contact stress and speed. Also it is not necessary that for given set of conditions, only one type of wear occurs. Different wear mechanisms can occur simultaneously depending upon the conditions. Following are the most common types of wear mechanisms.

Abrasion - Abrasion involves mechanical action of hard asperities of one material on the softer asperities of the other material. This results in localized removal of material from the softer surface. The harder asperities may be an integral part of the material or they may be loosely held between the sliding surfaces. In the former case, it is referred to as 'two body abrasion' whereas in the later case, it is referred to as 'three body abrasion'.

Adhesion - When two surfaces come into contact, they may adhere to one another at localized sites. As the two surfaces move relative to one another, adhesion wear occurs by one surface pulling the material out of the other surface at these sites. The pulling out occurs from the material which is softer and has relatively low melting point. Adhesive wear usually occurs at high temperatures and high sliding speeds.

Delamination - Delamination involves removal of material in the form of larger flakes from one of the surfaces while they are in relative motion. Due to repeated rolling, sliding or impacting, material in contact with surfaces experiences cyclic stresses. This stress cycling develops cracks or damage on the surface. With continuous cycling, the cracks propagate, eventually intersecting with the surface and themselves. This ultimately results in the removal of large flakes from the surface. Delamination wear is sometimes referred to as 'fatigue' wear.

Oxidation - In the context of wear, the term 'oxidation' implies the reaction of surface material with environment which results in the formation of oxide layer and hence the material composition at the surface is altered. Oxidative wear is likely to occur under corrosive environments and at higher temperatures. It is sometimes also referred to as 'chemical wear'.

1.3 Organization of Thesis

In this work, Chapter 2 briefly discusses the effect of different particulate reinforcements on the wear resistance of Aluminum and its alloys. In the experimental part, which is covered in Chapter 3, Al6061 alloy was selected as a matrix material and was reinforced with varying Carbon Nanotubes (CNTs) proportion. Powder metallurgy route was followed for the processing and preparation of composites. The composite which displayed best properties was selected for detailed wear analysis along with the monolithic material for comparison. Wear tests for the specimens were conducted using Pin-on-Disk tribometer. The wear resistance of the monolithic Al6061 and the composite

were compared in terms of wear rate and friction coefficient. SEM and EDS analyses were carried out for worn surfaces and the debris to determine the wear mechanisms. Chapter 4 presents all the experimental results and Chapter 5 discusses these results in relation to the existing relevant literature [1-3]. Finally, in Chapter 6, important conclusions are given and possible future research is proposed.

CHAPTER 2

LITERATURE REVIEW

2.1 Metal Matrix Composites and Nanocomposites

Metal Matrix Composites (MMCs) is a class of material in which a hard, strong and brittle reinforcement (usually ceramic in nature) is embedded into a ductile metallic matrix for improving its mechanical properties. MMCs find wide range of applications in aerospace and automobile industry. Among various types of reinforcements, particulate based reinforcements with size 1 to 100 microns are more commonly used because of easy and economical processing route as well as the isotropic nature of the composite. Among various metals, Aluminum and its alloys have gained much significance because of their wide applications and high strength to weight ratio. Several types of ceramic reinforcements such as silicon carbide and alumina have been extensively tested as reinforcements for Aluminum and results have been very encouraging. With the discovery of exceptionally strong and light materials like carbon nanotubes (CNTs), the modern aerospace and automobile industry got a new hope for developing metal matrix nanocomposites with exceptional strength and very low weight. Carbon nanotubes have also been extensively studied as nanoreinforcements in Aluminum matrix for imparting low weight-high strength characteristics to the matrix material. It has been shown that dramatic improvement in mechanical characteristics of Al is possible upon CNTs addition if proper dispersion & consolidation methods are used. Noguchi et al. [4]

reported around five times improvement in strength of Al upon CNT addition. Deng et al. [5,6] also reported considerable enhancement in hardness, strength & stiffness of Al2024 alloy when reinforced with CNTs. Zhang et al. [1] & Morsi et al. [7] observed significant improvement in hardness of Al upon CNT addition. Agarwal et al. [8] reported considerable improvement in stiffness of Al-Si alloy upon CNT addition, but at the cost of ductility. Kawasaki et al. [9] showed about four times improvement in strength of Al upon 1 wt. % CNT addition. The results so far have been very encouraging; however there are several aspects such as uniform distribution of CNTs across the matrix and subsequent consolidation of the composite, which need comprehensive research before these types of Aluminum nanocomposites can be employed in practical applications.

2.2 Carbon Nanotubes

Carbon nanotubes (CNTs), discovered by Iijima [10] and proved exceptionally strong by Wong and co-workers [11], have been manifested as very promising nanoreinforcements for enhancing various mechanical and physical properties of different metallic and non-metallic materials. The shape of CNTs can be considered in a way that a Graphene sheet rolls into a tubular form with very high aspect ratios (1000 or more). This is due to a unique structure of CNTs that they exhibit such a high value of strength and elastic modulus and are thus candidate nanoreinforcements for improving mechanical properties of various metallic and non-metallic materials.

2.2.1 Dispersion of Carbon Nanotubes

Due to their very high surface energy (due to high surface area to volume ratio), CNTs have strong tendency to form clusters. As a consequence, their uniform distribution across the matrix material remains major challenge in the development of CNT based composites. Depending upon the matrix, there exist several methods for obtaining nearly homogeneous of CNTs. When the matrix is metal and in the powder form, Sonication (sometimes called 'ultrasonication) and Ball Milling have been the popular and promising techniques for obtaining nearly uniform distribution of CNTs across the matrix particles. In sonication, which involves the application of sound energy to agitate the particles, the CNTs and the matrix powders are usually mixed in an organic liquid such as ethanol and the sound waves are applied in the mixture using a probe vibrating at an ultrasonic frequency. The application of high energy sonic waves not only minimizes the CNT agglomeration but also causes homogeneous distribution of CNTs across the matrix particles.

Ball milling, which involves mechanical action of metallic balls enclosed in a rotating metallic container, is another method for dispersing CNTs uniformly across the matrix particles. Although ball milling was mainly developed for reducing the particle and crystallite size and for mechanical alloying of the metallic powders, it has been extensively used for obtaining homogenous distribution of CNTs across matrix particles. Usually, when the ball milling is used for this purpose, the process is carried out a relatively lower RPM and for shorter durations. In such case, it is sometimes referred to as 'ball mixing'.

Due to agglomeration of CNTs, their proportion must be limited to an optimum value for maximum properties. Esawi et al. [12] reported enhancement in mechanical properties upon addition of lower proportion of CNTs. For higher CNT contents, opposite trend was observed which was attributed to the presence of CNT clusters, which represented sources of weakness in the samples. Similar trend was observed by Lee et al. [2] who found highest hardness & wear resistance for Al in case of 1 wt. % CNTs and for higher CNT content, poor characteristics were attributed to CNT agglomeration & formation of aluminum carbide. Esawi et al. [13] also found that whereas addition of 2 wt. % CNTs imparts highest properties to Al, CNT content as high as 5 wt. % causes degradation in mechanical properties of Al due to clustering of CNTs & formation of aluminum carbide. Similarly, Sridhar et al. [14] reported maximum tensile & compressive properties for 0.5 wt. % CNTs & decreasing trend was observed for much higher CNT percentages. Bae et al. [3] also found that 4.5 vol. % CNTs is the optimum percentage for best wear resistance of Al. For much higher CNTs content, poor densification caused poor wear resistance. Since different fabrication routes result in different distribution of CNTs across the matrix, different CNT proportions turn out to be optimum for best mechanical properties of the nanocomposite when different processing methods are followed.

2.3 Spark Plasma Sintering

Spark plasma sintering (SPS) is a novel field assisted sintering technology that produces almost 100 % densification with very fine microstructure without noticeable grain growth, thus imparting superior mechanical properties to the specimen. The process is capable of extremely fast heating (upto 500 ^{o}C/min) which does not only saves time but

also eliminates the problem of grain growth which is common in other conventional sintering methods. The theory of SPS is based on the electrical spark discharge phenomenon wherein a high energy pulse current momentarily generates spark plasma at a very high localized temperature between powder particles enclosed in a graphite die. The spark energy vaporizes contaminants and oxidation on the surface of the particles prior to neck formation. Heat is concentrated on particle surfaces producing thermal bonding without considerable neck and grain growth. The process is pressure-assisted utilizing up to 300 tons of force depending upon the equipment capability. The atmosphere is highly evacuated with the ability to use inert gas. Temperature feedback is provided via thermocouples or pyrometer. Almost all the SPS systems include programmable pressure, temperature and power settings and data acquisition. The process is schematically illustrated in Fig 2.1. The driving force for sintering in SPS is DC pulse discharge which could generate: spark plasma, spark impact pressure, Joule heating, and an electrical field diffusion effect. Fig 2.2 illustrates the flow of DC pulse current through the particles during SPS.

It has been shown that conventional sintering methods such as hot pressing [15] & furnace sintering [4] are not capable of properly densifying these nanocomposites as these methods provide less instantaneous interfacial energy between particles for bonding. Thus the ultimate result is poor densification & mechanical properties of the composite. Field assisted consolidation methods which are capable of providing high instantaneous energy such as SPS, which is also used in the current work, have been proved more suitable for sintering Al-CNT nanocomposites [2,7,9,14]. These advance

sintering methods do not only densify the nanocomposite to maximum extent, but also retain the microstructure of matrix particles due to minimum grain growth.

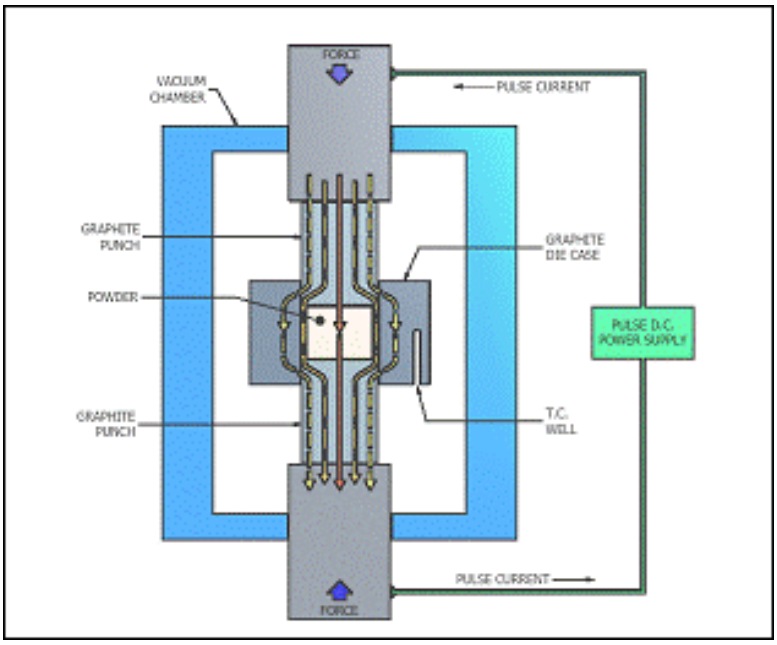

Fig 2.1 Schematic illustration of SPS process

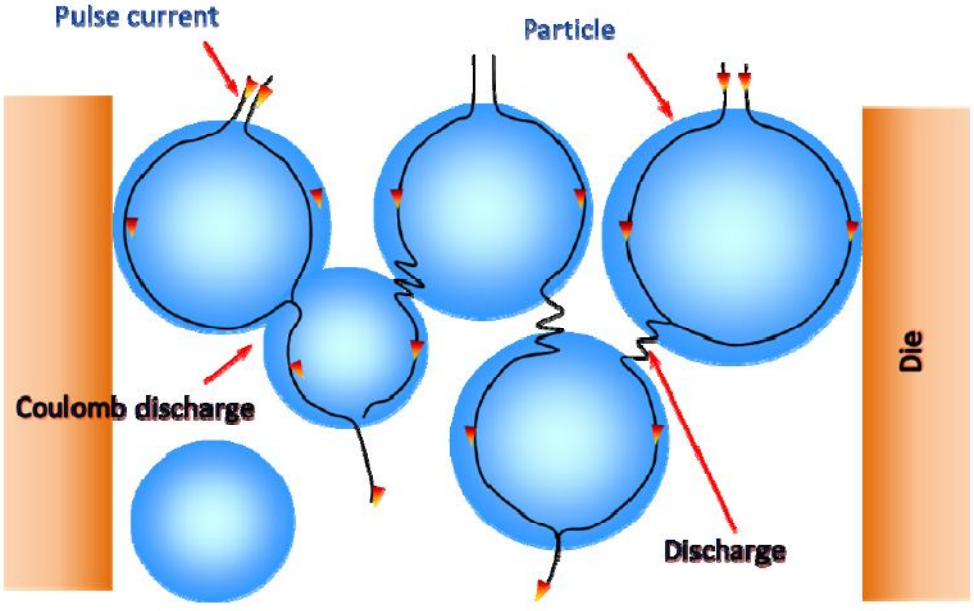

Fig 2.2 DC Pulse Current flow through the particles

2.4 Wear Behavior of Al-MMCs

One of the solutions proposed in the early studies to improve the wear resistance of Aluminum was to form Aluminum Metal Matrix Composite (Al-MMC) i.e. to reinforce aluminum with some hard ceramic particles which improves both its hardness and wear resistance. Several particulate reinforcements like alumina, silicon carbide and tungsten carbide have been successfully employed to improve the wear resistance of aluminum and its alloys. The following sections briefly discuss the various reinforcements which have been tested for improving wear resistance of Aluminum and its alloys.

2.4.1 Al – SiC MMCs

As reported by Lee et al. [16], SiC particles play major role in improving the wear resistance of Al6061. They reported that the wear rate of Al6061 decreases as the percentage and particle size of SiC increases. Similar results were found by Axen et al. [17] who observed about two times improvement in wear resistance of Al-Mg-Si alloy when reinforced with SiC particles. Venkataramana et al. [18] reported the formation of mechanically mixed layers consisting of Al and SiC from the test specimen and also Fe from the counter face. These mechanically mixed layers, formed during wear tests, were found responsible for improved wear resistance of Al. Takagi et al. [19] reported that wear resistance of Al-Ti-Fe-Cr alloy increases as the particle size of SiC, used as reinforcement, increases. Using same reinforcement and pure aluminum as matrix for specimen and bonded alumina abrasive belts as counter face, Cimenoglu et al. [20] reported that abrasive wear rate of the Al–SiC composites, which had 13 and 37 microns

SiC particle size, increased with increasing the size of the abrasive grains. On relatively fine abrasive alumina grains (<150 microns) the composite having coarse SiC particles (37 microns) exhibited higher wear resistance than the composite containing fine SiC particles (13 microns). However, the contrary was true on coarse abrasive alumina grains (>150 microns). Tsao et al. [21] reported that friction coefficient and the fluctuation of the friction coefficient of Al-SiC composites can be reduced by adding Ni coated graphite. However, the wear rates of all the composites with Gr–Ni additions were found to be higher than the wear rate of base Al/SiC material with no Gr–Ni addition. Sahin [22] also observed that SiC particles improve the wear resistance of Al-Cu based alloys. Using Al–Si–Cu–Mg–Ni alloy reinforced with SiC, Kim et al. [23] observed that wear amount of composite decreased with an increase in sliding speed and SiC particle size. Izcilera et al. [24], who studied the wear behavior of SiC reinforced Al 2124 alloy against rubber, reported that wear rate of the composite is quite low, although the applied loads were very high. Das et al. [25], who studied the wear behavior of SiC reinforced Al-Si alloy against SiC abrasive papers, observed that in the case of cast alloy, at low load regime, the wear constant was found to have higher value and decreased drastically to lower value with increase in applied load. In the case of heat-treated alloy and composites, the wear constant decreased monotonically with load. In this study, SEM observation of wear surface and subsurface suggested that at low load regime, the wear of material is controlled by nucleation and propagation of crack, however, at high load regime, the material removal is dominated by plastic deformation. Salazar et al. [26] studied the effect of heat treatment on wear properties of Al 6092-SiC composites and reported that the heat treatment T6 for 7 hours was the one that provided the matrix

greater hardness, and therefore it was the one which gave the composite the stronger wear resistance. Similarly, Muratoglu et al. [27] reported that wear rate of aged Al 2124-SiC composite specimens are lower than that of non aged composite specimens. Mondal et al. [28] also observed the enhancement in wear resistance of Al-Si alloy with addition of SiC particles. In this work, it was found that the wear rate increases linearly with applied load irrespective of the material and abrasive size. It was also found that the wear resistance increases linearly with increase in SiC content and decreases with increase in reinforcement size. Also, the wear rate decreased linearly with increase in SiC content and hardness. Rao et al. [29], studying wear behavior of Al–Zn–Mg–Cu alloy reinforced with SiC, reported that wear coefficient decreases with increasing applied pressure reaching to a minimum value and then again increases when the applied pressure reaches near to the seizure of the specimen. Also, the transition load and speed is increased when it goes from one region to the other due to addition of SiC particles. The same researchers [30], studying the effect of heat treatment on wear behavior of Al–Zn–Mg alloy with same reinforcement, reported improvement in hardness and wear resistance of composites which were aged for 6 hours. Studying the wear behavior of Al 2014-SiC composite, Sahin [31] observed that the abrasive grain size exerts the greatest effect on the wear, followed by the hardness. Moreover, larger particle sizes of composites led to more wear resistance than those of smaller particle sizes of composites. One recent study conducted by Saha et al. [32], in which they studied wear characteristics of Al–Cu–Mg alloy reinforced with SiC, reports that specific wear rate of the composite increases with the decrease of reinforcement size for a certain volume percentage of SiC. Also, wear

resistance initially improves with the increase of the content of SiC, but there is no further enhancement in wear resistance beyond 20 vol. %.

2.4.2 Al – Alumina MMCs

There has been considerable research regarding the effect of alumina particles on the wear properties of aluminum and its alloys. Cordovilla et al. [33], using Al-Si and Al-Si-Mg alloys reinforced with SiC and alumina, reported improved wear resistance of alumina reinforced alloys, however the wear rates were higher than that of SiC reinforced alloys. Yang [34] observed that the value of wear coefficient for Al6061/alumina decreases as the volume fraction of alumina increases and the main wear mechanism was found to be adhesive wear. The same researcher [35] for the same alloy and reinforcement, observed that the wear coefficient values obtained for the specimens with a smaller nominal contact area were lower as compared to those with larger area as the wear asperity volume available in the former ones is smaller. Rosenberger et al. [36] studied the wear behavior of Al 1060 alloy reinforced with alumina under different loads and reported the formation of mechanically mixed layer which is responsible for protecting the composite from subsequent wear. This layer was, however, not observed at higher loads. Al-Qutub et al. [37] showed that addition of up to 30 vol. % sub-micron alumina in Al6061 increases its wear resistance as high as 145 percent. In another study, Al Qutub et al. [38] demonstrated that lower concentrations of alumina result in increased wear resistance of Al6061 in severe wear regimes. Higher concentration of alumina decrease the wear resistance of the material in severe wear regimes due to increased abrasive action. Al-Qutub [39] also studied the effect of heat treatment on wear

characteristics of Al6061 reinforced with sub-micron alumina and observed that heat treatment of composite can increase the transition load to severe wear by 30% compared to untreated composite. On the other hand, at high loads, the heat treatment results in larger delaminated flakes on the worn surface indicating reduced fracture toughness. This causes the higher wear rates compared to the untreated composite surface. Moreover, dry friction coefficient was found to be unaffected by the heat treatment.

2.4.3 Al Reinforced with other Particulate Reinforcements

Effect of several other types of ceramic particulate reinforcements and their combinations on the wear characteristics of Al and its alloys have also been examined by many researchers. Bermudez et al. [40] compared the effect of adding Ti and AlN particles on the wear properties of pure Al. They found that the wear rate of Al decreases to great extent upon adding these reinforcements. Moreover, the wear rate for AlN reinforced Al was considerably less than Ti reinforced Al. Riahi et al. [41] studied the wear characteristics of two types of Al composites: A356 Al-SiC-Graphite and A356 Al-Alumina-Graphite. It was reported that the graphitic composites displayed a transition from mild to severe wear at load and sliding speed combinations, which were higher than those of the unreinforced A356 Al alloy and the non-graphitic A356 Al composites. Effect of granite particles on wear behavior of Al-Si alloy was investigated by Singh et al. [42] and they reported that frictional heating and friction coefficient was much reduced in case of composite as compared to the matrix alone. Wang et al. [43] studied the wear characteristics of Ni_3Al reinforced 6092 Al alloy and observed that at low loads the composite offered superior wear resistance as compared to the matrix. In contrast, the

matrix alone showed superior wear resistance to the composite at very high loads. Sharma [44] studied the wear behavior of garnet reinforced Al6061 alloy and concluded that the wear resistance of composite is superior to that of unreinforced matrix alloy and that the wear resistance increases with increasing wt. % of garnet. Hemanth [45] studied the effect of adding glass particles in Al-Zn-Mg alloy and the subsequent wear behavior of composite. It was found that wear resistance increases as the volume fraction of glass particle increases. The same researcher [46] studied the effect of boron particles on wear properties of same matrix. It was found that wear resistance improves as sliding speed increases from low to intermediate, beyond which, wear resistance reduces again. Chena et al. [47] studied the wear behavior of two types of composites: Al-Alumina and Al-Alumina-SiC. It was found that Al-Alumina-SiC composites have better wear resistance and cause a lower wear rate on the counter face steel than the unreinforced Al-Alumina composites. The addition of SiC particle plays a dual role on the wear behavior of the composite: by providing load-support to give higher wear resistance at very low load and promoting/maintaining a beneficial iron oxide debris layer in the wear track to reduce friction. Niranjan et al. [48] reported that the wear weight loss of beryllium aluminum silicate reinforced Al–Si–Mg alloy is considerably less as compared to the matrix itself. Korkut [49] compared the wear behavior of Al 2024-SiFe and Al 2024-SiFe-Alumina composites. It was reported that under severe wear condition, alumina particulates were broken and they affected wear behavior badly. Moreover, the influence of α intermetallic phases for Al 2024-SiFe alloy is primarily on the transition load and they decreased the wear rate as well as the coefficient of friction for Al2024 alloy. Wear properties of Al-Alumina and Al-Alumina-Al_4C_3 composites were studied by Abouelmagd [50] and he

found that composites with Al_4C_3 exhibited higher wear resistance. Haseeb et al. [51] compared Al-SiC and Al-B_4C composites regarding wear characteristics. They found that higher sliding velocity leads to lower wear rate and lower friction coefficient for both composites. Moreover the amount of the constituents of the counter body in the transfer layer, which formed on the composite, was seen to increase as sliding velocity increases. It was suggested that the transfer layer on composite acts as a protective cover and helps reduce both wear rate and friction coefficient. Bhattacharya et al. [52] studied the wear behavior of Al reinforced with nano sized Pb dispersions. It was found that the nanodispersed Pb particles in Al lead to significant improvement in friction and wear characteristics. This improvement was attributed to the formation of uniform Pb rich tribolayer during sliding. Zhiqiang et al. [53] tested Al–Cu–Mg reinforced with Si particles for wear characteristics. They found that Si particle reinforced composites exhibited reduced wear loss than the unreinforced alloy specimens. Ramesh et al. [54] experimented with TiO_2 reinforced Al6061 and reported that composites exhibited higher hardness and lower wear coefficient when compared with the matrix alloy. Suarez et al. [55] found that reinforcing AlB_2 dispersoids in Al-Mg alloy results in improved wear resistance of the alloy. Ramesh et al. [56] tested 3 types of composites: Al6061 reinforced with SiC, alumina and cerium oxide, respectively. They observed that increased contents of reinforcement results in decreased wear rates of composites. Among all the composite systems studied, Al6061-cerium oxide possessed the lowest wear rates under identical test conditions. Al 5083 alloy reinforced with B_4C has been examined for wear behavior by Tang et al. [57]. They reported that wear rate of composite decreases as the percentage of B_4C increases. A356 Al alloy reinforced with fly ash particles was tested by Sudarshan

et al. [58]. They reported that incorporating fly ash particles into A356 Al alloy results in decrease in dry sliding wear rates at low loads and wear rates decrease as the fraction of fly ash particles increases. Significant increase in the friction coefficient was observed when volume fraction of fly ash particles was increased. Pure Al reinforced with $NiAl_3$ has been examined for wear resistance by Bermudez et al. [59] who concluded that the addition of small wt.% Ni slightly improves the wear resistance of mechanically alloyed Al at room temperature and low loads.

2.4.4 Al – CNT MMCs

The current trend of nanotechnology and nanomaterials made some of the researchers to examine the effect of nanoreinforcements on the wear characteristics of Al. Carbon Nanotubes (CNTs) have been one candidate to act as effective nanoreinforcements for Al and its alloys. Several studies [9,60,61] have reported considerable enhancement in hardness, strength and elastic modulus of Al when it is reinforced with CNTs. This is because the CNT is not only the strongest known material but also these nanoparticles play effective role in resisting dislocation movement inside the matrix material. However, there is still a lot of room for further research in the area of Al-CNT composites as the behavior varies considerably as the different parameters like CNT content, CNT dispersion method, Al alloy type and the consolidation method are varied. Wear resistance of Al-CNT composites has also been examined recently. The following paragraphs discuss in detail, the wear characteristics of Al-CNT composites which have been reported so far.

Zhang et al. [1] studied the effect of CNTs on the wear resistance of Aluminum. Five compositions were used: 0, 5, 10, 15 and 20 vol.% CNTs. The composites were prepared using pressureless infiltration process. Pin on disk tests were conducted using single load and very low speed value of 30 N and 0.1571 m/s, respectively. The specimens were prepared in the form of disks whereas spherical pins with a radius of 5 mm, fabricated by quenched and tempered medium carbon steel, acted as counterface. Within the range of volume fraction of CNTs from 0 to 20 percent, the wear rate of the composite showed a steadily decreasing trend with increasing volume fraction of CNTs in the composite, as shown in Fig 2.1. It was concluded that as the CNT content in Al increases, more CNTs are available at the pin-disk interface and due to the lubricating action of these CNTs, the wear rate and friction coefficient decreased with increasing CNT content. During the steady-state wear process, the oxidation wear was found to be the main wear-mechanism for the CNTs reinforced Al composites. It is to be noted in this study that although the hardness was highest for 15 vol.% CNTs composite, the wear resistance was highest for the composite with 20 vol.% CNTs. This shows that in case of Al-CNT nanocomposites, wear resistance is not directly dependent upon the hardness only as the lubricating effect of CNTs is also important which increases with increasing CNT content.

Kim et al. [2] compared the wear properties of Al-1 wt. % CNT composites prepared by two methods: Hot pressing (HP) and spark plasma sintering (SPS). Pin on disk wear tests, using pins as specimens and 0.2 % plain carbon steel disk as counterface, were conducted. Wear tests were conducted at loads with different magnitudes, 2.94, 4.9 and 11.7 N, at a very low sliding speed of 0.02 m/s approx. For dispersing CNTs in Al matrix, three different types of dispersion methods were used. However, the best method was

found to be as follows: performing the acid treatment, next, mixing aluminum powder and then performing sonication for 20 min, as this method resulted in lowest friction coefficient and wear amount for composites. This is illustrated in Fig 2.2. Condition 1 corresponds to the above mentioned method. However, no explanation was given for the superiority of this dispersion method. In terms of processing method, SPS was found superior to HP as it resulted in better strength, hardness and stable friction coefficient over longer sliding distance. This is shown in Fig 2.3. The superiority of SPS method was attributed to the small grain size of Aluminum obtained through it. Particle growth in HP was solely held responsible for degradation of hardness and wear resistance. This can be true only if HP specimens achieved good densification, which is not mentioned. Otherwise, poor densification/sintering which caused Al-CNT agglomerates and porosity, can be the important reason for degradation of hardness and wear resistance in case of HP composites.

Two body abrasion was observed in HP specimens. Abrasion was attributed to separated microdebris from adhesion and large debris from fatigue. Fatigue wear which is evident in the form of micro cracks was considerable for HP specimens. Three body abrasion, which generally results in lower wear loss as compared to two body abrasion, was observed in SPS specimens. In case of SPS specimens, three body abrasion was observed. Considerable quantities of oxygen and iron were found in SPS specimens which supported the formation of iron oxide film during wear test. It was inferred that this iron oxide film serves as a protective film and hence the wear loss for SPS specimen is low. In contrast, no such film was observed in HP specimen and hence its wear loss is high.

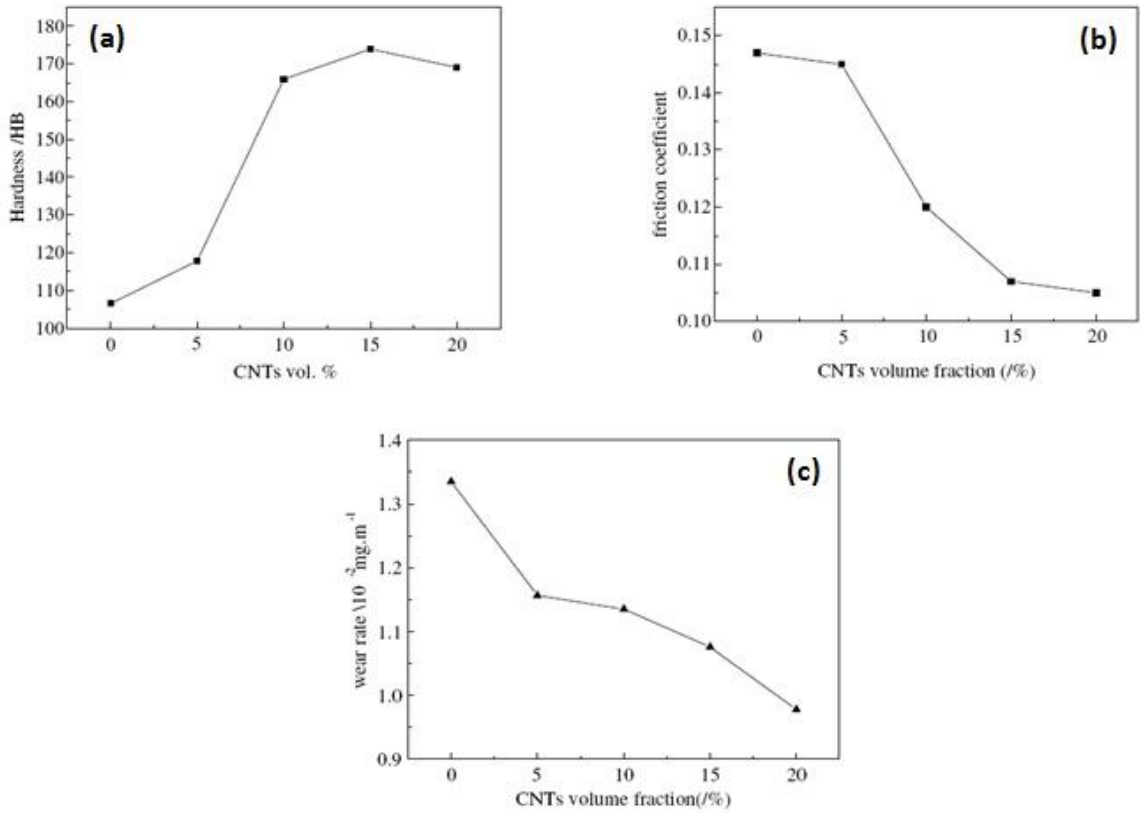

Fig 2.3 Effect of CNT vol. % on (a) Hardness (b) Friction Coefficient (c) Wear Rate [1]

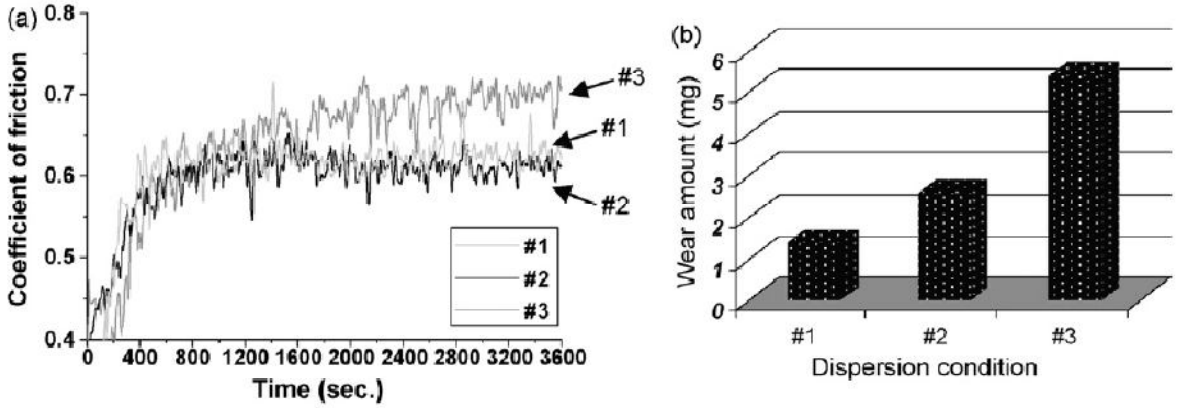

Fig 2.4 Friction coefficients and wear amounts of CNT–aluminum composites according to dispersion conditions: (a) friction coefficients and (b) wear amounts. [2]

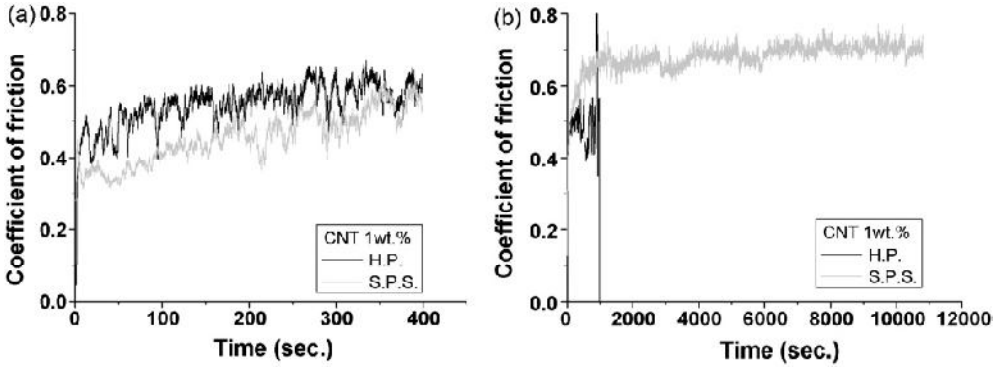

Fig 2.5 Friction coefficient of CNT–aluminum composites according to the fabrication techniques (a) applied load of 2.94 N and (b) applied load of 4.9 N. [2]

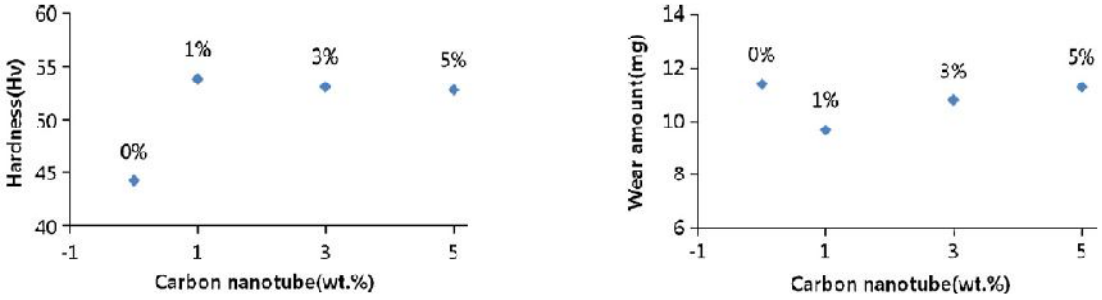

Fig 2.6 Hardness and wear amount of SPS composites according to CNT content. [2]

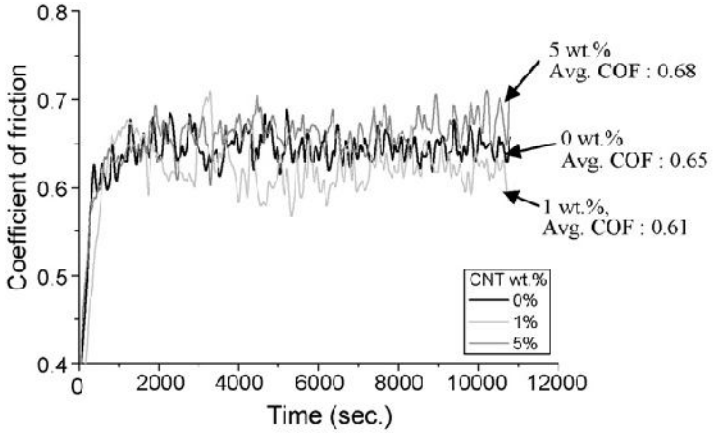

Fig 2.7 Friction coefficients of SPS composites with varying CNT content. [2]

Once it was found that SPS is superior to HP in terms of friction and wear, the subsequent experimentation was done only for SPS specimens with varying CNT content. Three compositions, 1, 3 and 5 wt. %, of CNTs were used to prepare SPS Al-CNT composites. Hardness of composites was measured and although considerable improvement was found in case of 1 wt. %, there was only marginal decrease in case of 3 and 5 wt. % CNTs. Consequently, the wear resistance was highest in case of composite with 1 wt. % CNTs. This is shown in Fig 2.4. It was concluded that an optimum level of CNTs, which is 1 wt. % in this case, is required for filling micovoids in Al matrix. The excess of CNTs agglomerates with Al particles and hinders proper sintering which results in defects and consequently degradation of wear and mechanical properties. As shown in Fig 2.5, friction coefficient was found to be lowest and highest in case of 1 wt. % and 5 wt% CNTs, respectively. Both adhesive and abrasive wears were observed. It was inferred that higher the CNT content, the higher the amount of abrasive wear due to the separation of agglomerated particles that have a weak bonding energy with the surface. Moreover, it was concluded that material transition is actively occurring owing to adhesive wear. However, the explanation for varying amounts of oxygen and iron in composites with different CNT content, was not given.

Aluminum carbide formation was held responsible for poor wear resistance of composite with 5 wt. % CNTs. Moreover, the graphite content decreased as the CNT content increased. This was another reason given for better wear resistance of composite with lower CNT content. However, again, the reason for decrease in graphite content with increase in CNT content was not given.

A much comprehensive study on Al-CNT composites has been done recently by Choi et al. [3]. Wear characteristics were investigated for ultra fine grained Al and Al-CNT composites. Ball milling was used for dispersing CNTs inside Al matrix. Ball milling was done for longer periods at higher rpm to obtain more uniform dispersion and fine grain size. Composite powders were prepared with varying CNT content: 1.5, 3.0, 4.5 and 6.0 vol. %. The powders were first hot pressed using copper container followed by hot rolling. So the specimens were prepared in the form of thin sheets. Wear tests were conducted using ball on disk type tribometer in which specimen sheets, acting as disks, were rubbed against alumina balls. Mechanical testing of composites was done prior to wear tests. The results are summarized in Table 2.1.

It can be seen that poor densification was obtained in case of composite with 6 vol. % CNTs. It was inferred that high vol. % of CNTs impeded the consolidation process which resulted in the generation of number of voids which not only decreased the density but also served as a source of crack initiation during tensile testing. Wear behavior of the materials is shown in Fig 2.6.

As evident from Table 2.1, no hardness tests were performed and reported, which may be more important in case of wear characterization, as done previously where it was mentioned that wear resistance of Al-CNT composite is directly proportional to its hardness [2]. As mentioned in this study, the friction coefficient of the material increases with increasing strain hardening exponent and decreasing the ratio yield stress/young's modulus. Relation to hardness was neither found nor mentioned. The ratio yield stress/young's modulus was found to increase with increasing the CNT content, as shown in Table 2.1, and hence the decrease in friction coefficient, as shown in Fig 2.6 (I) (a).

Self lubrication by carbon was also considered as a reason for decrease in friction coefficient with an increase in CNT content. For composite with 6 vol. % CNTs friction coefficient and wear loss were high. This behavior was attributed to poor consolidation and presence of microvoids. It is to be noted here that according to Fig 2.6 (I) (a) and (II) (b), lowest friction coefficient and wear loss occurred in case of 4.5 vol. % CNTs which corresponds to approximately 2.2 wt. % of CNTs (since the density of MWCNTs ranges from 1.3 to 1.4 g/cm^3 and for Al, it is 2.7 g/cm^3). While reported in earlier study [2], lowest friction coefficient and wear loss occurs at 1 wt. % of CNTs.

These results seem to be contrasting. However, one thing worth mentioning here is that the consolidation method used in the two studies [2] and [3] are entirely different i.e. SPS and hot rolling. Moreover, the types of wear tests and the counterfaces in the two studies are also different i.e pin on disk with steel as counterface [2] as compared to ball on disk with alumina as counterface [3].

As shown in Fig 2.6 (II), as the grain size of matrix was reduced to about 150 nm, which was achieved after 6 h of ball milling, the wear resistance increased almost twice. This finding is consistent with the previous one [2] where wear resistance of SPS composites having much smaller grain size was far better than HP composites, having larger grain size. As shown in Fig 2.6 (II) (b) and (c), the wear loss increases with increasing applied load and decreases with increasing sliding speed. This consistency shows that wear mechanism is not varied with the sliding condition.

Table 2.1 Summary of the density, Young's modulus, yield stress, and normalized yield stress for starting aluminum, ultrafine-grained aluminum, and aluminum-based composites containing MWCNT. [3]

MWCNT Volume (Fabrication Method)	Density (g/cc)		Young's Modulus (E, GPa)		Yield Strength (Y, MPa)		Y/E (10^{-3})	
	Cal.[a]	Exp.[b]	Cal.	Exp.	Cal.	Exp.	Cal.	Exp.
Starting Aluminum	2.7	2.69	-	-	-	40.43	0.43	-
0 % (milled for 6 h)	2.7	2.68	-	70.026	262.03	262.02	3.74	3.74
1.5 % (milled for 6 h)	2.68	2.66	84.17	82.542	389.92	386.53	4.63	4.68
3.0 % (milled for 6 h)	2.66	2.6	98.33	95.131	517.84	483.26	5.27	5.08
4.5 % (milled for 6 h)	2.64	2.56	112.5	110.05	645.76	610.17	5.74	5.54
6.0 % (milled for 6 h)	2.62	2.31	126.67	-	773.76	Failed	6.11	-

[a] & [b] denote the calculated & experimental data, respectively.

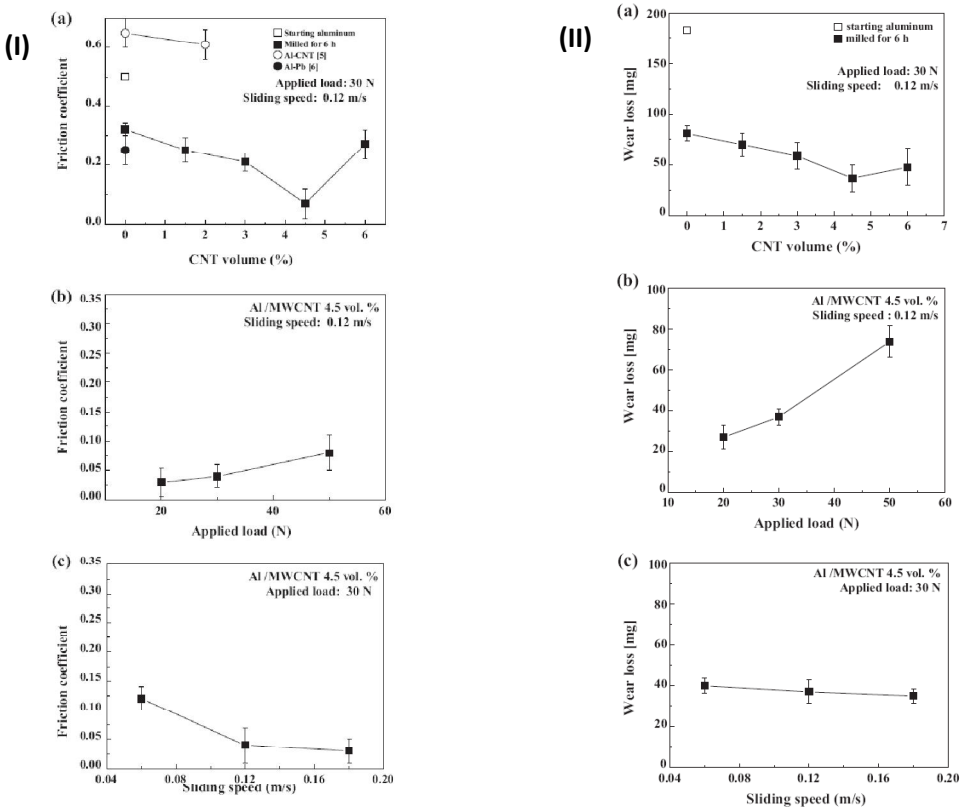

Fig 2.8 (I) The coefficient of friction varied according to (a) the MWCNT volume, (b) an applied load, and (c) a sliding speed. **(II)** The wear rate varied according to (a) the MWCNT volume, (b) an applied load, and (c) a sliding speed. [3]

To examine the element bonding state in composite before and after the wear test, Raman spectra was analyzed. The amorphization of MWCNTs or the formation of aluminum carbide was not found to be significant during the ball milling, consolidation as well as wear tests for 4.5 vol. % CNTs. This seems to be consistent with the previous study where the formation of aluminum carbide was reported through XPS analysis for composite with 5 wt. % CNTs. Severe material delamination was observed for the specimens tested under higher load and lower sliding speed, which is consistent with the trend shown in Fig 2.6 (II) (b) and(c).

Above studies are [1-3] are elaborative and reveal a considerable knowledge regarding wear characteristics of Al-CNT nanocomposite. However, there are some aspects which are worth mentioning at this stage. The first aspect is the optimum percentage of CNTs for best wear resistance. As already mentioned, Kim et al. [2] reported 1 wt. % as the optimum level of CNT content for minimum wear loss, whereas it was reported as 2 wt. % in [3]. In contrast, Zhang et al. [1] found steady increase in wear resistance up to 20 vol.% CNTs. However, it must be realized that the dispersion method of CNTs inside Al matrix and the processing methods in these studies are quite different. Not only the processing method, the wear properties were even found to be sensitive to the dispersion method used for CNTs [2]. Moreover, the type of wear tests and the counterface material in the studies are quite different. Considerable difference in the range of sliding loads and speeds is also evident.

Generally, hardness is the mechanical property of any material which has been found to be most closely related to its wear behavior. General observations have shown that wear resistance of the material increases with hardness. Similar trend was observed by Kim et

al. [2]. However, hardness was not given any significance by Choi et al. [3] where the ratio of material's yield strength to its elastic modulus was given much significance and inverse relationship between this ratio and wear resistance was mentioned. Although decrease in hardness with increase in CNT content beyond 1 wt. % was observed in [2], continuous increase in stiffness and yield strength with increasing CNT content was found in [3]. Zhang et al. [1], found maximum hardness at 15 vol. % CNTs but the wear resistance was highest for 20 vol. % CNTs.

Densification is another important parameter which should be given equal significance. Kim et al. [2] underestimated this aspect and the formation of aluminum carbide was solely held responsible for poor hardness and wear resistance of composites with higher CNT content. Poor densification of composites with higher CNT content could be the important reason for degradation in their hardness and wear resistance. However, Choi et al. [3] not only reported the densification of composites with varying CNT content but also compared the experimental values of density with theoretically calculated one. Poor densification of composite with high CNT content was held responsible for its poor wear resistance which seems quite justified as the unsintered Al-CNT agglomerates would definitely cause inhomogeneous microstructure and higher material loss during wear tests. Formation of aluminum carbide was not reported in this work.

As far as the variation of sliding speed and load is concerned, the second study [2] was conducted at a very low sliding speed of only 0.02 m/s approximately which seems to be very infeasible when compared with many practical applications. Similarly, very limited range of load, 3 to 12 N approximately, was used. Moreover, the study lacks some important information regarding the effects of sliding speed and load i.e. friction

coefficient and wear loss were not reported as a function of sliding speed and load. The speed used by Zhang et al. [1] was much higher, 0.1571 m/s, but still not comparable to practical applications. The third study [3], however, reports much comprehensive analysis for these parameters, as shown in Fig 2.11. The applied loads, 20 to 50 N, were considerably higher but the sliding speeds, 0.08 to 0.16 m/s, were again very low. Friction coefficient and wear loss were found to increase with applied load. With an increase in sliding speed, friction coefficient decreased considerably whereas slight decrease in wear loss was observed with increase in sliding speed. As far as the effect of speed and load on friction coefficient and wear loss of Al-MMC are concerned, mixed trends have been observed as evident in many studies [18,29,33,40,41,51,52,56,58,59]. One important aspect however is that the studies [1-3] used such contact geometries which does not give real idea of contact pressures employed in wear tests. The value of contact pressure is more significant in most of the tribological systems as it gives a much clear picture about the severity of wear conditions and related properties.

2.5 Objective

The purpose of the present research is to investigate the influence of carbon nanotubes (CNTs) as reinforcement on wear and friction behavior of Al6061 alloy under different loads and constant sliding speed. The objective is to compare the wear rates, transition load, friction coefficient and wear mechanisms of monolithic Al6061 and Al6061/CNT nanocomposite. In the first phase, the Al6061/CNT nanocomposite will be developed through novel fabricating route which results in uniform distribution of CNTs and finest microstructure. As far as CNT content is concerned, the one which results in highest

hardness will be selected for further analysis. Wear tests will be conducted using a pin-on-disk tribometer designed and fabricated according to ASTM G99 standards. In addition to wear rate and friction coefficient measurement, the worn surfaces and debris will also be examined using the scanning electron microscopy (SEM) and energy dispersive spectroscopy (EDS) for identifying the wear mechanisms.

CHAPTER 3

EXPERIMENTAL PROCEDURES

3.1 CNTs Dispersion in Matrix

Al6061 prealloyed powder supplied by the Aluminium Powder Co. Ltd., UK, was used as a matrix material with the composition illustrated in Table 3.1. The particles varied in shape & size, however, most of the particles were found to be nearly spherical with an average diameter of 50 microns.

Multi walled CNTs (MWCNTs)(Purity > 95%) with diameter 40 to 60 nm and length 5 to 15 μm, were used as reinforcing agent. As compared to Single walled CNTs (SWCNTs), MWCNTs consist of multiple layers of graphite superimposed and rolled on each other to form a tubular shape. In the case of SWCNTs, covalent functionalization can break some C=C double bonds, leaving "holes" in the structure of the nanotube and thus modifying its mechanical properties. In the case of MWCNTs, only the outer wall is modified. Hence MWCNTs should be preferred over SWCNTs as reinforcements, especially in the applications involving severe mechanical contact.

Composite powders were prepared by nearly uniform dispersion of CNTs in Al6061 powder. Dispersion of CNTs in Al powder was achieved in 4 steps: (1) Dissolving CNTs and Al6061 powder in ethanol. (2) Sonication of wet slurry for 30 minutes using ultra probe sonicator (Model: CV 33, provided by Sonics Inc., USA). The frequency of

sonication was 20 kHz and the probe vibration was set to 40 percent of the maximum amplitude. (3) Ball milling of ultrasonicated slurry at 200 rpm for 1 hour using planetary ball mill (Model: Pulverisette 5, provided by Fritsch GmbH, Germany). The balls weight to powder weight ratio of 10:1 was maintained and milling was done under argon environment to avoid any oxidation. Stainless steel vials and balls were used for milling to avoid any contamination and micro corrosion inside powders and after drying of powder, (4) the dry powder was again ball milled under same conditions for 15 min to avoid any agglomeration between particles. SEM analysis of the powders was performed to examine their morphology.

3.2 Consolidation

The choice of consolidation method was based on maximum densification for the material. It is necessary that the powder metallurgy specimen is fully densified if it is to be tested for wear properties. Otherwise, the pores inside the material act as macroscopic defects and cause excessive wear of the material. In the present work, four different types of consolidation methods namely Spark Plasma Sintering (SPS), Microwave Sintering (MW), Hot Isostatic Pressing (HIP) and Furnace Sintering (FS), were first tested and the one which imparted highest densification to the material was selected for consolidating all the specimens including the composites. The conditions used for these processes in the present work are as follows.

Table 3.1 Composition of Al6061 powder

Al	Fe	Si	Cu	Mn	Pb	Mg	Zn	Ni	Ti	Zr	Cr	Ga	Co
97.83	0.192	0.69	0.29	0.016	< 0.001	0.83	0.012	0.030	0.015	0.002	0.086	0.015	0.001

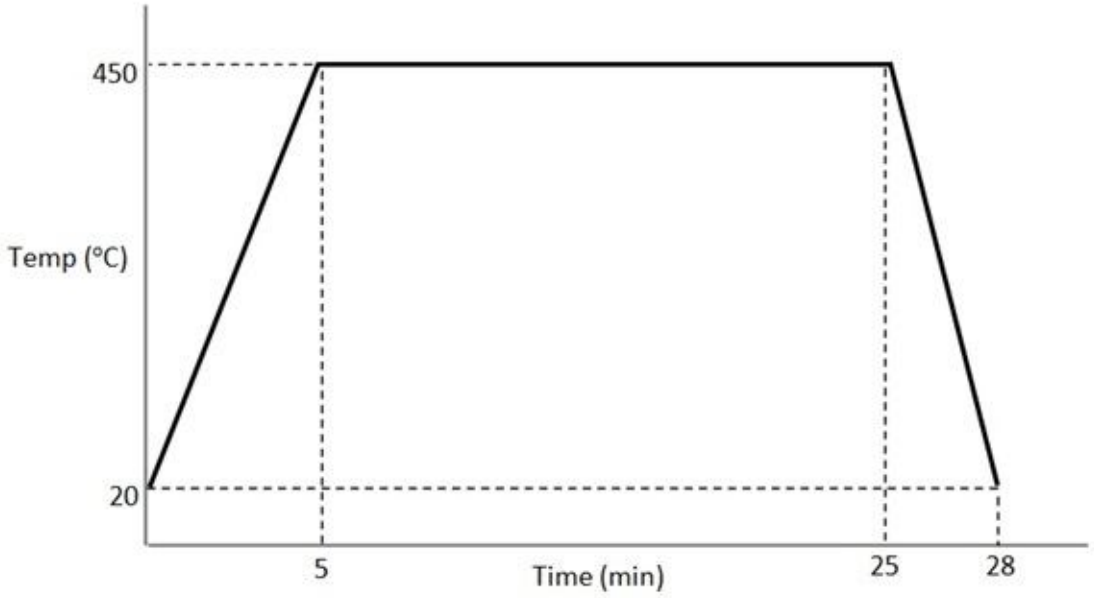

Fig 3.1 Time – Temperature path followed for SPS

Spark Plasma Sintering (SPS)

SE 607, computer controlled SPS system, provided by GmbH, Germany, was used for the processing of specimens. The system provides excellent control over temperature, force and time under which the specimen is processed. The powders were filled directly into the graphite die as precompaction of powders in case of SPS is not required. This is one of the primary advantages of this method which saves considerable energy and time. Powders were pressed under a pressure of 35 MPa and at three different temperatures of 400, 450 and 500 ^{o}C, respectively, under highly evacuated environment. The temperature of specimen was raised from room temperature to the desired temperature in 5 minutes and then it was held at this temperature for 20 min. After this, the system was cooled to room temperature within 3 minutes and the specimen was removed. This is represented in Fig 3.1. To prevent any damage to graphite die, powders and the die were separated by a thin graphite sheet.

Microwave Sintering (MW)

Microwave heating and sintering, which is a pressureless process, is fundamentally different from the conventional sintering, which involves radiant/resistance heating of the specimen via microwaves followed by transfer of thermal energy via conduction to the inside of the body being processed. Microwave heating is a volumetric heating involving conversion of electromagnetic energy into thermal energy, which is instantaneous, rapid and highly efficient. The microwave sintered compacts achieve high density under reduced temperature and cycle time. Moreover, by eliminating grain growth and improving crystalline structure, microwave sintering results in enhanced mechanical properties of sintered compacts [62].

In the present work, MW sintering was performed using a Puschner MW sintering system. Before MW sintering, the powders were compacted in an automated uniaxial press under a pressure of 52 MPa and cylindrical compacts with diameter 20 mm and height 12 mm were produced. These compacts were then MW sintered at 400, 450 and 500 ^{o}C, respectively, for 20 min under evacuated environment.

Hot Isostatic Pressing (HIP)

The HIP process subjects a component to both elevated temperature and isostatic gas pressure simultaneously in a high pressure containment vessel. The pressurizing gas most widely used is argon. An inert gas is used, so that the material does not chemically react. Due to increased cycle time and consequently greater probability of grain growth, the process is not usually employed when preservation of specimen's microstructure is critical.

In the present experimentation, AIP 6-30H hot isostatic press was used for consolidation of the same compacts as prepared for MW sintering. Two different sets of pressure and temperature were employed and the sintering was carried out for 30 min using argon as a pressurizing gas.

Furnace Sintering (FS)

Furnace sintering is the oldest and most conventional type of sintering method which involves heating of precompacted specimens for prolonged durations under inert environment without the application of pressure. Due to increased cycle time and consequently greater probability of grain growth, this process is also not usually employed when preservation of specimen microstructure is critical. In the present

experimentation, a conventional sintering furnace was used for sintering the same compacts as prepared for MW sintering. Sintering was carried out for 3 hours at 400, 450 and 500 ^{o}C, respectively, under argon environment.

As already mentioned, among the above four process, the process which resulted in best densification of the monolithic specimens was used for consolidating all the subsequent specimens, including the composites. Also, detailed characterization was done only for the specimens produced from that specific consolidation method.

3.3 Characterization Techniques

3.3.1 Element Bonding State

X-Ray Diffraction (XRD) analysis was carried out for the matrix and composite in unsintered and sintered state to examine the element bonding state. Differential Scanning Calorimetery (DSC) analysis was also performed for the monolithic Al6061 powder and the composite powder to examine any possible reaction between Al6061 and CNTs.

3.3.2 Densification

Electronic Densimeter (Made : GENEQ, Model : MD 300), having an accuracy of 0.001 g/cm^3 , was used for measuring the density of sintered specimens. The theoretical density of pure Al6061 is 2.7 g/cm^3 whereas the theoretical density of composites was calculated using the rule of mixtures. The average density of MWCNTs is taken as 1.4 g/cm^3.

It is necessary to determine the theoretical density of composite to see the densification obtained after sintering. The theoretical density of composite '$\boldsymbol{\rho_c}$' is calculated using rule of mixtures as follows:

$$\boldsymbol{\rho_c = \rho_m V_m + \rho_r V_r} \quad \ldots (1)$$

Where $\boldsymbol{\rho_m}$ & $\boldsymbol{\rho_r}$ are the densities of matrix (Al6061) & reinforcement (CNTs) with the values of 2.7 g/cm^3 & 1.4 g/cm^3, respectively. $\mathbf{V_m}$ & $\mathbf{V_r}$ represent the volume fractions of matrix & reinforcement, respectively. The values of $\mathbf{V_m}$ & $\mathbf{V_r}$ are calculated as follows:

Volume of matrix in composite = Mass of matrix in composite / Density of matrix

$$= 98 \text{ (g)} / 2.7 \text{ (g/cm}^3\text{)}$$

$$= 36.29 \text{ cm}^3$$

Volume of reinforcement in composite = Mass of reinforcement in composite / Density of reinforcement

$$= 2 \text{ (g)} / 1.4 \text{ (g/cm}^3\text{)}$$

$$= 1.43 \text{ cm}^3$$

Therefore,

$\mathbf{V_m} = (36.29) / (36.29 + 1.43) = 0.96$

And

$\mathbf{V_r} = 1 - 0.96 = 0.04$

Therefore, (1) implies

$\boldsymbol{\rho_c} = (2.7)(0.96) + (1.4)(0.04)$

$\boldsymbol{\rho_c} = 2.648$ g/cm^3

In a similar way, $\boldsymbol{\rho_c} = 2.674, 2.681, 2.687$ g/cm^3 for composite with 1, 0.75 and 0.5 wt. % CNTs, respectively.

3.3.3 Hardness

The Vicker's micro hardness values of the specimens were measured using Digital Micro Hardness Tester (Made: Buehler, USA). The Hardness values shown represent the average of 10 readings taken at different locations in the specimen. The applied load was 100 gf and the dwell time for the indenter was 12 sec. The formula for Vicker's hardness (HV) is given as follows

$$HV = \frac{0.1891F}{d^2}$$

Where, 'F' is the applied load and 'd' represents the diagonal length of an indent.

3.3.4 Compression Tests

Compression tests were performed on the cylindrical specimens with diameter 6 mm and length 12 mm at a strain rate of 0.1 mm/min using Instron 3367 testing machine. The objective of compression tests was to analyze the effect of CNTs on the stiffness and ductility of Al6061 alloy.

3.3.5 Scanning Electron Microscopy

A JEOL scanning electron microscope (SEM) model JSM 6460 was used to analyze the morphology of matrix particles as well as the microstructure of sintered samples. SEM images of fractured surface of the sintered composite were also taken to analyze the CNT distribution and adhesion of CNTs with the matrix.

3.4 Wear Tests

Pin on disk wear tests were conducted at room temperature and under dry conditions using standard Pin-on-Disk tribometer satisfying ASTM G99 standard. Specimens were prepared in the form of cylindrical pins having a diameter of 6 mm and a length of 12 mm. The flat surface of the pin was carefully ground with 600 grit size abrasive paper and polished using a 9 micron diamond polishing suspension. The AISI 4140 steel disk with an average hardness of 24 HRC acted as counterface. The surface finish of the disk, which is an important parameter for the wear tests, was designed to have an average R_a value of 0.3 microns by grinding the disc with alumina abrasive wheel. Before running the tests, the surface of the pin as well as the disk were cleaned with ethanol.

In order to set the sliding distance for steady state wear conditions, some initial wear tests were conducted. These initial tests were conducted on Al6061 pins at the minimum and maximum applied loads of 5 N and 20 N for the sliding distances of 100, 200 and 500 m. The sliding speed was kept constant at 0.5 m/s. The friction coefficient was continuously recorded throughout the test using XY plotter attached to the tribometer.

For determining wear loss, the weight of the specimens was measured before and after the wear tests using electronic balancer with an accuracy of 0.1 mg. To examine the topography of worn specimens and debris, JEOL scanning electron microscope was used. For ensuring correct interpretation of wear mechanisms, EDS analysis was also performed for the worn surfaces as well as the carefully collected debris formed during the entire test.

3.5 Uncertainty Analysis

Since there are several parameters upon which the accuracy of wear rate is dependent, uncertainty analysis for wear rate was carried out. The symbols used in upcoming calculations are explained here:

w = Wear rate (mm^3/km)

ΔV = Volume loss of pin during wear test (mm^3)

ρ = Density of pin material (g/cm^3)

m_1 = Mass of pin before wear test (g)

m_2 = Mass of pin after wear test (g)

v = Sliding speed (m/s)

R = Radius of circular wear track (mm)

N = RPM of counterface disk

t = Wear test duration (sec)

The wear rate 'w' is defined as the volume loss per unit sliding distance and hence expressed as:

$$w = \frac{\Delta V}{vt}$$

Where

$$\Delta V = \frac{m_1 - m_2}{\rho}$$

And

$$v = \frac{2\pi RN}{60}$$

Therefore

$$w = \frac{9.5(m_1 - m_2)}{\rho RNt} \quad \ldots(1)$$

The data reduction equation expresses wear rate as a function of measured parameters in the form

$$w = f(m_1, m_2, \rho, R, N)$$

Uncertainty in time has been neglected.

The variables m_1 and m_2 are fully correlated since they are measured using the same instrument. Hence the Bias in wear rate 'B_w' is given by

$$B_w^2 = \left(\frac{\partial w}{\partial m_1}\right)^2 B_{m_1}^2 + \left(\frac{\partial w}{\partial m_2}\right)^2 B_{m_2}^2 + 2\left(\frac{\partial w}{\partial m_1}\right)\left(\frac{\partial w}{\partial m_2}\right) B_{m_1} B_{m_2}$$

$$+ \left(\frac{\partial w}{\partial R}\right)^2 B_R^2 + \left(\frac{\partial w}{\partial N}\right)^2 B_N^2 + \left(\frac{\partial w}{\partial \rho}\right)^2 B_\rho^2$$

Dividing whole equation by w^2, we get

$$\left(\frac{B_w}{w}\right)^2 = \left(\frac{1}{w}\frac{\partial w}{\partial m_1}\right)^2 B_{m_1}^2 + \left(\frac{1}{w}\frac{\partial w}{\partial m_2}\right)^2 B_{m_2}^2 + 2\left(\frac{1}{w}\frac{\partial w}{\partial m_1}\right)\left(\frac{1}{w}\frac{\partial w}{\partial m_2}\right) B_{m_1} B_{m_2}$$

$$+ \left(\frac{1}{w}\frac{\partial w}{\partial R}\right)^2 B_R^2 + \left(\frac{1}{w}\frac{\partial w}{\partial N}\right)^2 B_N^2 + \left(\frac{1}{w}\frac{\partial w}{\partial \rho}\right)^2 B_\rho^2 \quad \ldots(2)$$

From (1), the partial derivatives are obtained as follows

$$\frac{\partial w}{\partial m_1} = \frac{w}{m_1 - m_2}$$

$$\frac{\partial w}{\partial m_2} = -\frac{w}{m_1 - m_2}$$

$$\frac{\partial w}{\partial R} = -\frac{w}{R}$$

$$\frac{\partial w}{\partial N} = -\frac{w}{N}$$

$$\frac{\partial w}{\partial \rho} = -\frac{w}{\rho}$$

Substituting these partial derivatives in (2), we get

$$\left(\frac{B_w}{w}\right)^2 = \left(\frac{B_R}{R}\right)^2 + \left(\frac{B_N}{N}\right)^2 + \left(\frac{B_\rho}{\rho}\right)^2 \quad \ldots (3)$$

Bias in m_1 and m_2 gets cancelled out due to correlation between them.

The precision in wear rate 'P_w' is given by

$$P_w^2 = \left(\frac{\partial w}{\partial m_1}\right)^2 P_{m_1}^2 + \left(\frac{\partial w}{\partial m_2}\right)^2 P_{m_2}^2 + \left(\frac{\partial w}{\partial R}\right)^2 P_R^2 + \left(\frac{\partial w}{\partial N}\right)^2 P_N^2 + \left(\frac{\partial w}{\partial \rho}\right)^2 P_\rho^2$$

Dividing whole equation by w^2, we get

$$\left(\frac{P_w}{w}\right)^2 = \left(\frac{1}{w}\frac{\partial w}{\partial m_1}\right)^2 P_{m_1}^2 + \left(\frac{1}{w}\frac{\partial w}{\partial m_2}\right)^2 P_{m_2}^2 + \left(\frac{1}{w}\frac{\partial w}{\partial R}\right)^2 P_R^2 + \left(\frac{1}{w}\frac{\partial w}{\partial N}\right)^2 P_N^2 + \left(\frac{1}{w}\frac{\partial w}{\partial \rho}\right)^2 P_\rho^2$$

Substituting partial derivatives, we get

$$\left(\frac{P_w}{w}\right)^2 = \left(\frac{P_{m_1}}{m_1 - m_2}\right)^2 + \left(\frac{P_{m_2}}{m_1 - m_2}\right)^2 + \left(\frac{P_R}{R}\right)^2 + \left(\frac{P_N}{N}\right)^2 + \left(\frac{P_\rho}{\rho}\right)^2 \quad \ldots (4)$$

The values of 'm_1' and 'm_2' were recorded by using a Shimadzu AUW220D dual range electronic balancer. The scale has a resolution of 0.1 mg for a range of 220 g and a resolution of 0.01 mg for a range of 82 g. The device has a linearity of 0.2 mg for a range of 220 g and a linearity of 0.1 mg for a range of 82 g. Since a range of 82 g was used, a linearity of 0.1 mg is used as bias. The manufacturer's data sheet lists a repeatability of 0.1 mg for a large range and a repeatability of 0.05 mg for a small range. A repeatability of 0.05 mg is thus used as precision.

The track radius 'R' was set using a specially designed arm having graduations in mm which were made during arm fabrication. The accuracy was insured using a Starret 721A electronic digital caliper having accuracy of 0.03 mm which is taken as bias. The pin holder is adjusted manually with the graduation. So in this adjustment, the human error of 0.25 mm is taken as precision.

The bias in 'N' is based on the work carried out previously [63] in which 1 Hz of input frequency corresponds to 41 rpm using same tribometer setup as in present work. The bias in that work was found to be 13 rpm and precision as 0 rpm. In present work, 1 Hz of input frequency corresponds to 18 rpm. So the current bias in N can be calculated as (18/41)*13 = 5 rpm (approx.). The precision remains same as 0 rpm.

The density 'ρ' of specimens was measured using MD 300 electronic densimeter for which the error in measurements could be 0.001 g/cm^3 according to manufacturer's data sheet. So this value is taken as bias. In density measurement, the density of the same

specimen varied by 0.001 g/cm^3 during repetitions and hence this value was taken as precision.

Table 3.2 summarizes the bias, precision and nominal values for all the variables. Substituting values from Table 3.2 in (3) and (4), we get

$$\left(\frac{B_w}{w}\right)^2 = 4.4\ x10^{-4}$$

$$\left(\frac{P_w}{w}\right)^2 = 5.5\ x10^{-4}$$

Finally, the uncertainty in wear rate 'U_w' is given by

$$\left(\frac{U_w}{w}\right)^2 = \left(\frac{B_w}{w}\right)^2 + \left(\frac{1}{\sqrt{n}}\frac{P_w}{w}\right)^2$$

Where 'n' is the number of repetitions for same experiment and its value is 3.

Hence

$$\left(\frac{U_w}{w}\right)^2 = 6.23\ x10^{-4}$$

$$\frac{U_w}{w} = 0.025$$

Or

$$U_w = 2.5\ \%$$

Hence the uncertainty in reported wear rate is 2.5 percent.

Table 3.2 Bias, Precision and Nominal values for different variables

Variable	Bias	Precision	Nominal Value
m_1	0.1 mg	0.05 mg	$0.80572*10^3$ mg
m_2	0.1 mg	0.05 mg	$0.80217*10^3$ mg
R	0.03 mm	0.25 mm	20 mm
N	5 rpm	0 rpm	239 rpm
ρ	0.001 g/cm^3	0.001 g/cm^3	2.700 g/cm^3

CHAPTER 4

EXPERIMENTAL RESULTS

4.1 Morphology of Powders

The morphology of Al6061 powder is shown in Fig 4.1(a). The powder consists of particles with various shapes including spherical, elongated and irregular ranging between 10 and 90 microns. Fig 4.1(b) also shows that large particles themselves are made from very small crystals (grains). Fig 4.2 shows x-ray diffraction spectrum of the Al6061 powder. The major phase present is the solid solution α-aluminum with FCC crystal structure. The spectrum does not clearly reveal other phases that may form due to the presence of other elements with concentrations that exceed the solubility limit in the α-aluminum. This is due to the fact that the amount of these phases, if they are present, is not enough to be clearly revealed in the XRD spectrum. The morphology of MWCNTs is shown in Fig 4.3. It is evident that CNTs are in a fairly separated state without any noticeable agglomeration.

Fig 4.4 (a-e) shows the morphology of composite powders obtained by the route mentioned earlier. As can be seen in Fig 4.4(a), some particles got slightly flattened although wet milling for only for 1 hour was done. This flattening is more pronounced in case of dry milling for much larger time periods [3]. Fig 4.4(b) shows the implantation of CNTs on these flattened particles surface. Some of the CNTs got located deeper inside the matrix through the plastic deformation of matrix. This is desirable because as the

proportion of CNTs lying outside the matrix particle increases, the sintering capability of the matrix decreases due to hindrance caused by CNTs between adjacent particles. Fig 4.4(c) reveals that many particles still maintained the spherical shape whereas Fig 4.4(d) shows that these particles are uniformly surrounded by the segregated CNTs which were unable to locate themselves deeper inside the matrix. As the wet balled mixture of powder was left in open air for drying, therefore during drying, the movement of vapor from inside the droplet to outside leads to transport of low density CNTs to the surface of particle [60]. It is evident in Fig 4.4 (a-d) that dispersion of CNTs is fairly uniform and no considerable clustering of CNTs, except at few locations as shown in Fig 4.4(e), occurred during wet ball milling and subsequent drying of composite powders. As reported in previous study [64], this clustering which becomes more pronounced in case of higher CNT content, is highly undesirable as it results in poor sintering and densification and consequently poor mechanical properties of the composite.

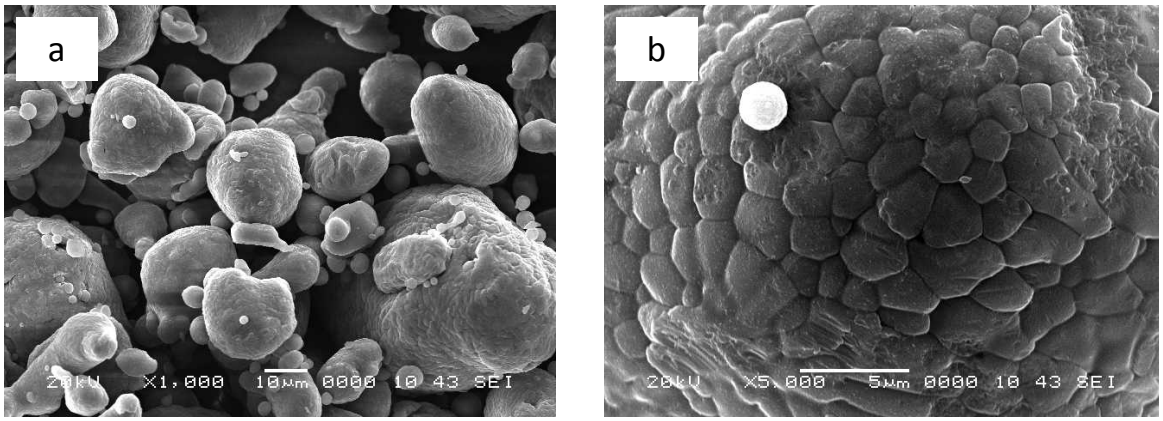

Fig 4.1 Al6061 powder morphology (a) x1000 (b) x5000

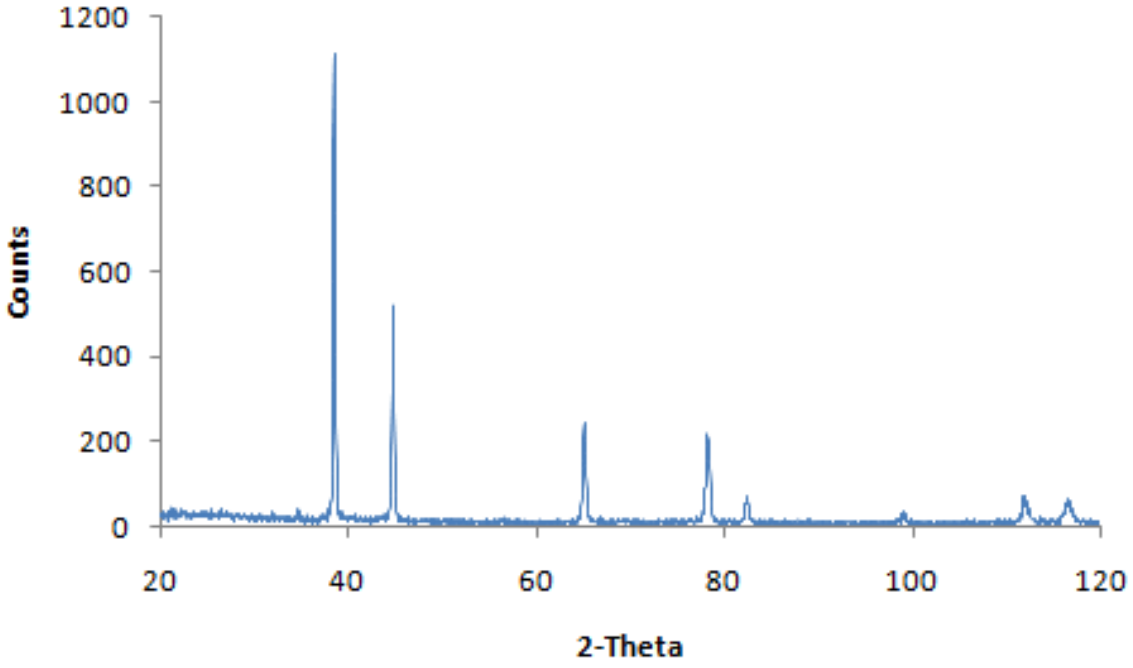

Fig 4.2 X-ray diffraction spectrum of as received Al6061 powder

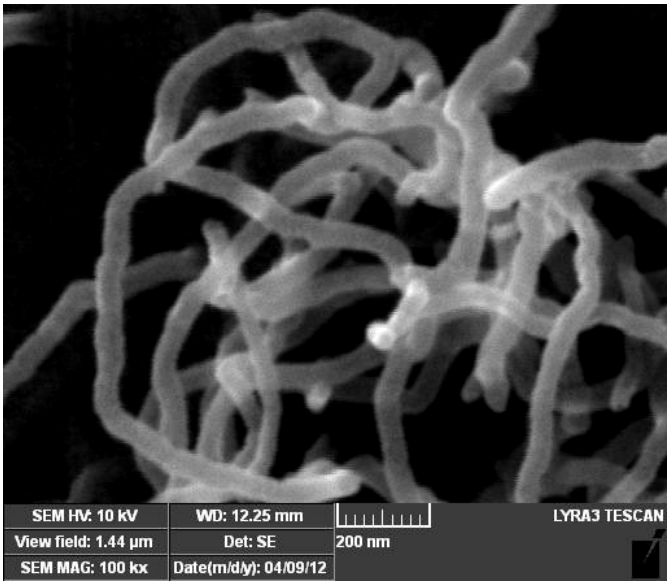

Fig 4.3 Morphology of MWCNTs

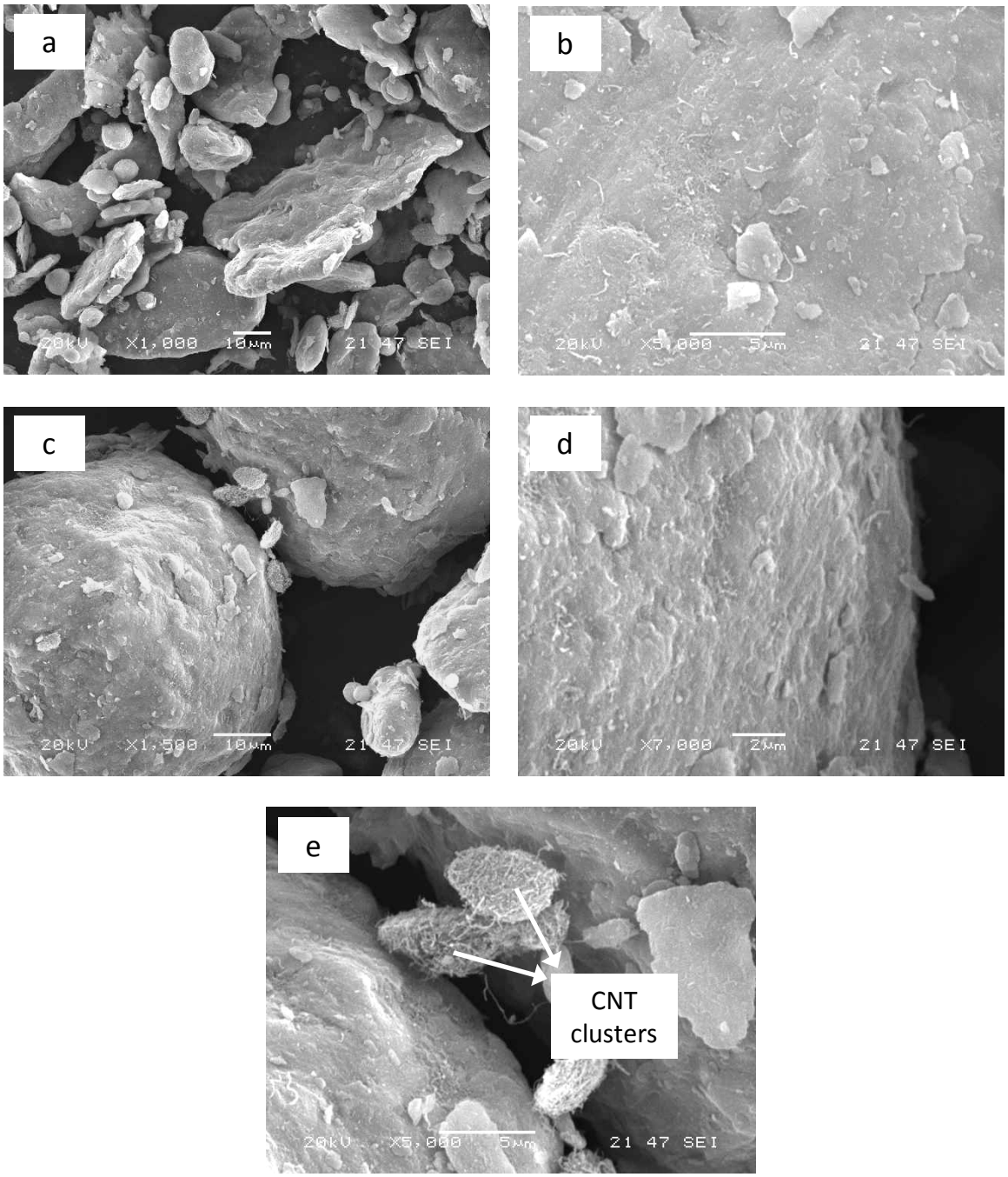

Fig 4.4 SEM micrographs of the composite powders showing (a) some flattening of particles during ball milling, (b) implantation of CNTs on flattened particles surface, (c) spherical particles, (d) uniform surrounding of spherical particles by CNTs and (e) some CNT clusters.

4.2 Density of Monolithic Specimens

Table 4.1 illustrates the density of monolithic Al6061 alloy when sintered through different processes under different conditions. It can be seen that FS resulted in a density of around 2.3 g/cm^3 as compared to 2.7 g/cm^3 which is the actual density of Al6061. Hence satisfactory densification through FS is not possible even after 3 hrs. Also the effect of increasing temperature is not pronounced. As far as HIP is concerned, densification remained considerably low even when the pressure and temperature were increased to significant extent. Results of MW sintering are almost similar and the densification remained below 2.5 g/cm^3 for all the sintering temperatures. In contrast, the results of SPS are very different from MW, HIP and FS processes. It can be seen that 100 % densification was achieved as the temperature was increased to 450 ^{0}C in SPS. Based on these results, SPS was selected for consolidating all the subsequent specimens, including the composites, and all the specimens were consolidated under a pressure of 35 MPa at a temperature of 450 ^{0}C for 20 min.

4.3 Density and Hardness of Sintered Specimens

Shown in Fig 4.5 (a) is the density of sintered specimens as a function of CNT content. It can be seen that the monolithic Al6061 achieved full densification, however, the density decreased considerably as the CNTs were added. This was expected because the agglomeration of CNTs at some locations might have resisted proper neck formation between adjacent matrix particles and hence caused void formation. It can also be seen that densification for 0.5 and 0.75 wt. % CNTs is considerably low and it increased

slightly for 1 and 2 wt. % CNTs. Among the four CNT percentages used, 1 wt. % CNTs resulted in highest densification.

Shown in Fig 4.5 (b) is the hardness of sintered specimens as a function of CNT content. It is evident that addition of CNTs resulted in increased hardness. However, the maximum hardness was found in case of 1 wt. % CNTs. For 2 wt. % CNTs, the hardness decreased drastically. In case of 2 wt. % CNTs, the excessive CNTs form their agglomerates and also conglomerate with the matrix and hence cause defects in the material. Theses defects, which are mainly composed of CNT agglomerates, are weak regions and as the indenter comes in contact with the material, these defects do not only cause indents of greater size but also relatively nonuniform indent. This results in reduced hardness of the composite. The hardness results are very much similar to those observed by Kim et al. [2] who also used SPS for fabricating the Al – CNT composites. They also observed that Al – CNT composites displayed highest hardness and wear resistance in case of 1 wt. % CNTs. Addition of further CNTs results in reduced hardness and may consequently to poor wear resistance. Although, in case of higher CNT proportions, lubricating action of CNTs is more effective. But if excessive subsurface fracturing and delamination is going on, the CNTs fail to form a stable lubricating film and hence the lubricating action of CNTs, despite higher proportion, becomes ineffective.

It can be seen that with small amount of carbon nanotubes addition, the relative density and hardness of the composites increased with increasing CNT content, while the proportion as high as 2 wt. % of reduced the relative density and especially the hardness of the composites. This can be attributed to the fact that small amount of CNT addition could fill up the microvoids causing increase of the density of composites, however, large

amount of CNTs are prone to excessive clustering. Thus the CNT agglomeration will not only hinder the densification of the specimens, but will also become the defect source. Hence, the relative density and hardness of the composites decreases. Similar trends for density and hardness in case of Al2024-CNT composites were reported elsewhere [6].

Based on these results, the composite with 1 wt. % CNTs was selected for further analysis and wear tests.

Table 4.1 Density of monolithic Al6061 under different processes and sintering parameters

PROCESS	PRESSURE (MPa)	TIME (min)	DENSITY (g/cm^3) @ TEMPERATURE (^{0}C)		
			400	450	500
FS	-	180	2.279	2.397	2.229
HIP	69	30	-	2.416	-
	103		-	-	2.252
MW	-	20	2.459	2.480	2.498
SPS	35	20	2.540	2.700	2.692

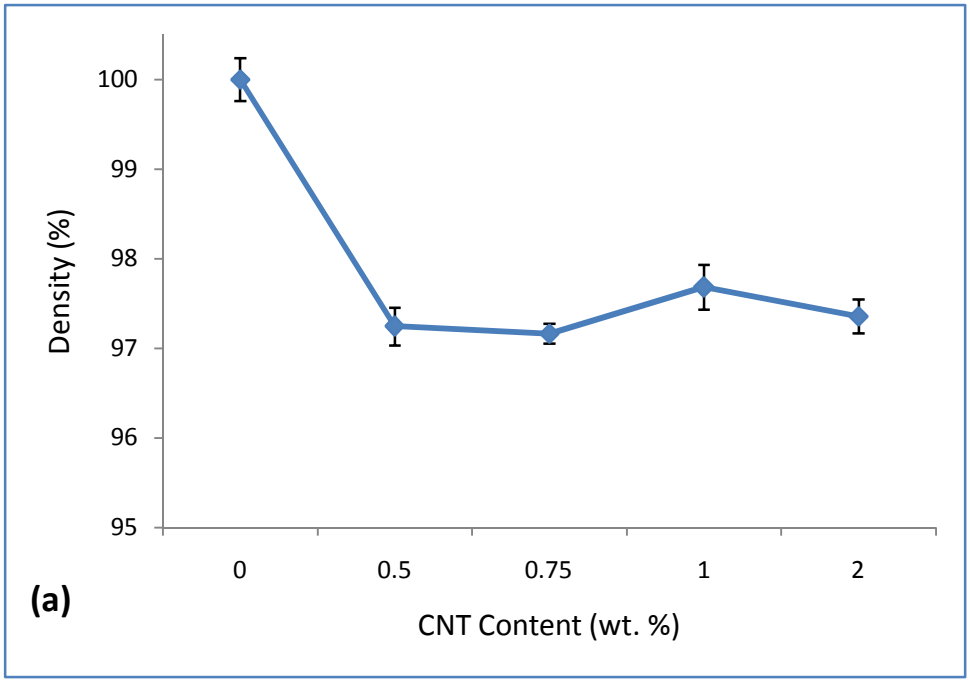

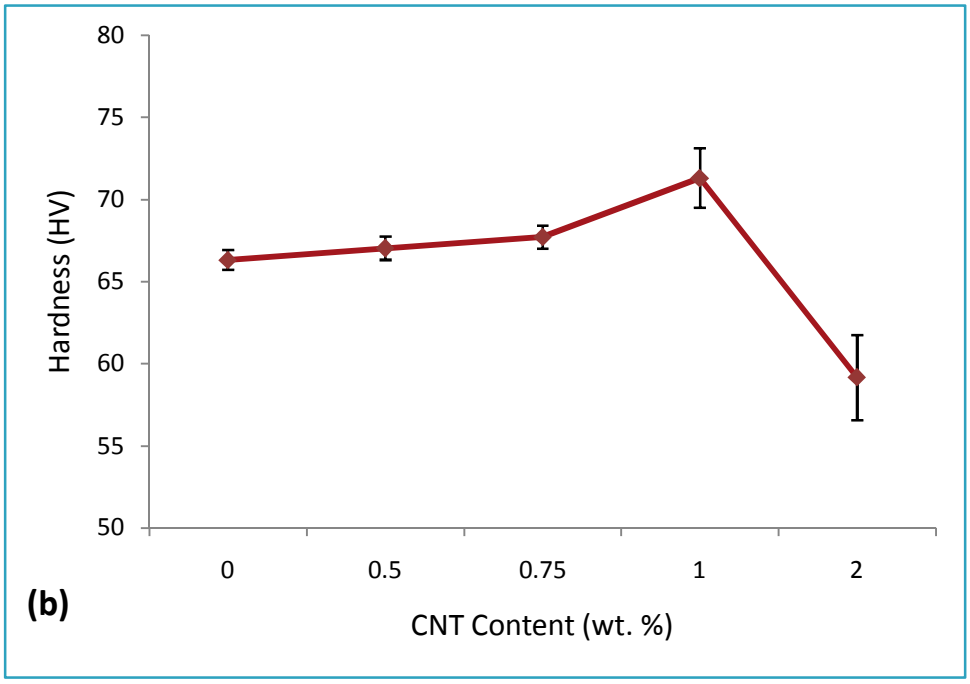

Fig 4.5 (a) Density and (b) Hardness of SPS'ed Al6061 alloy as a function of CNT content

4.4 Microstructure of Sintered Specimens

Fig 4.6 shows the SEM image of the spark plasma sintered Al6061. At same magnification, Fig 4.7 shows the SEM image of the SPS'ed Al6061 with 1 wt. % CNT composite. Slight porosity is evident in case of the composite. This was expected as slight agglomeration of CNTs at some locations hinders proper sintering of the matrix and consequently some porosity. Fig 4.8 further clarifies this aspect where one of the pores is magnified. It is evident that agglomeration of CNTs at this region hindered proper sintering of the matrix.

Fig 4.9 shows the morphology of fractured surfaces of the spark plasma sintered Al6061 with 1 wt. % CNT composite at higher magnification. As can be seen in Fig 4.9(a), CNTs show good adhesion with the matrix particles without any significant clustering. Also, very less CNTs are found over the fractured surface which shows that CNTs were able to penetrate deep inside the matrix particles during processing. Fig 4.9(b) shows another location inside the same material where some CNT agglomeration can be found, as circled in the figure. However, this agglomeration was observed at limited locations and most of the regions were characterized by fairly uniform distribution and good adhesion of CNTs with the matrix. Also marked with arrows in the figures is the CNT pull out from the matrix which occurred due to fracture.

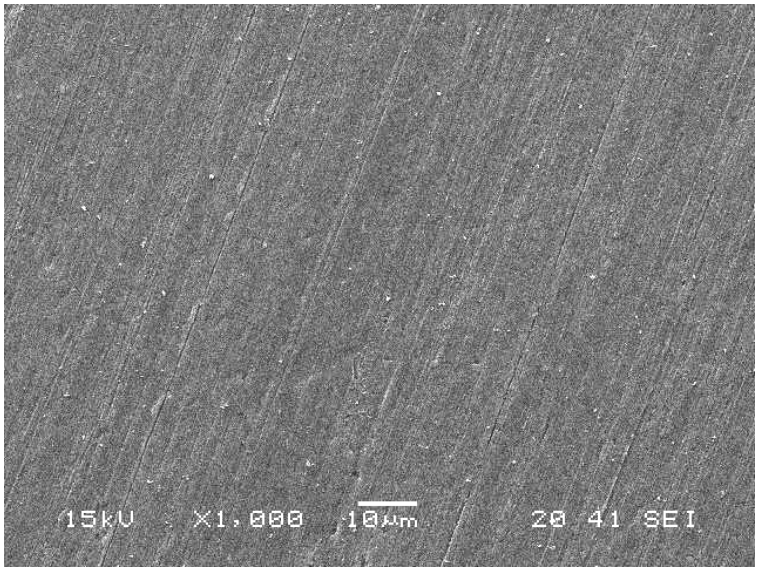

Fig 4.6 SEM image of SPS'ed Al6061 (T = 450 ^{o}C, P = 35 MPa, t = 20 min)

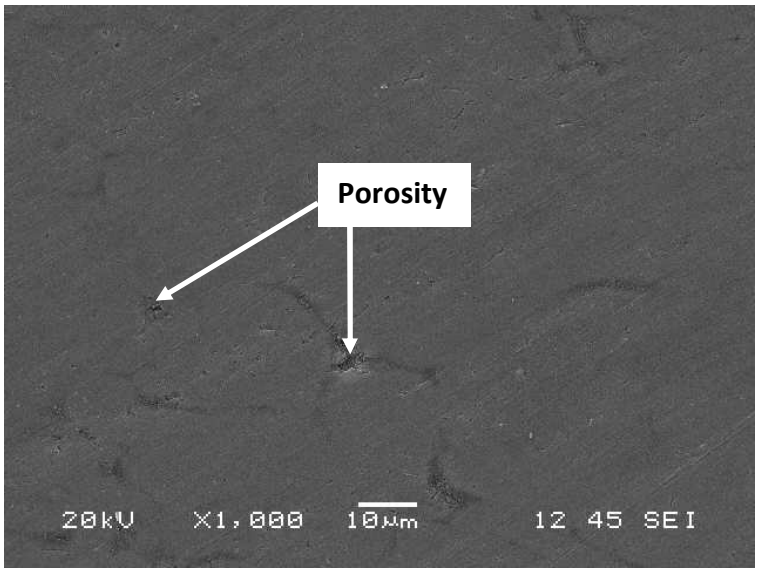

Fig 4.7 SEM image of SPS'ed Al6061 + 1 wt.% CNT composite (T = 450 ^{o}C, P = 35 MPa, t = 20 min)

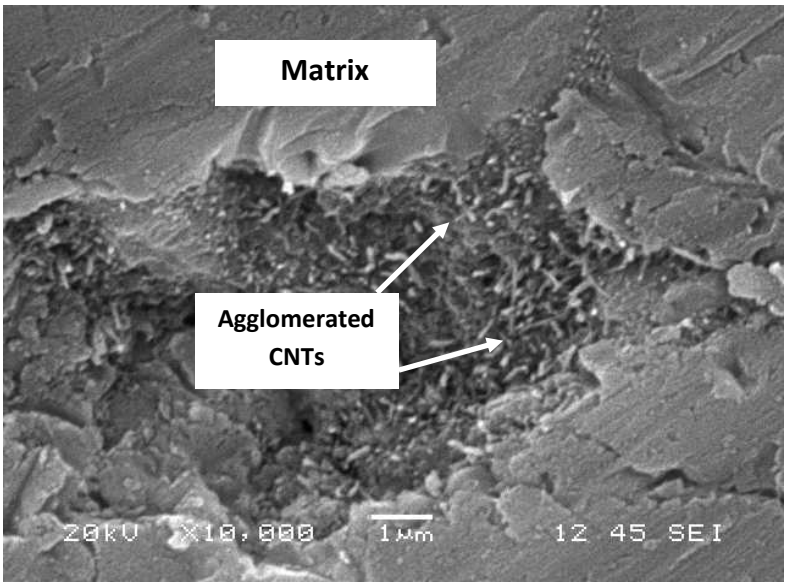

Fig 4.8 SEM image of SPS'ed Al6061 + 1 wt.% CNT composite at higher magnification showing porosity caused by agglomeration of CNTs at some regions (T = 450 ^{o}C, P = 35 MPa, t = 20 min)

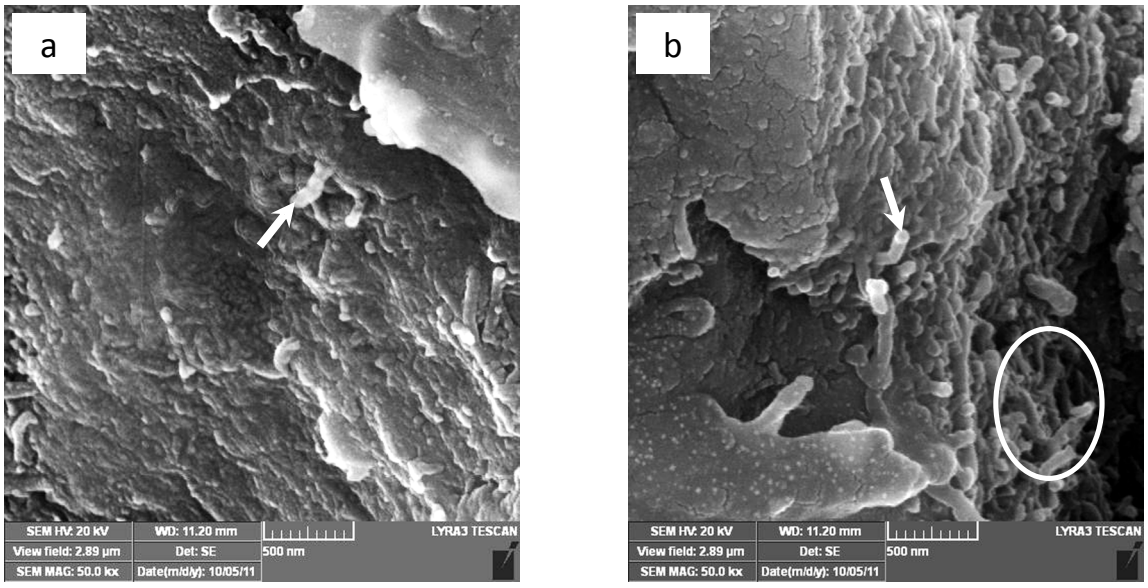

Fig 4.9 SEM images of fractured surface of Al6061 + 1 wt. % CNTs composite with (a) fairly uniform distribution of CNTs and (b) some agglomeration as circled. Pulled out CNTs marked with arrows in (a) and (b). (50,000X)

4.5 X-Ray Diffraction

The XRD spectrum of the composite powder is shown in Fig 4.10(i) which is similar to that of pure Al6061 powder shown in Fig 4.2. This was expected as only 1 % CNTs are two low to reveal any chemical or phase transformation in XRD analysis, if occurred. XRD spectra of SPS'ed Al6061 and spark plasma sintered Al6061 with 1 wt.% CNT composite are shown in Fig 4.10(ii) and 4.10(iii) respectively. Both spectra are not only similar to each other but also to the XRD spectrum of Al6061 powder shown in Fig 4.2. This reveals that no significant chemical reaction or phase transformation occurred during powder preparation as well as consolidation. Although CNT content is quite low i.e. 1 wt. %, which is undetectable for XRD machine, it has already been reported that significant and detectable formation of Aluminum Carbide occurs for CNT content as high as 5 wt. % [2].

4.6 Differential Scanning Calorimetery

Differential Scanning Calorimetery (DSC) signals for the Al6061 powder and composite powders with sonication and sonication followed by ball milling are shown in Fig 4.11. It can be seen that the DSC pattern for the composites is almost the same throughout as that of the matrix and does not reveal any special exothermic peak. This confirms that no significant reaction took place between Al and CNTs during sonication and ball milling and hence the formation of aluminum carbide did not occur. This is in agreement with the XRD pattern shown in Fig 4.10 which also does not show any special peak for the composite. It is worth mentioning here that the formation of aluminum carbide in case of

Al 2024 powder with 1 wt. % CNT has already been reported [5]. Formation of aluminum carbide was observed in the form of exothermic peak at about 675 ^{o}C in DSC analysis. The Al 2024 alloy has significant proportion of copper (about 4 %) which might have acted as catalyst for the reaction between Al and CNTs and hence aluminum carbide is formed. In contrast, the Al6061 alloy used in the present study has negligible proportion of copper (about 0.3 %) and hence no catalytic action exists for Al and CNTs to react.

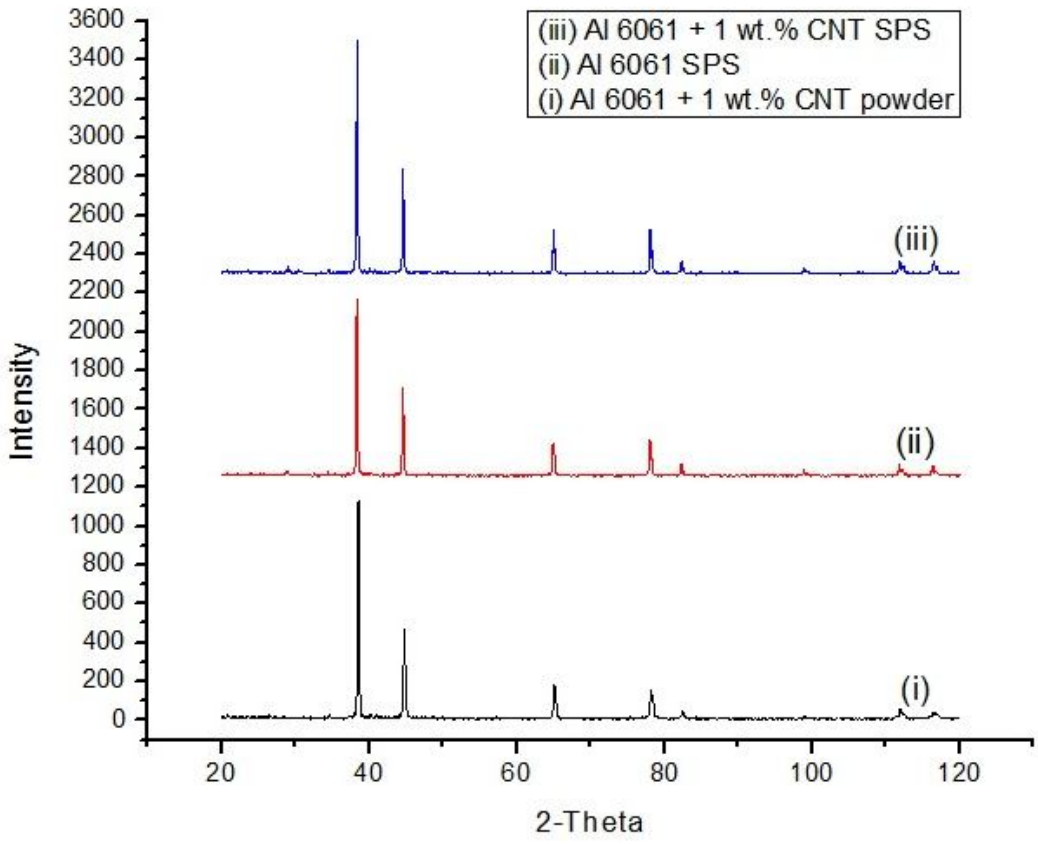

Fig 4.10 X-ray diffraction spectrum of (i) Al6061 + 1 wt. % CNT powder (ii) SPS'ed Al6061 (iii) SPS'ed Al6061 + 1 wt.% CNT (T = 450 ^{o}C, P = 35 MPa, t = 20 min)

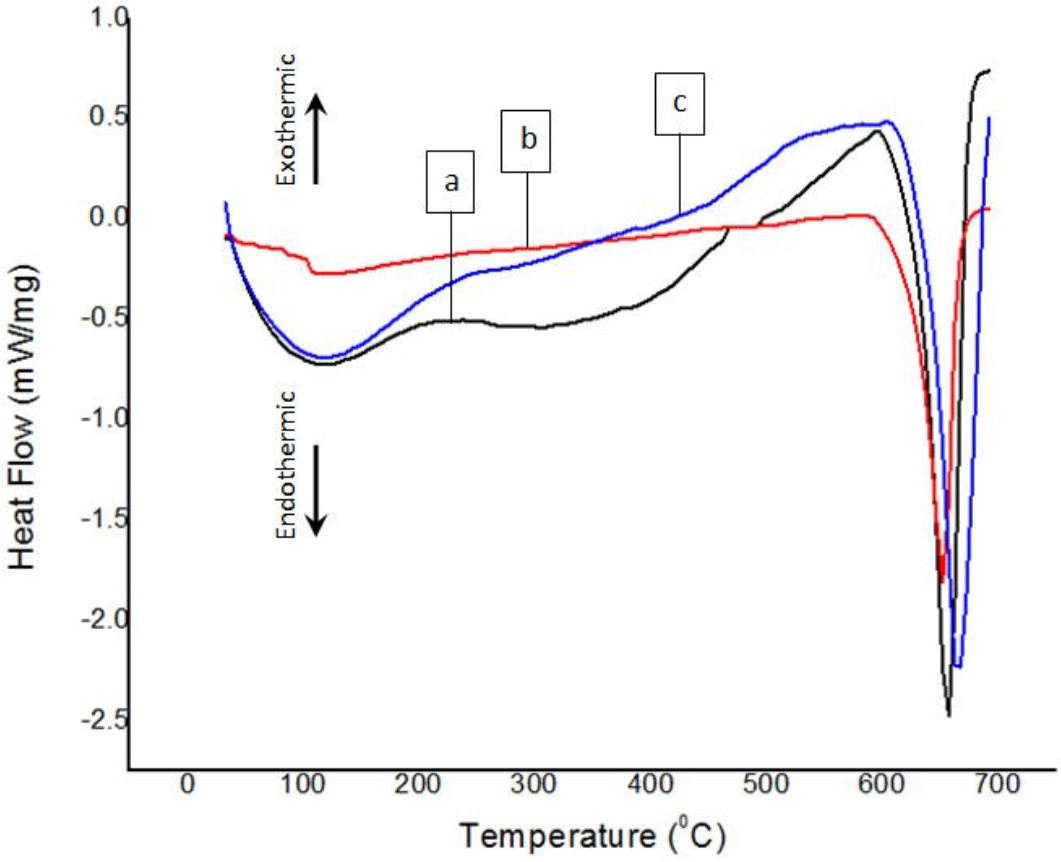

Fig 4.11 DSC signals for (a) Al6061 powder, (b) Al6061 + 1 wt. % CNTs powder after sonication and (c) Al6061 + 1 wt. % CNTs powder after sonication and ball milling

4.7 Density and Mechanical Properties

Table 4.2 shows the theoretical and experimental values of density as well as the relative density for the spark plasma sintered matrix and the composite. It can be seen that the composite is not fully densified. This is in agreement with the SEM analysis where some porosity due to agglomeration of CNTs at some location was evident.

Improvement in hardness (approx. 8 %) can be observed due to the addition of CNTs. It was necessary to take many readings throughout the specimens because in case of sintered specimens, hardness does vary from location to location. This aspect is more important in case of composites, especially for nanocomposite as in the present situation, where due to nonuniform distribution of nanoparticles, hardness varies from location to location within the specimen. In the present measurements also, the variation was observed more in case of composite. The locations where the CNTs distribution is fairly uniform exhibit relatively high hardness because at these locations, CNTs play an effective role in resisting dislocation movement. On the other hand, the locations where the specimen exhibit relatively low hardness are the locations where the CNTs distribution is relatively nonunifrom and CNTs agglomerates exist which do not play effective role in resisting dislocation movement and rather decreases the strength of the composite. However, in the present case hardness didn't vary considerably across the composite and the standard deviation for the 10 readings taken was found to be only 1.8 HV.

The compression test results show improvement in stiffness of the material upon 1 wt. % CNT addition but at the cost of ductility, which decreases by almost 10 %. This reduction

in ductility, which is due to the brittle nature of reinforcement phase, can significantly affect the wear characteristics of the composite. Also, the yield stress for the composite is lower as compared to pure Al6061.

4.8 Surface Finish of Counterface

It is important to measure the surface roughness of counterface as it greatly affects the wear behavior of the material being tested. Fig 4.12 (a) and (b) show the arithmetic mean of surface roughness (R_a) values. The R_a value of 0.17 microns and 0.42 microns along and across the grinding direction on the disc, respectively, was observed. So the average R_a value for the disc can be considered as 0.30 microns approximately. The R_a values were measured using Mitutoyo SJ – 400 profilometer.

Table 4.2 Density and mechanical properties for the SPS'ed matrix and composite (T = 450 ^{o}C, P = 35 MPa, t = 20 min)

Material	Density			Hardness (HV)	Compression (%)	Compressive Elastic Modulus 'E' (MPa)	Compressive Yield Stress 'Y'(MPa)	Y/E
	Theoretical (g/cm^3)	Experimental (g/cm^3)	Relative (%)					
Al6061	2.700	2.700	100	66.31	40.94	1200.09	28.5	0.023
Al6061 + 1 wt. % CNTs	2.674	2.612	97.7	71.30	31.21	1509.13	21.25	0.014

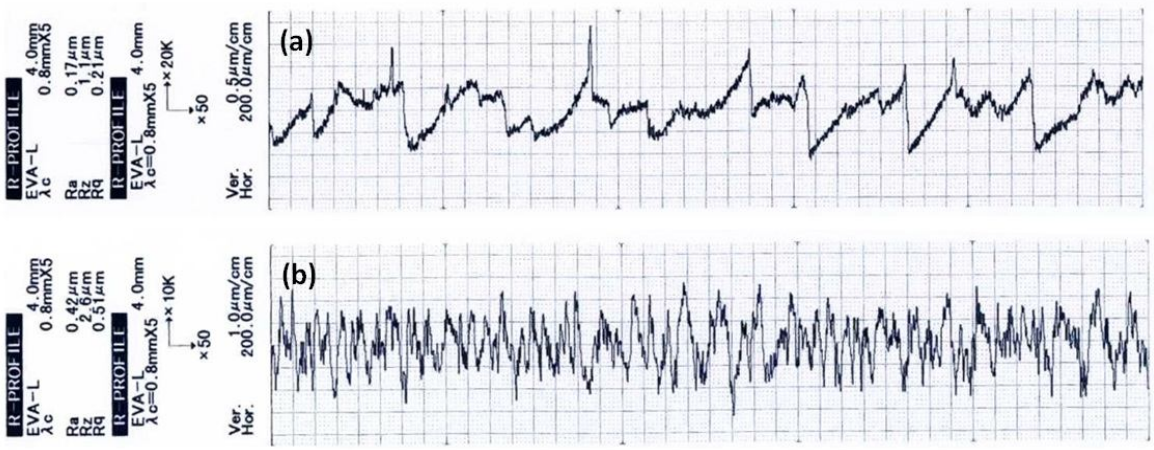

Fig 4.12 R_a values for the counterface disc (a) along and (b) across the grinding direction

4.9 Wear Tests

4.9.1 Wear Rate

Fig 4.13 shows the wear rate per unit sliding distance as a function of sliding distance for Al6061 pins. It can be seen that wear rate increases sharply as the sliding distance was increases from 100 m to 200 m. However, for the sliding distance of 500 m, the wear rate was almost similar to that of 200 m sliding distance. This shows that steady state friction conditions prevail over the sliding distance range of 200 m to 500 m. So for all the subsequent tests, the sliding distance was kept constant at 500 m. To study the effect of applied load on wear and friction and to compare the transition loads for the matrix and composite, the load range was extended to 30 N. So the applied load was varied from 5 N to 30 N with an increment of 5 N resulting in a total of six applied loads. The sliding speed was kept constant at 0.5 m/s for all tests.

Fig 4.14(a) shows the wear rate for the monolithic Al6061 and the composite as a function of applied load. The wear rate for both materials increased linearly with the applied load. It can be seen that at lower loads of 5 N to 15 N, the composite displayed better wear resistance. However at higher loads of 20 N to 30 N, the wear resistance of monolithic Al6061 is far better than the composite. As far as the transition load is concerned, it can be seen that the wear rate of composite increased drastically as the load was increased from 15 to 20 N which shows that the composite underwent sharp switch in wear mechanism and hence transition from 15 N to 20 N. As far as monolith is concerned, such drastic increase was not observed until 25 N of load. However, as the

load was increased to 30 N, the wear rate displayed dramatic increase. This shows that transition in the composite occurs at lower load as compared to monolithic Al6061.

Fig 4.14 (b) and (c) show the wear rates for both the materials as a function of stress with standard deviation. These graphs actually correspond to mild and severe wear regimes. It can be seen that the composite displayed nearly three times improvement in wear resistance as compared to monolith under mild wear conditions. Also, the standard deviation in results is considerably low in mild wear regimes. However, as the conditions switched to severe, the wear rate for the composite increased considerably as compared to monolith. Also, the standard deviation in results in severe regime is relatively high.

For the experimental conditions used, the wear rates for both the materials indicate that CNTs act as effective reinforcements for improving wear resistance of Al6061 at lower loads only. At higher loads, CNTs give no advantage and rather decreased the wear resistance of Al6061 alloy. This behavior may be attributed to considerable difference in the microstructure and the subsequent wear mechanisms of both the materials under different values of applied load. The details will be discussed in later sections.

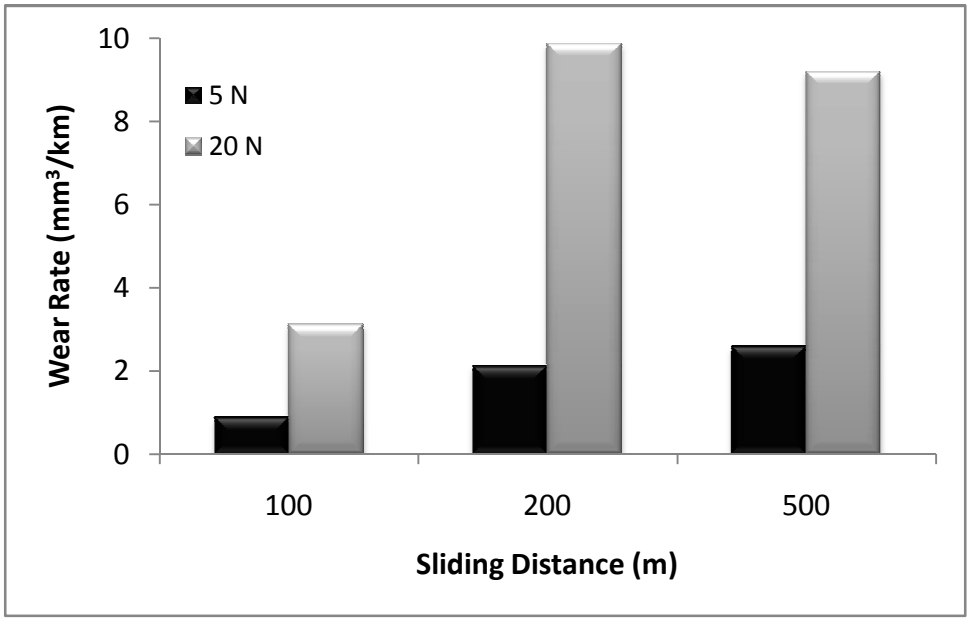

Fig 4.13 Wear rate vs sliding distance for the Al6061 specimens tested at 5 N and 20 N

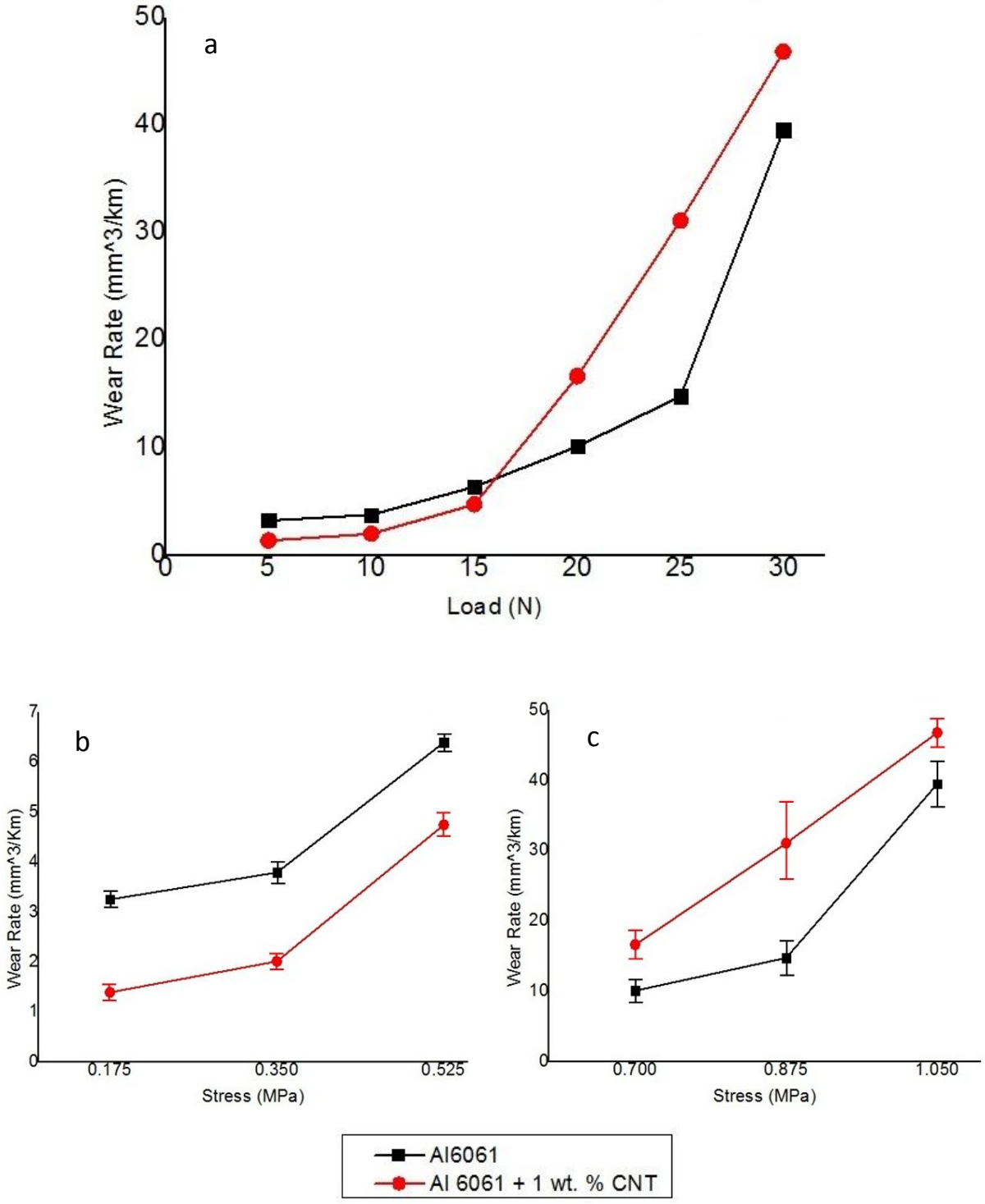

Fig 4.14 Wear rate for monolithic Al6061 and the composite as a function of (a) load and (b, c) stress. (b) and (c) represent mild and severe wear regimes, respectively.

4.9.2 Friction Coefficient

Fig 4.15 (a – c) show the friction coefficient for monolithic Al6061 and the composite throughout the test for the applied load of 5 N, 15 N and 25 N, respectively. Fig 4.15 (a) shows that friction coefficient for Al6061 increased continuously during the first 100 m. After 100 m, it decreased slightly and remained steady at an average value of about 0.45 for the remaining 400 m. In case of composite, the friction coefficient showed considerable variation during first 200 m. However for the remaining 300 m, the friction coefficient remained steady at an average value of 0.35. It is also evident that the friction coefficient for the composite is not only less but also has considerably less fluctuation as compared to monolithic Al6061. The lower value and fluctuation of friction coefficient in case of composite may be attributed to stable lubricating action of CNTs during the wear test.

Fig 4.15 (b) compares the friction coefficient for both the materials at 15 N. It can be seen that both the materials displayed considerable variation in friction coefficient for approximately 100 m. However for the remaining sliding distance, the friction coefficient for the monolithic Al6061 and the composite remained almost steady at an average value of 0.6 and 0.5, respectively. It is also evident that unlike at 5 N, the fluctuation in friction coefficient for the composite increased considerably. This may be attributed to increased micro fracturing and delamination due to increased brittleness of composite.

Fig 4.15 (c) compares the friction coefficient for both the materials at 25 N. It is evident that for both the materials, not only the friction coefficient increased to considerable extent but also the fluctuation increased considerably. Moreover, it can be seen that the

friction coefficient for the composite is now much higher as compared to monolithic Al6061. During the first 300 m, the friction coefficient for the monolithic Al6061 remained steady at an average value of 0.65 whereas in case of composite, this value is as high as 0.8. During last 200 m, too much fluctuation in the form of sharp peaks is evident for both the materials. Especially for the composite, excessive value and fluctuation of friction coefficient represent seizure of material which may be attributed to excessive sub surface fracturing and delamination at such high value of applied load.

Shown in Fig 4.16 (a) and (b) is the minimum, maximum and average value of friction coefficient as a function of applied load for the monolithic Al6061 and the composite, respectively. It is clear that the friction coefficient increased linearly with applied load for both the materials. For monolithic Al6061, the friction coefficient increased steadily with the applied load without any sharp increase. However, in case of composite, the increase is sharper, especially from 20 N to 25 N, where the friction coefficient jumped from about 0.6 to almost 1.0. Such drastic increase corresponds to sharp switching in wear intensity from mild to severe fracturing and delamination.

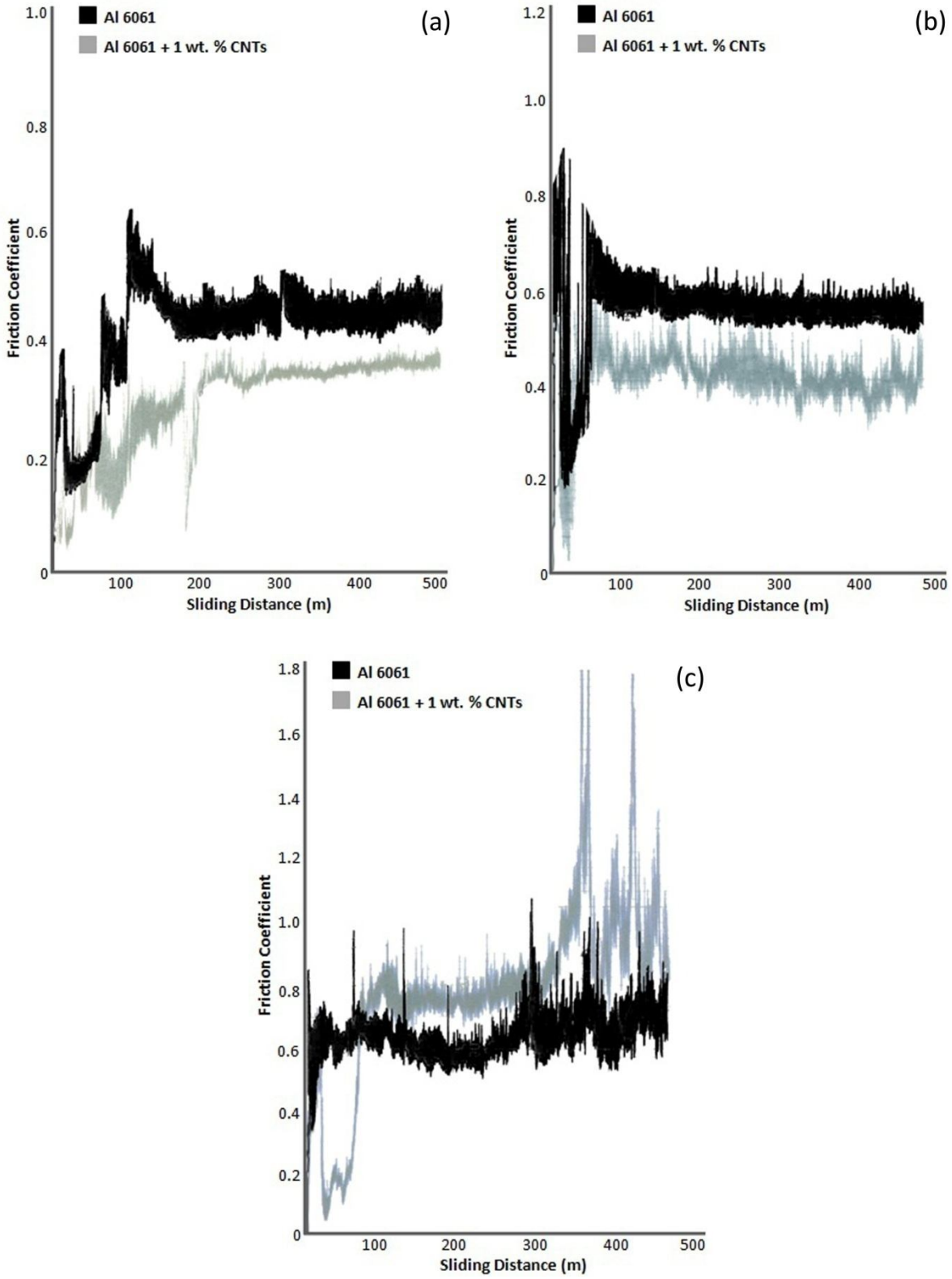

Fig 4.15 Friction Coefficient for monolithic Al6061 and composite (a) 5 N (b) 15 N (c) 25 N

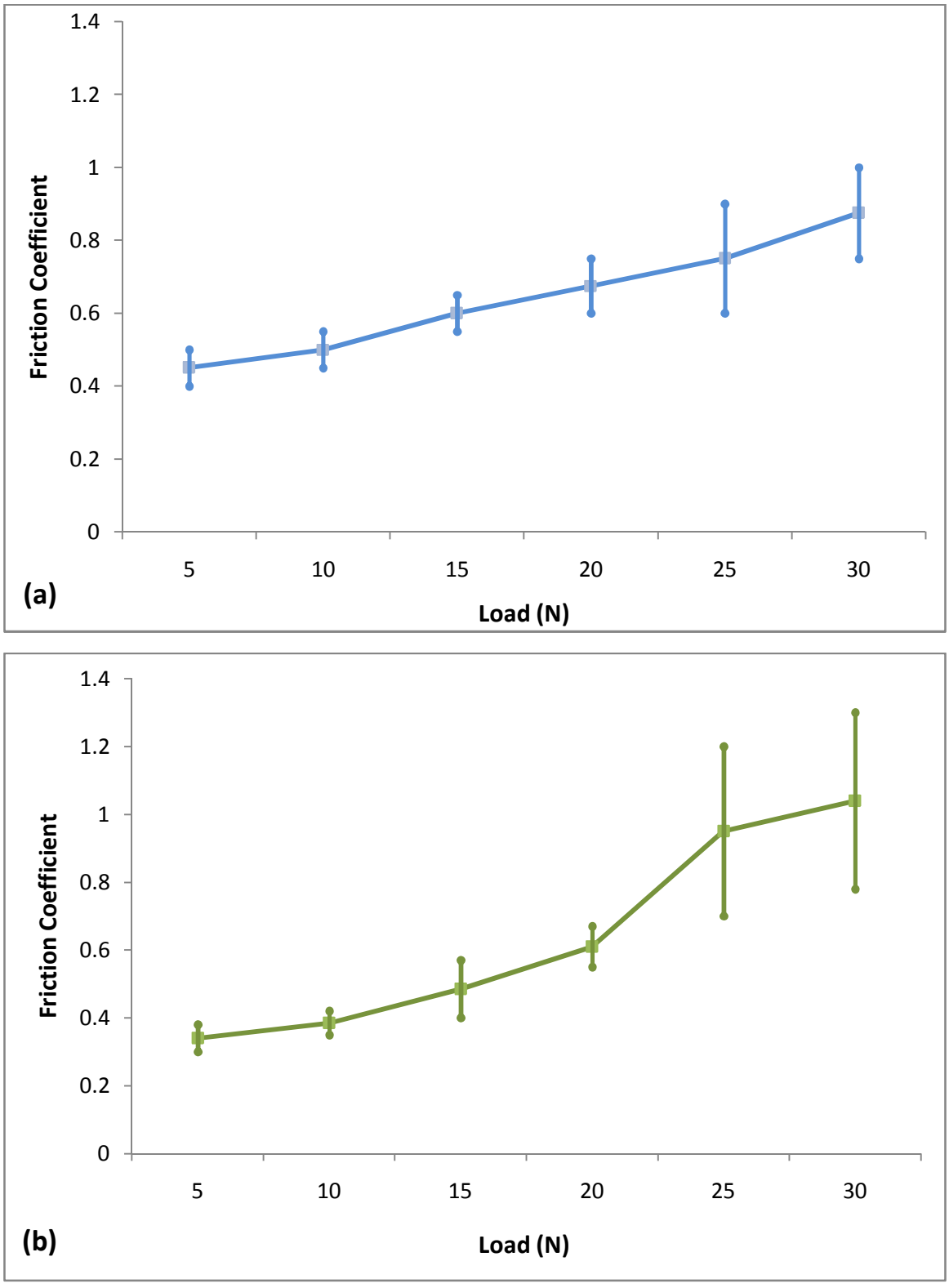

Fig 4.16 Friction Coefficient as a function of load for (a) monolithic Al6061 and (b) composite

4.9.3 SEM Analysis

Fig 4.17 (a) and (b) compares the worn surfaces of the monolithic Al6061 and the composite, respectively, at an applied load of 5 N. It is evident that abrasion is dominant for both the materials; however, the intensity is very much less in case of composite. Slight delamination can also be seen in monolithic Al6061 whereas the composite does not display any delamination and its surface is characterized by only minor scratches. This is due to greater hardness and strength imparted to the material by CNTs.

Fig 4.18 (a) and (b) compares the worn surfaces of the monolithic Al6061 and the composite, respectively, at an applied load of 15 N. Besides abrasion, considerable delamination can now be seen for monolithic Al6061. In case of the composite, partially delaminated large flakes can be seen along with crack initiation at few locations. The partially delaminated flakes could also be a sort of mechanically mixed layer. This will be confirmed later through EDS analysis.

Fig 4.19 (a) and (b) compares the worn surfaces of the monolithic Al6061 and the composite, respectively, at an applied load of 25 N. The monolithic Al6061 is characterized by severe delamination with some possible adhesion which will be confirmed through EDS analysis. As far as composite is considered, the surface is characterized by severe sub surface fracturing and deep pits. It seems that the cracks initiated at lower loads as a result of surface fatigue, grew and propagated freely at higher load which resulted in heavy delamination and hence very high wear rate for the composite. It is already shown that CNTs agglomeration at some locations resulted in about 3 % porosity in the composite. So these pores are the source of crack nucleation

and initiation inside the composite which caused excessive fracturing and formation of deep pits as a result of crack formation and propagation at higher loads. It can be clearly seen that at 30 N, the worn surface of monolithic Al6061 is characterized by smaller flakes. In contrast, the worn composite's surface is characterized by larger flakes. This proves that development & long distance propagation of cracks in case of composite remained dominant which resulted in the formation of larger flakes; the detachment of which caused very high wear rate for composite.

Fig 4.20 (a) and (b) show the SEM images of the worn specimens at a lower magnification of monolithic Al6061 and the composite, respectively, at an applied load of 30 N. The monolithic Al6061 is characterized by the formation of long and deep groove. Such groove could have formed due to continuous abrasion from a large fragment adhered to the counterface from the specimen due to softening. However, such grooves are not evident in case of the composite. The composite's surface is characterized by severe fracture and delamination, especially at the edges. This breaking of sharp edge during wear test at high loads may be attributed to increased brittleness imparted to composite by the CNTs.

Fig 4.21 (a) and (b) show the SEM images of the edges of the worn specimens shown in Fig 4.20 (a) and (b), respectively, at a higher magnification. The images clearly reveal the deep groove and severe fracture in monolithic Al6061 and the composite, respectively, which formed at the highest applied load of 30 N.

Fig 4.22 (a) and (b) show the morphology of wear debris for monolithic Al6061 and the composite, respectively, formed at 10 N. At a lower load of 10 N, the debris for both the

materials consist of small particles and flakes showing that abrasion occurred predominantly at lower loads. However, as the load was increased to 20 N, clear difference in debris morphology is observable, as shown in Fig 4.23. The monolithic Al6061 debris consist mainly of small delaminated flakes indicating transition from abrasive to delamination wear. In contrast, at 20 N, the composite debris consists mainly of large delaminated flakes indicating excessive surface fracturing and delamination. This was expected as the wear rate and intensity of composite is considerably high as compared to monolithic when the load was increased to 20 N. At maximum applied load of 30 N, as shown in Fig 4.24, the debris of monolithic Al6061 consists mainly of large delaminated flakes indicating that the wear mechanism is now mainly delamination. In case of composite, at 30 N, the debris contains much larger delaminated flakes which clearly shows long distance crack propagation on worn surfaces and subsequent fracturing and detachment of material in the form of larger flakes.

The SEM results are in very much accordance to the wear rates shown in Fig 4.14. At a lower load of 5 N, abrasion is dominant for both the materials. However, this abrasion is very much less in case of composite due to its increased hardness and strength and hence its wear rate is less. At much higher load of 15 N, the composite continued to display better wear resistance than monolithic Al6061, however the surface of composite is characterized by some tiny cracks. These cracks may be attributed to increased brittleness of composite. As the load increased to much higher values of 25 and 30 N, these cracks propagated and caused excessive fracturing which resulted in very high wear rate for the composite. Such cracking and fracturing is not evident in case of monolithic Al6061 and its surface is characterized by mild delamination and possible adhesion. Such big

difference in the wear mechanism of the two materials at high loads resulted in very high wear rate for the composite as compared to monolithic Al6061.

The SEM results of the worn surfaces can also be well compared with friction coefficient results discussed previously. For both the materials, the lower value of friction coefficient at lower loads corresponds to dominant abrasive wear without any considerable fracturing and delamination. As the load increased, delamination increased which not only increased the friction coefficient but also its fluctuation. At much higher loads of 25 N and 30 N, excessive fracturing of surface in case of composite combined with adhesion resulted in very high value of friction coefficient along with too much fluctuation evident in the form of sharp peaks in friction coefficient plot shown in Fig 4.15 (c). This high value and fluctuation of friction coefficient is also evident in case of monolithic Al6061, however, the intensity is much less as the wear is mainly characterized by mild delamination and possible adhesion.

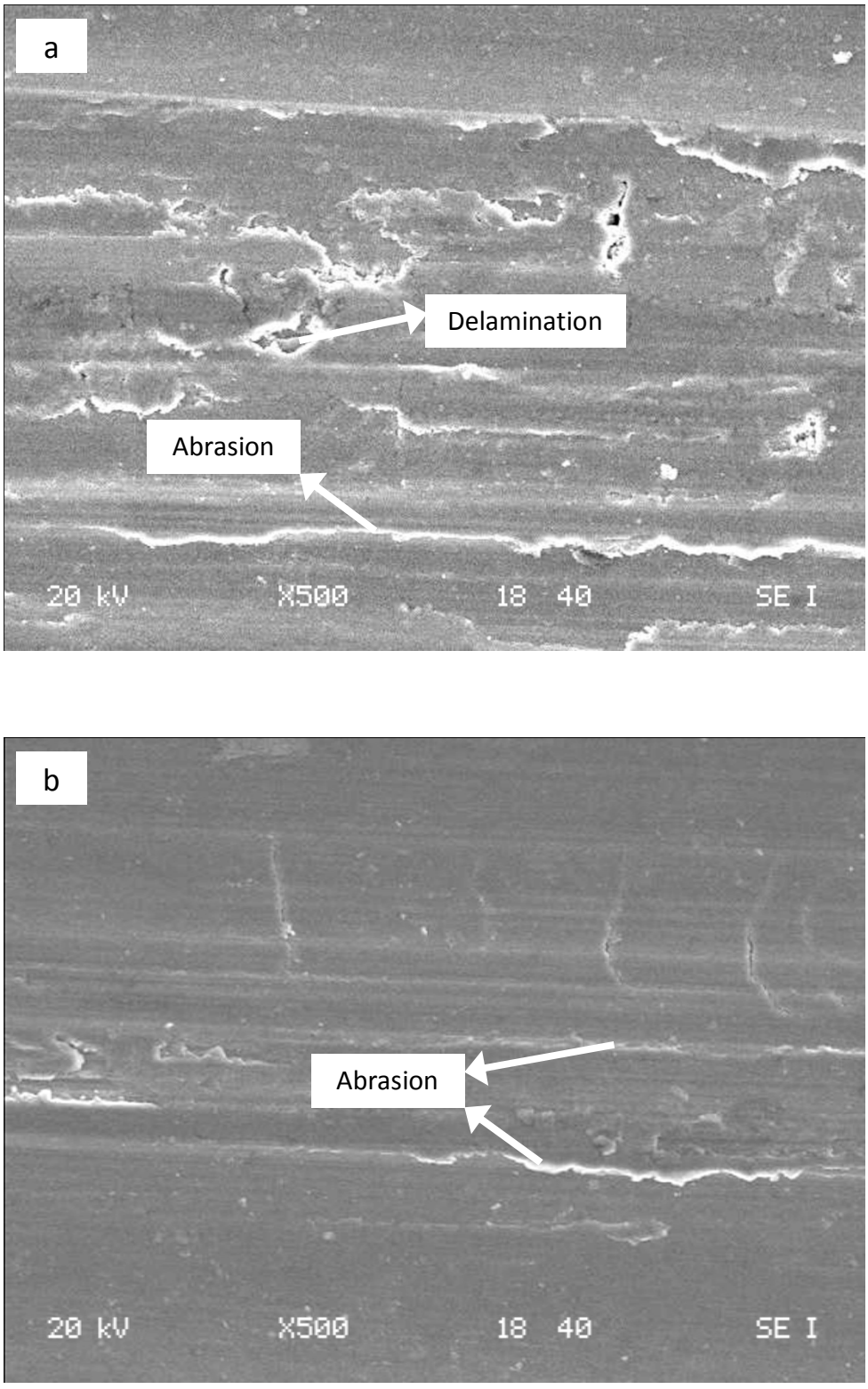

Fig 4.17 SEM micrographs of the worn surfaces at 5 N for (a) Al6061 and (b) composite

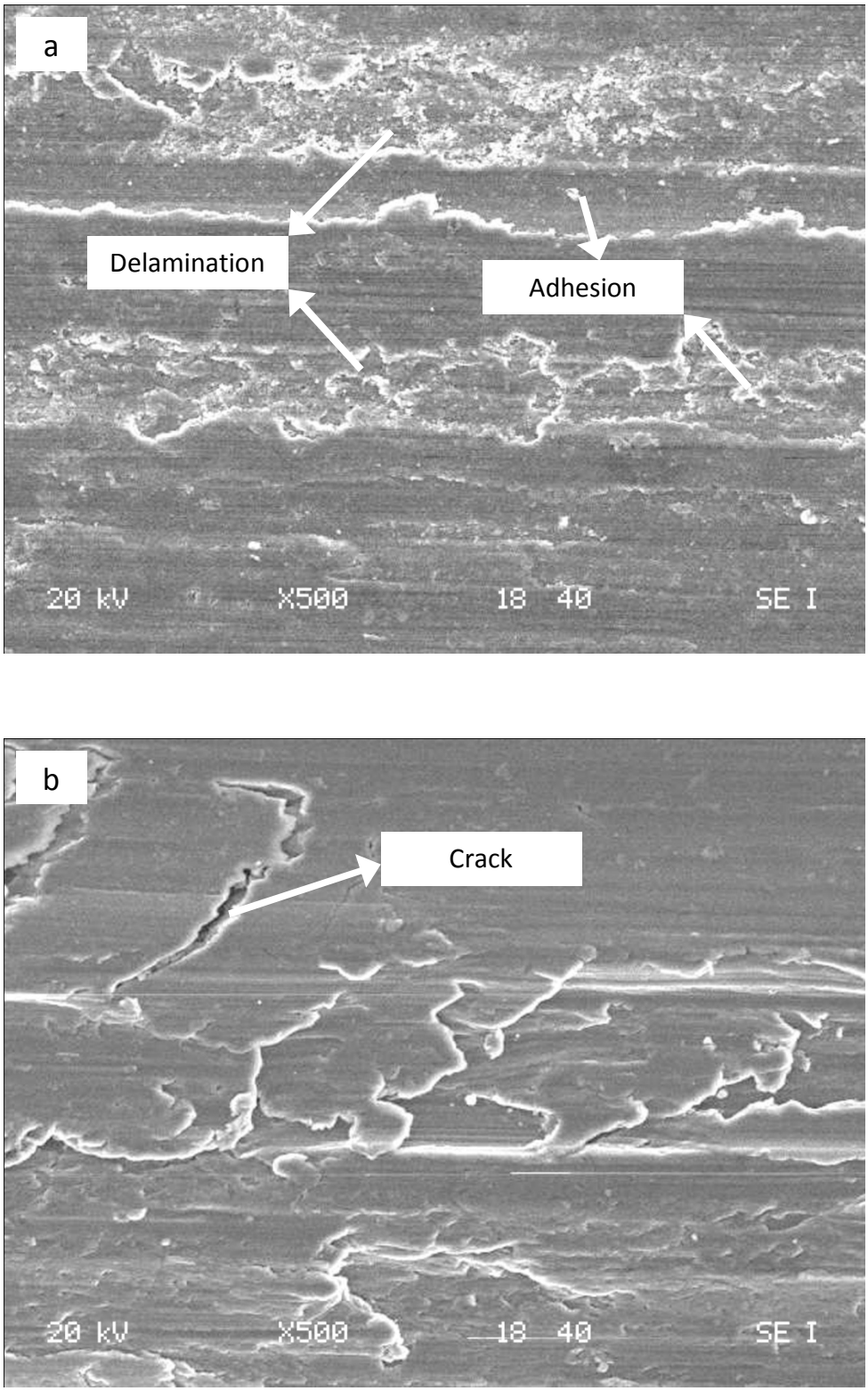

Fig 4.18 SEM micrographs of the worn surfaces at 15 N for (a) Al6061 and (b) composite

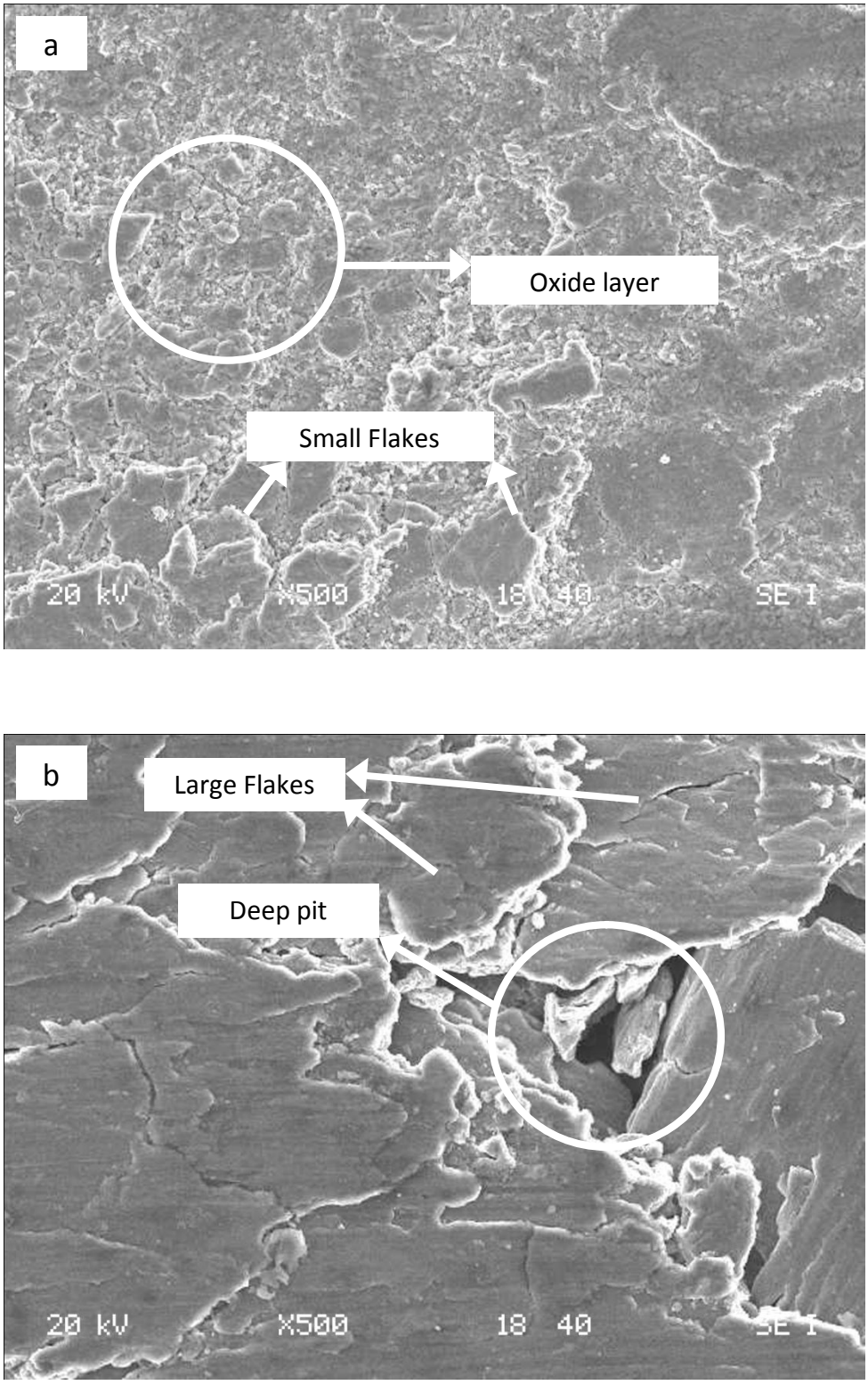

Fig 4.19 SEM micrographs of the worn surfaces at 25 N for (a) Al6061 and (b) composite

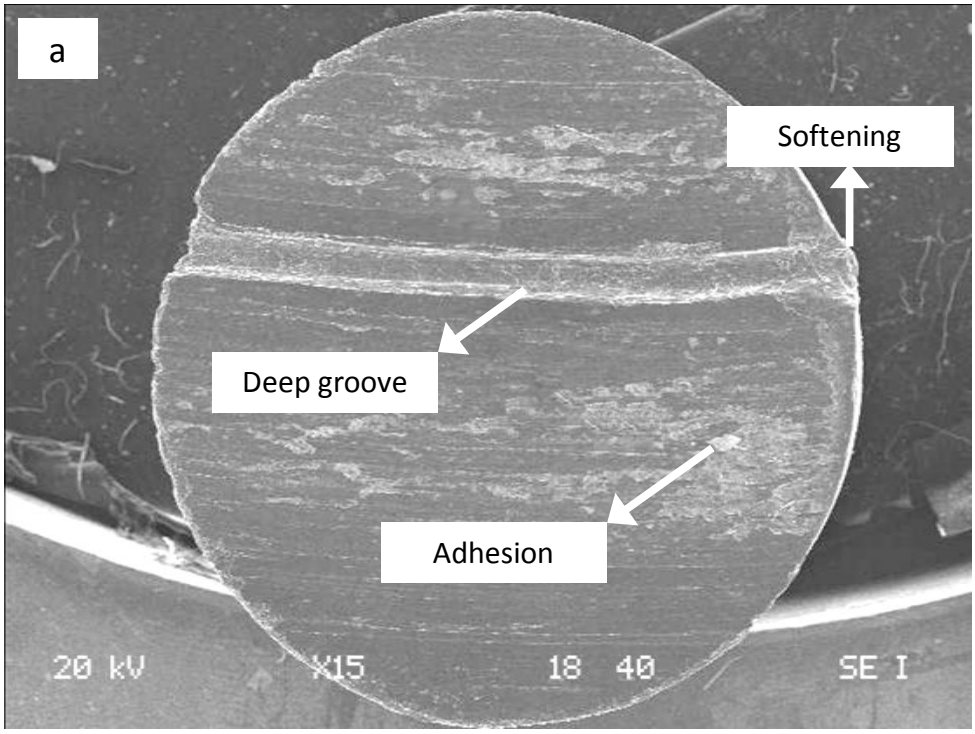

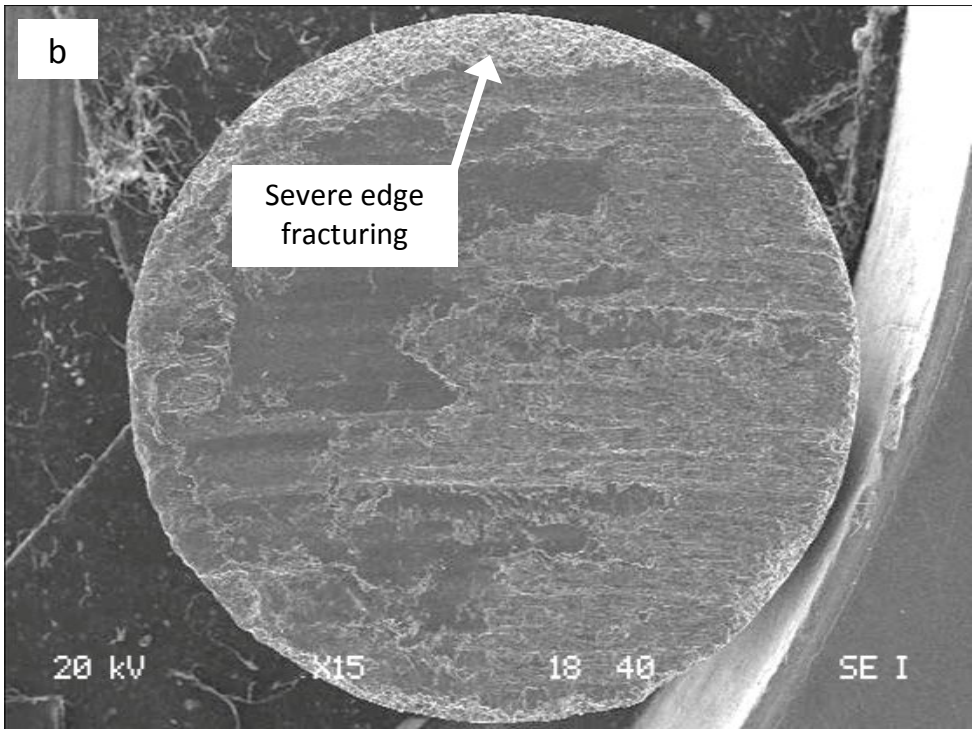

Fig 4.20 SEM micrographs of the worn surfaces at 30 N for (a) Al6061 and (b) composite

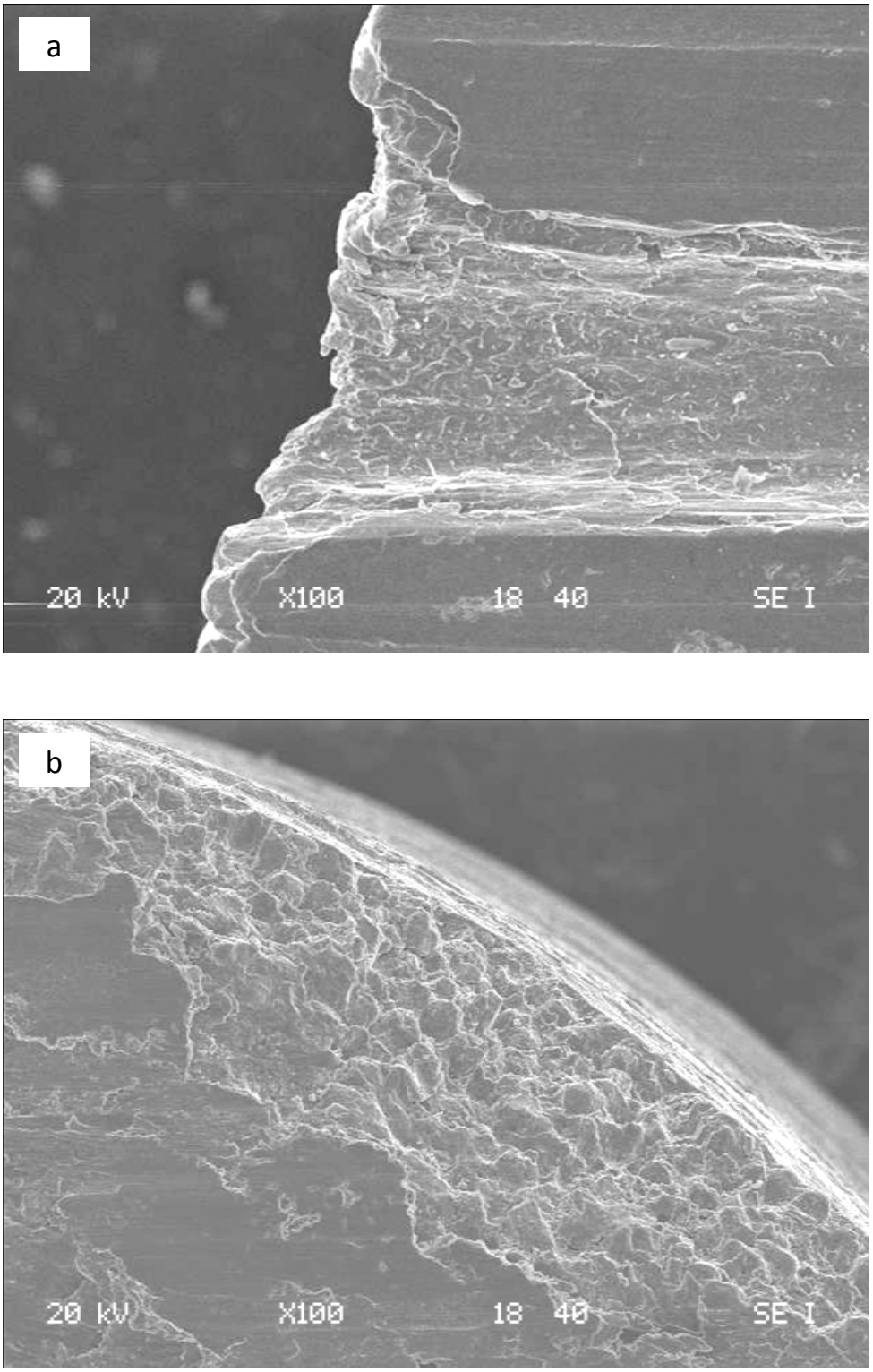

Fig 4.21 SEM micrographs of the edges of worn surfaces at 30 N for (a) Al6061 and (b) composite

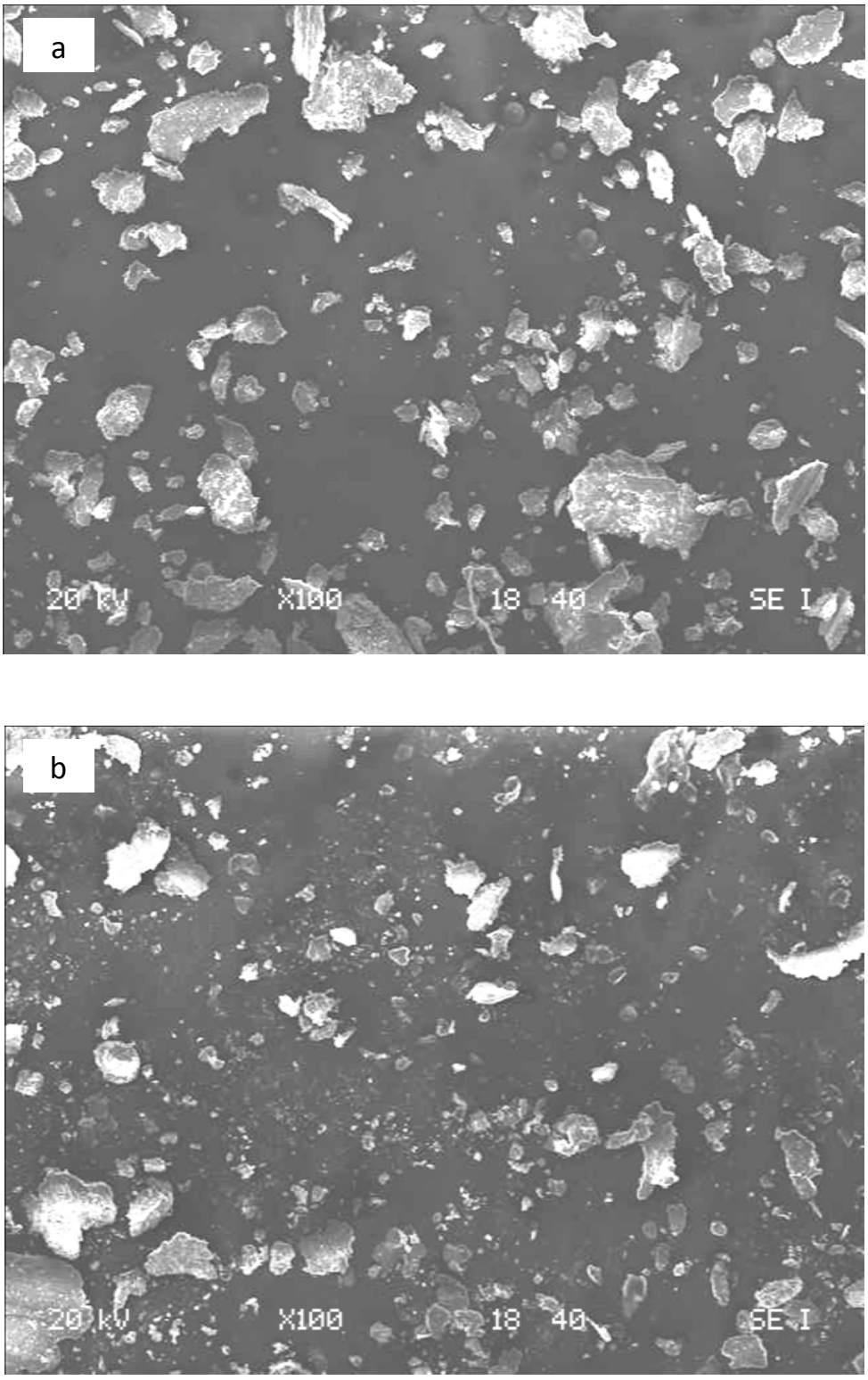

Fig 4.22 SEM micrographs of the debris formed at 10 N for (a) Al6061 and (b) composite

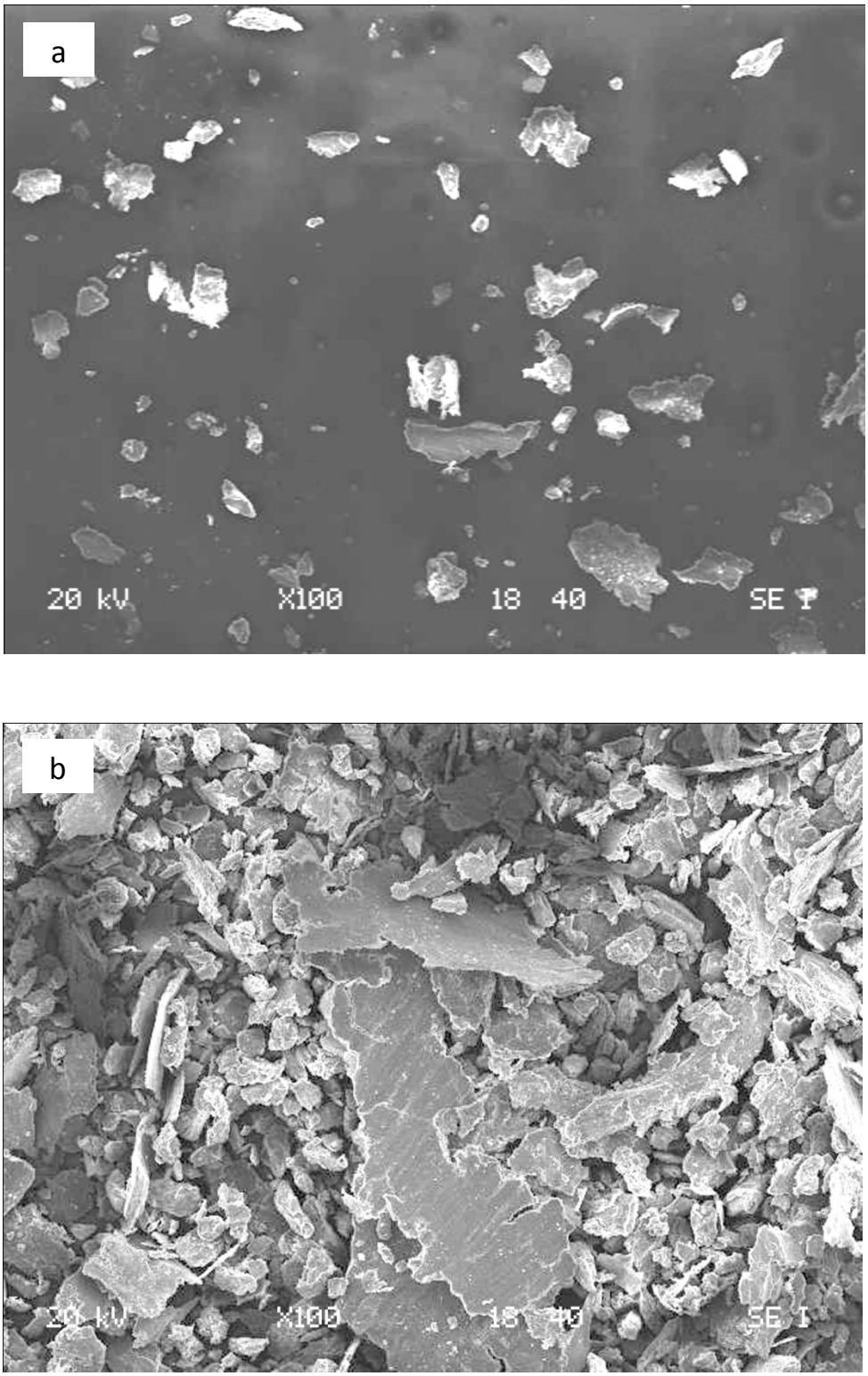

Fig 4.23 SEM micrographs of the debris formed at 20 N for (a) Al6061 and (b) composite

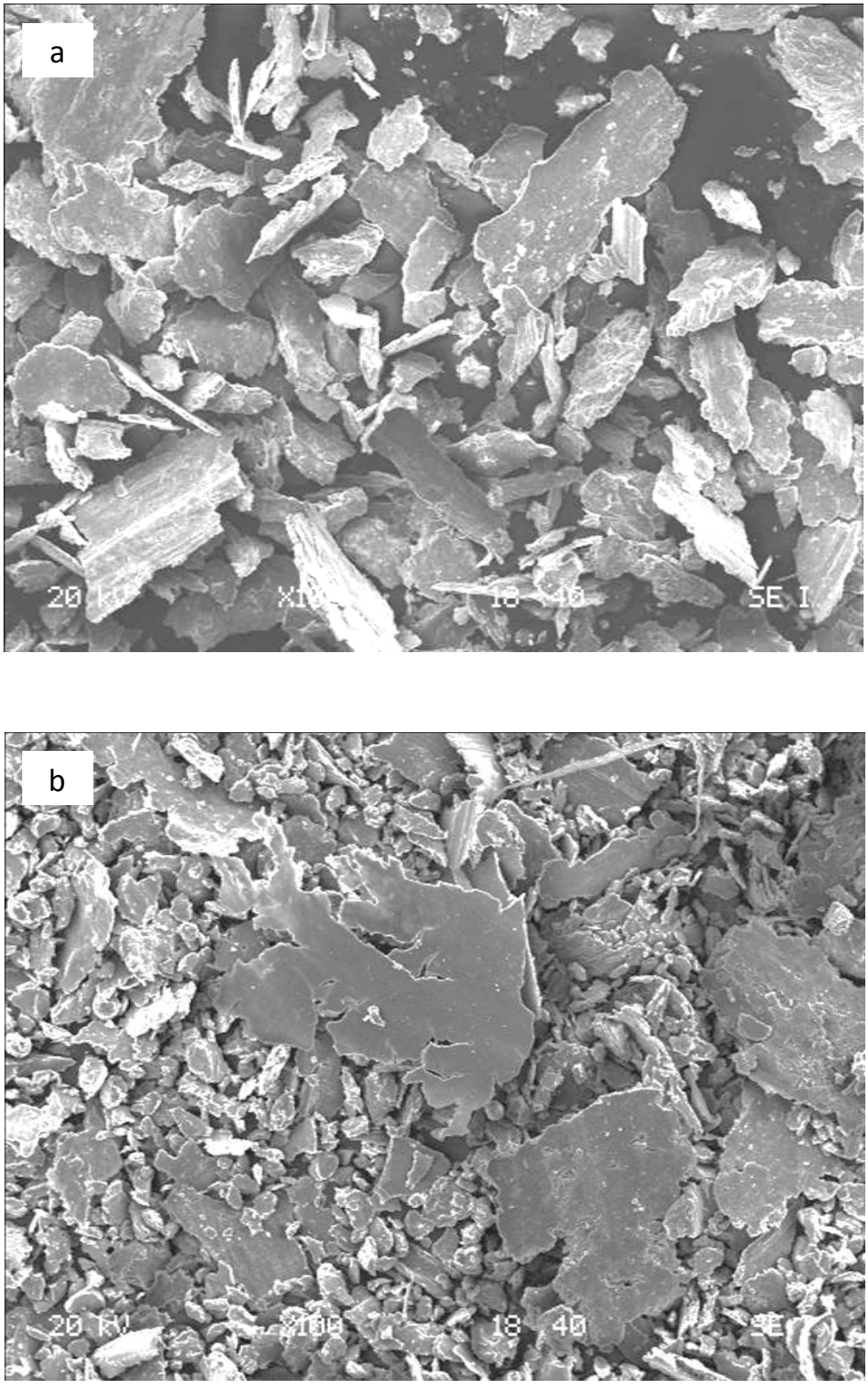

Fig 4.24 SEM micrographs of the debris formed at 30 N for (a) Al6061 and (b) composite

4.9.4 EDS Analysis

EDS analysis of the worn surfaces and the carefully collected debris was performed to determine the elemental composition and for further clarification of wear mechanisms. At the magnification of 100X, spectrums of three random square areas on the worn surface and on the debris were recorded to get an overall composition. This is shown in Fig 4.25. The reported values of elemental composition represent the average of the values obtained from these three spectra.

Fig 4.26 (a) and (b) show the EDS analysis of the worn out monolithic Al6061 and the composite pins, respectively, at varying loads. It can be seen that the monolithic Al6061 is characterized by considerable quantities of iron (Fe) and oxygen (O) revealing considerable oxidation wear with formation of Fe oxide layer during wear tests. The proportion of Fe increased significantly for higher loads showing excessive transfer of Fe on pin surfaces from the counterface disk. This is in agreement with the SEM results where tiny lumps where found on worn out monolithic Al6061 at higher loads. Thus, the major proportion of these tiny lumps is most probably composed of Fe or iron oxide. The Fe rich layer might have acted as a protective layer for monolithic Al6061 and thus caused lower wear rate as compared to the composite at higher loads. Considerable difference can be observed in case of the composite pins where negligible Fe was found especially at higher loads, as evident in Fig 4.22(b). Small proportion of Fe and O can, however, be found at lower loads showing small scale oxidation wear. For all the loads, the amount of other elements is quite low as compared to Al, especially at higher loads, where more than 90 percent of the surface is composed of Al. This shows that due to excessive fracturing and delamination in the composite at higher loads, stable Fe oxide

layer failed to form and if some oxide layer formed or some Fe adhered from the counterface, it failed to survive due to frequent fracturing and delamination of material from the pin surface.

Fig 4.27 (a) and (b) show the EDS analysis of the wear debris of monolithic Al6061 and the composite, respectively, at the loads of 10, 20 and 30 N. Again, it can be seen that the monolithic Al6061 debris contain significant amount of Fe and O whereas almost 70 percent of the composite debris is composed of Al. The EDS analysis results of debris are in good agreement with those of worn surfaces as both reveal almost similar compositional trend. These results show that, at higher loads, adhesion and oxidation are dominant wear mechanisms in case of monolithic Al6061 whereas excessive surface fracturing and delamination remains dominant in case of composite.

4.9.5 Microscopic Examination of Counterface

Fig 4.28 shows the microscopic images of the wear track formed on counterface disk at an applied load of 30 N. In case of monolithic Al6061, small lumps of Al were frequently observed on the track as shown in Fig 4.28 (a) which shows that adhesion of Al actively occurred from the pin to the counterface due to thermal softening of pin. In contrast, as evident from Fig 4.28 (b), no such lumps were found in case of composite which shows that adhesion from pin to the counterface didn't occur and severe sub-surface fracturing and delamination remained dominant in case of composite. To confirm that the lump shown in Fig 4.28 (a) is mainly composed of Al, few lumps were mechanically peeled off from the counterface & the EDS analysis of those lumps was carried out. Fig 4.29 (a) shows the SEM micrograph of the peeled off lump & Fig 4.29 (b) shows the EDS

analysis of this lump. As evident, the lump is mainly composed of Al and this confirms that the adhesion actively occurred from the pin on the counterface in case of monolithic Al6061. Significant proportion of Fe and O was also found in the lump which shows some transfer of Fe from counterface to pin as well as oxidation. It seems that during the initial and intermediate period of wear test, oxidation occurred on the specimen surface and as the test continued, the thermal softening of specimen resulted in the adhesion of some material to the counterface. These results are in good agreement with EDS results of worn out specimens and debris of monolithic Al6061 where significant proportion of Fe and O were observed.

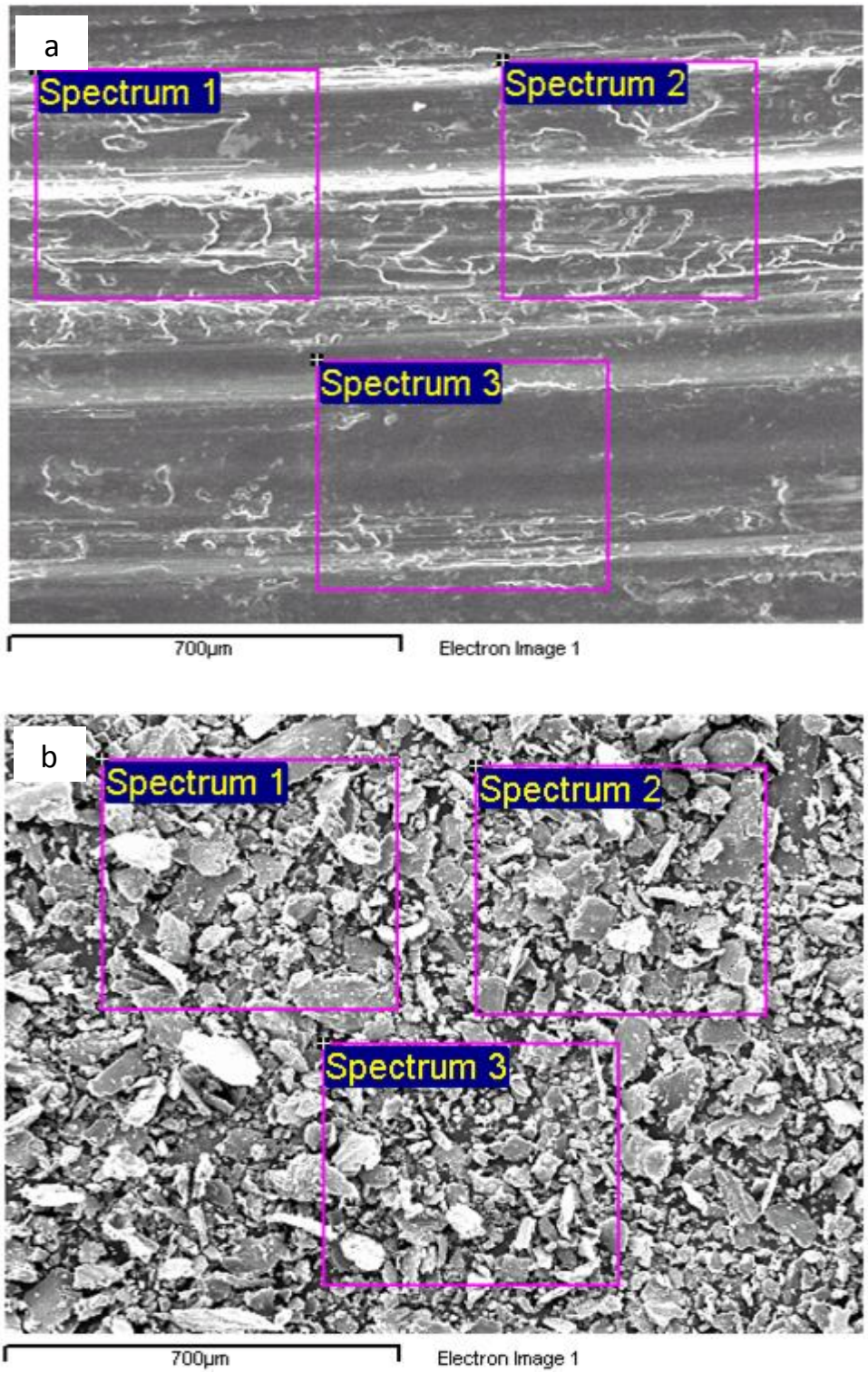

Fig 4.25 EDS analysis of worn surface done by recording 3 spectrums at random areas on (a) worn surface and (b) debris

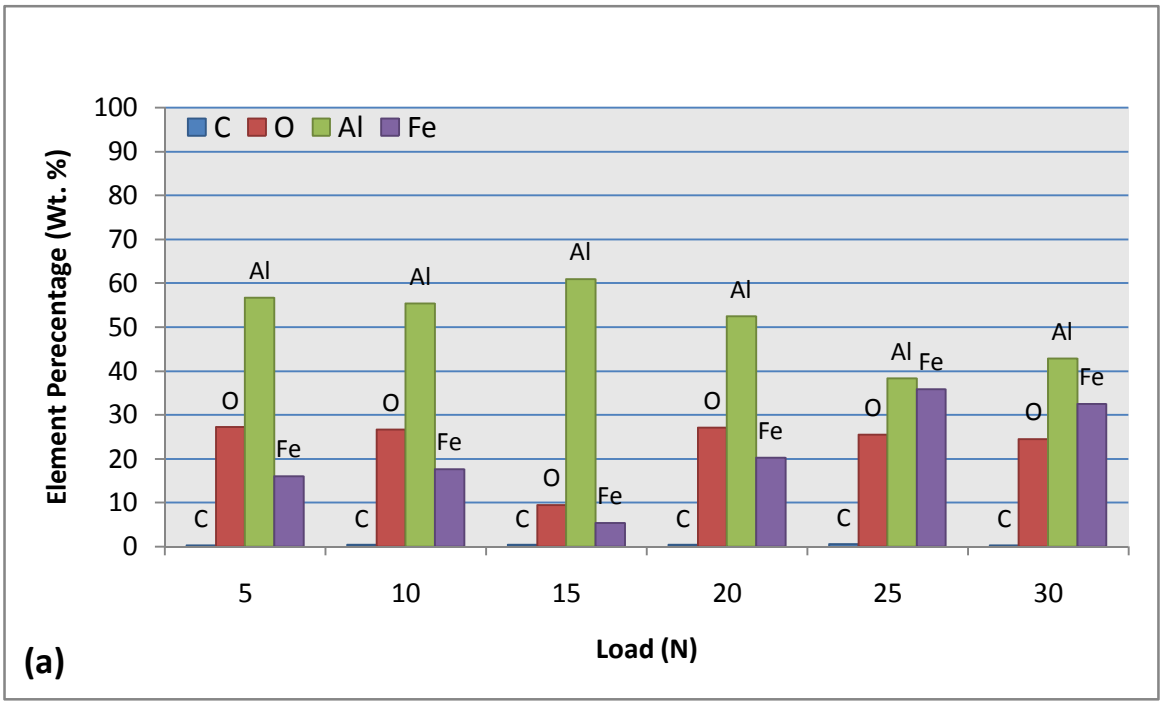

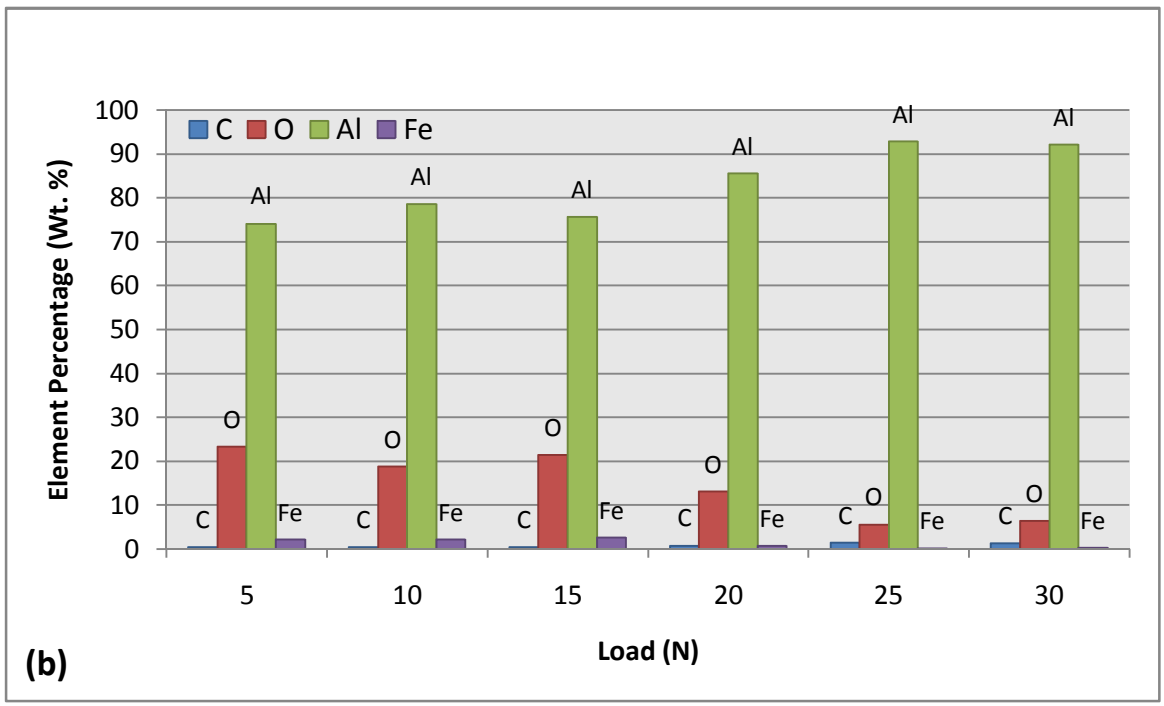

Fig 4.26 EDS analysis of worn surfaces of (a) monolithic Al6061 and (b) composite

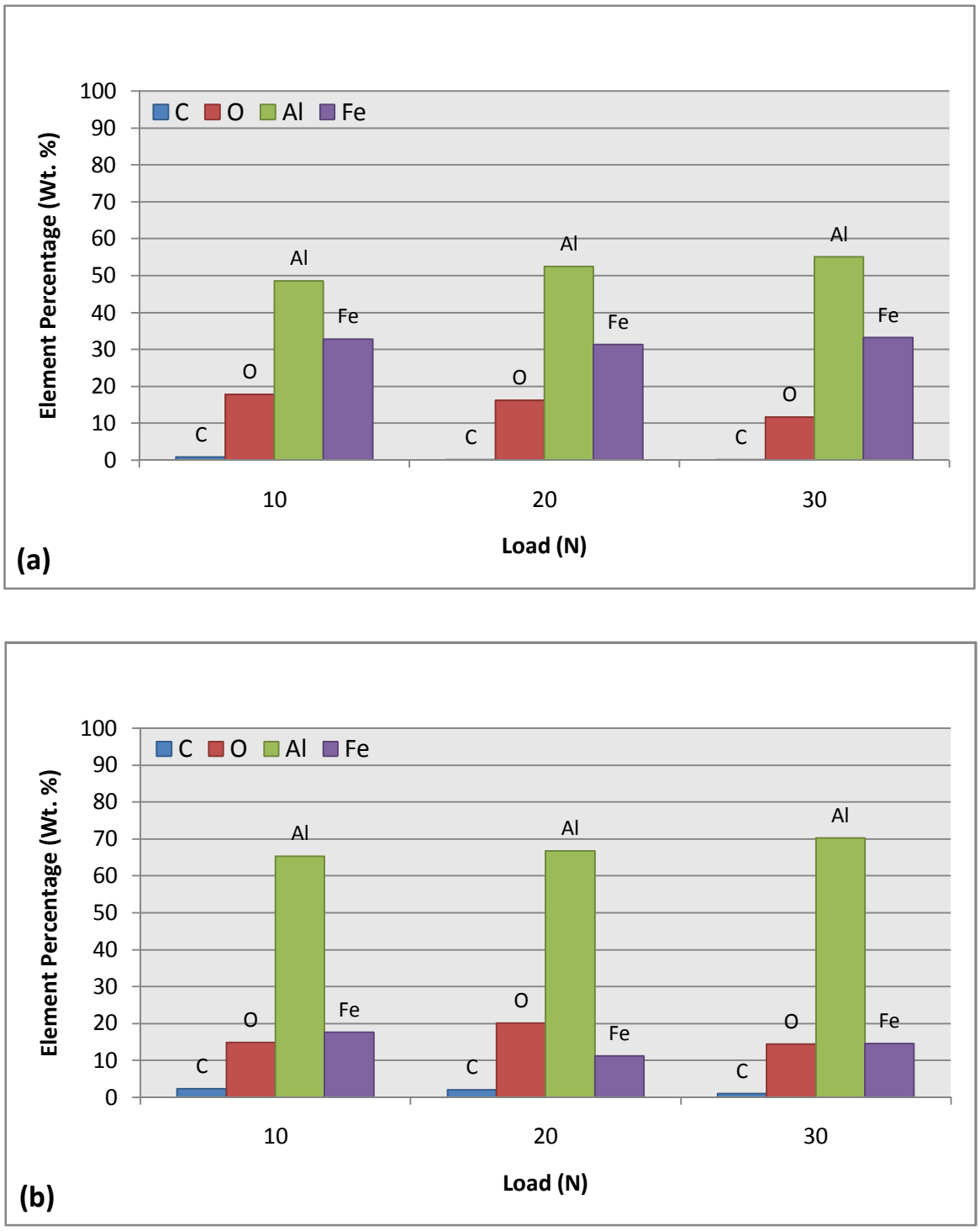

Fig 4.27 EDS analysis of wear debris of (a) monolithic Al6061 and (b) composite

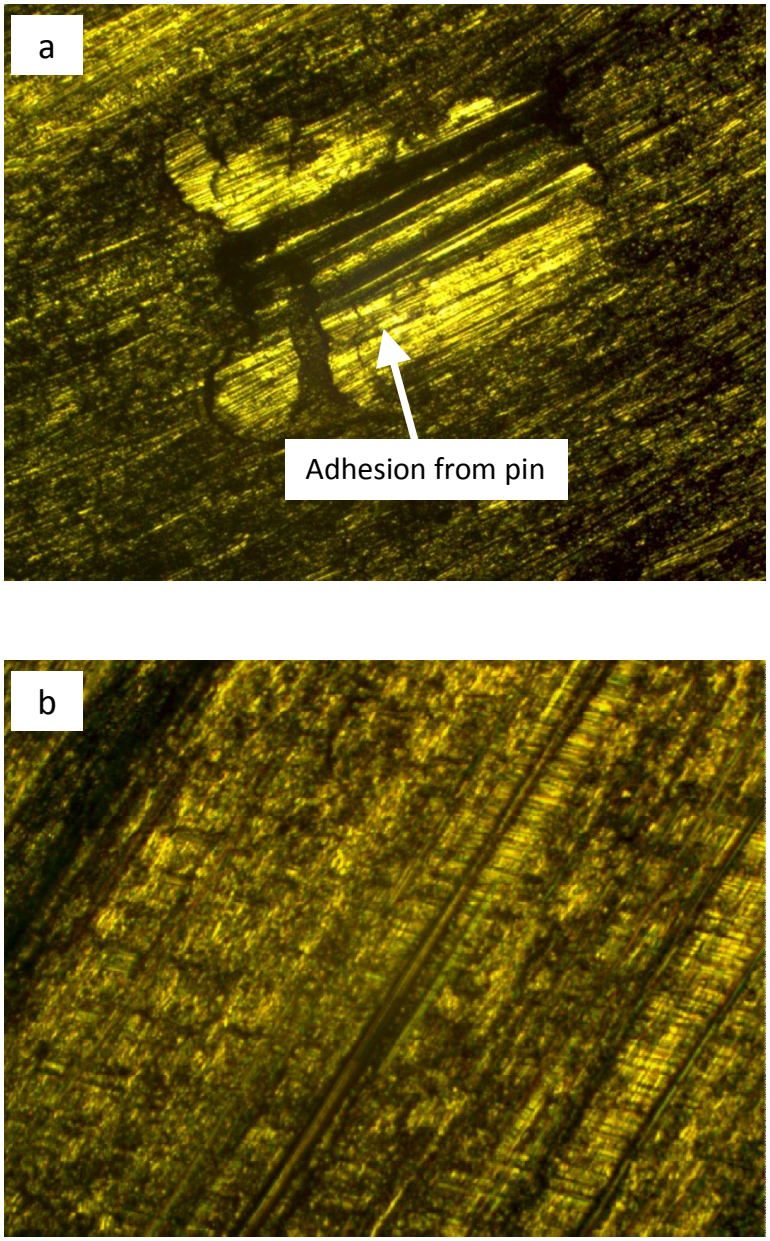

Fig 4.28 Microscopic images of counterface disk at an applied load of 30 N for (a) monolithic Al6061 and (b) composite

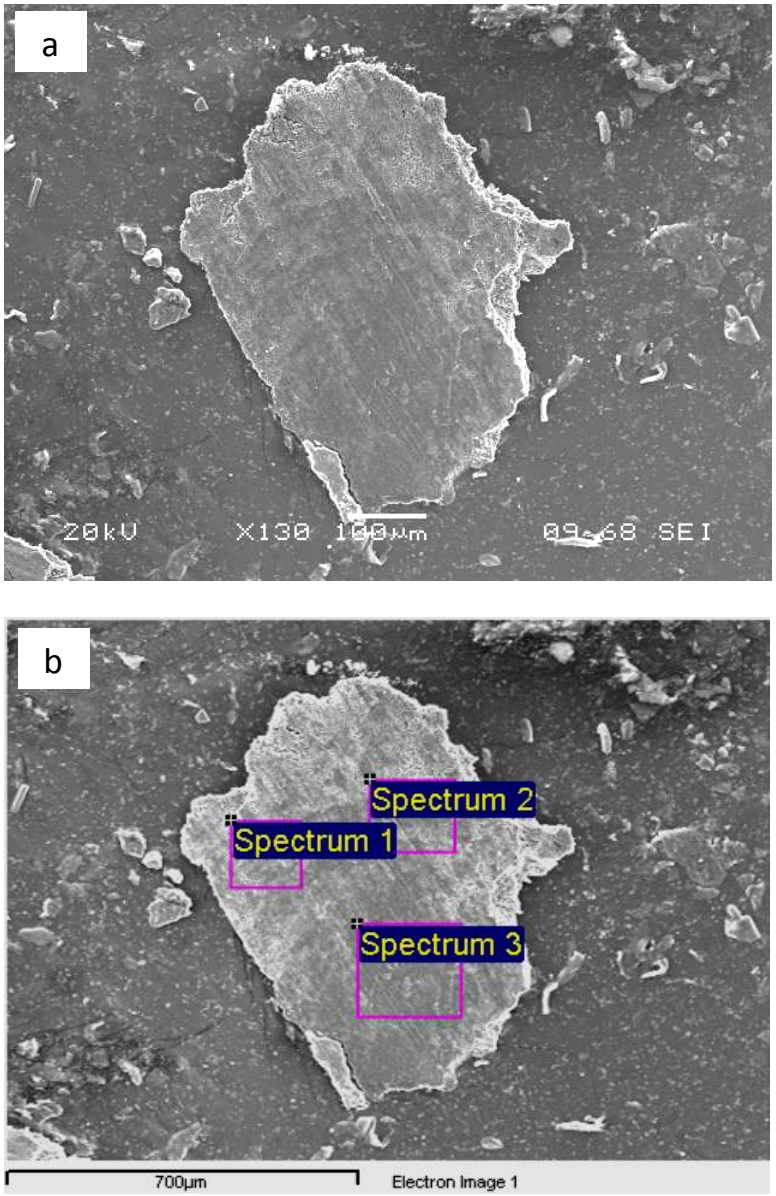

Spectrum	C	O	Al	Fe	Total
Spectrum 1	0.31	23.66	51.21	24.82	100.00
Spectrum 2	0.37	22.19	51.71	25.74	100.00
Spectrum 3	0.00	17.93	64.98	17.09	100.00

All results in Weight Percent

Fig 4.29 (a) SEM image and (b) EDS analysis of the peeled off lump from counterface in case of monolithic Al6061 pin at 30 N

CHAPTER 5

DISCUSSION

5.1 Synthesis of Al-CNT Nanocomposite

The most important aspect in the development of Al-CNT nanocomposite, as mentioned earlier, is the uniform distribution of CNTs inside the Al matrix. The SEM micrographs of composite powder reveals fairly uniform distribution and it was observed that most of the CNTs penetrated into the matrix particles which is desirable for effective resistance to dislocation movement. At the same time, the agglomeration of CNTs was not found to be significant except at few locations, which is undesirable due to very high surface energy of CNTs. This issue of CNT clustering/agglomeration is being constantly observed, especially for its higher proportions [2,3,6,12-14,65] which is not only responsible for poor densification and mechanical properties of the material but also the source of considerable discrepancy between the theoretically predicted and experimentally observed mechanical properties of the composite [8]. The uniform distribution of CNTs reflects the efficiency and effectiveness of the combination of sonication and ball milling; the two way dispersion route followed in the present work.

Researchers have also reported the formation of aluminum carbide [2,13] in case of higher percentage of CNTs which is another source of weakness inside the material. However, the problem of aluminum carbide formation is observed less commonly and is not a major concern as it can be controlled by processing parameters such as temperature

or by providing any suitable coating on CNTs. In the present work, the formation of aluminum carbide was not observed during all the processing stages of nanocomposite, as evident from XRD and DSC results presented in section 4.5 and 4.6.

As far as sintering method is concerned, it can be seen that only SPS resulted in proper densification of the monolith and the nanocomposite. Conventional sintering methods such as hot pressing [15] and furnace sintering [4] are not capable of properly densifying these nanocomposites as these methods provide less instantaneous interfacial energy between particles for bonding. Thus the ultimate result is poor densification and mechanical properties of the composite. Field assisted consolidation methods which are capable of providing high instantaneous energy such as SPS, which is also used in the present work, have been proved more suitable for sintering these nanocomposites [2,9,14,66]. These advance sintering methods do not only densify the nanocomposite to maximum extent, but also retain the microstructure of matrix particles due to minimum grain growth.

As far as CNT content is concerned, it can be seen that hardness increased linearly up till 1 wt. %. However, sharp decrease was observed as the content was increased to 2 wt. %. This may be closely attributed to higher CNT agglomeration for higher CNT content. Kim et al. [2] also observed that 1 wt. % CNT is best choice for Al for maximum hardness and wear resistance. It is to be noted that the sintering method used by Kim et al. is exactly the same as the one used in the present work i.e. SPS.

5.2 Wear Behavior

The results show that addition of 1 wt. % CNTs improves wear resistance of Al6061 alloy at lower loads (or mild conditions) only. At higher loads (or extreme conditions), the pores developed in the composite as a consequence of CNTs agglomeration, serve as a source of crack nucleation and cause severe sub surface fragmentation resulting in poor wear resistance of composite as compared to monolith. Moreover, increased brittleness of the composite could be another reason for its severe fracturing under severe conditions. Lee et al. [16] have shown in detail that the wear resistance of the material fabricated by powder metallurgy is very sensitive to the presence of porosity. As the porosity increases, the wear rate increases as these pores serve as a source of crack nucleation and propagation resulting in excessive sub-surface fracturing. The transition load for the monolith and the composite was found to be considerably different in the present work. The composite transited to severe wear as the load was increased from 15 N to 20 N. However, the pure Al6061 displayed transition to severe wear when the load was increased from 25 N to 30 N. This behavior may be attributed to increased brittleness and reduced fracture toughness of the composite. Another important aspect is the better wear resistance of composite at lower loads only. Several studies [43,49,58] have also reported that Al MMCs display better wear resistance at low loads only and that there exists a transition load after which the reinforcement has negative effect on the wear resistance of the matrix. Wang et al. [43] studied the effect of adding 15 vol. % Ni_3Al on the wear resistance of Al 6092 alloy. It was found that up till 91 N, the composite displays better wear resistance, however as the load is increased to 140 N, the reverse holds true. At low load, the wear mechanism for the composite was mainly oxidation whereas for the

monolith, adhesion was dominant. For both the materials, a mechanically mixed layer (MML), consisting of Fe, Al and O, was observed on the contact surface. The thickness of MML was found to be much less for the composite, especially at 140 N where it was only 27 % for the composite as compared to 63 % for the monolith. Wang et al. suggested that this thick MML, having greater stiffness as compared to the rest of the material, is the main reason for better wear resistance of pure material as compared to composite at 140 N. Moreover, the fragmentation of brittle Ni_3Al particles led to excessive wear rate and hence poor wear resistance of composite at higher load.

Korkut [49] also reported a similar trend for Al2024\SiFe\Alumina composites. It was found that as the conditions switch from mild to severe, the composite starts displaying higher wear rates as compared to the pure material. No considerable difference was observed in the wear mechanism of the monolith and the composite. It was found that up till mild wear conditions, the worn surface and the debris of the composite are mainly composed of Fe_2O_3 showing that Fe_2O_3 layer serves as a protective layer for composite and hence improves its wear resistance. However as the conditions approach to severe wear, the alumina particles started to break and caused excessive surface fragmentation. The worn surface at severe conditions was mainly composed of Al showing failure of oxide layer stability due to excessive breaking of alumina particles. Hence under the severe conditions, the composite displayed poor wear resistance as compared to monolith.

Sudarshan et al. [58] also reported similar trend while studying wear behavior of A 356 Al alloy reinforced with 6 and 12 vol. % fly ash particles. It was found that adhesion is dominant in case of monolith whereas abrasion was mainly observed in composites. The

composite reinforced with 6 vol. % fly ash particles displayed better wear resistance as compared to composite up till 20 N. At higher loads, opposite was true. However, the composite reinforced with 12 vol. % fly ash particles displayed better wear resistance from 20 N to 80 N. Sudarshan et al. suggested that particle fracture and damage occur in the matrix material if the fraction of fly ash particles on the contact area is small. The large plastic strains in the deformed layer give rise to void nucleation and subsurface crack propagation and in this process, eutectic silicon and fly ash particles play major role. The interface between the matrix and the particle provides preferential path for the growth of subsurface cracks. The crack finally reaches the contact surfaces and causes the delamination of subsurface layer. Hence, wear rates of lower volume fraction composite (6 vol. %) are higher. However, for larger volume fraction (12 vol. %) the sufficient proportion of fly ash particles at the interface suppresses this behavior and results in better wear resistance at higher load.

As far as present work is concerned, the porosity inside the composite seems to be the main reason for its poor wear resistance as compared to the monolith at higher loads. As long as the load remains below the critical value, CNTs continue to behave as efficient reinforcement and stable lubricant, resulting in lower wear rate and friction coefficient as compared to pure Al6061. However, as the load crosses the critical value, the role of CNTs does not remain effective due to excessive delamination caused by initiated cracks from the pores. These pores, formed mainly due to CNT agglomeration at few locations, can be considered as macroscopic defects inside the material which serve as nucleating sites for crack initiation and propagation. Another important reason could be the increased brittleness of composite as compared to pure Al6061. The monolith having

greater ductility, undergo some plastic deformation rather than complete fragmentation during the wear test. However, the composite, due to its increased brittleness, undergo severe fragmentation once the load crosses the ultimate value.

If we compare the present work with the existing literature regarding wear resistance of Al-CNT nanocomposites, we can compare various parameters except the optimum percentage of CNTs as we experimented with only one composition i.e. 1 wt. %. All the studies, however, do discuss about optimum percentage of CNTs for best wear resistance. Before we proceed with further discussion, it must be mentioned that the contact geometries used by Zhang et al. [1], Kim et al. [2] and Choi et al. [3] were such that the contact pressure cannot be determined, unlike in the present work where the contact pressure can be calculated as uniaxial load was applied on round cylindrical specimens. Thus the comparison of these three studies with the present work will have limited scope. The following sections compare different parameters of the present work with the above three studies.

5.2.1 Wear Rate

As far as wear rate is concerned, the first important aspect is that in the present work, the wear resistance of Al6061/CNT composite was found to be better than the monolithic Al6061 at lower loads only. Such behavior was, however, not reported previously for Al/CNT nanocomposite. Zhang et al. observed marginal improvement in wear resistance of Al-CNT composites. The wear rate of monolithic Al was found to be about 0.0135 mg/m which reduced to a minimum value of around 0.01 mg/m for 20 vol. % CNTs. Kim

et al. also observed only slight decrease in wear rate for Al/CNT composites. The wear rate of monolithic Al was found to be around 11.5 mg which reduced to a minimum value of about 9.5 mg for 1 wt. % CNTs. It is to be noted that in present work, the improvement in wear rate upon CNT addition at lower loads is significantly high. This can be attributed to high densification of nanocomposite (97 % approx.) in the present work. Zhang et al. and Kim et al. however did not report the density of the Al/CNT nanocomposite which might be relatively low. Also, if we look at the work of Choi et al., considerable improvement in wear resistance was observed on addition of CNTs. The wear rate of monolithic Al was found to be around 75 mg which reduced to almost 35 mg for 4.5 vol. % CNTs. Choi et al. also obtained very high densification of around 97 % for the nanocomposite. This gives us an idea that like other materials fabricated through powder metallurgy, densification of Al nanocomposites is also a key parameter for better wear resistance. Choi et al. [3] also observed that wear rate increased linearly with applied load at constant speed which is in accordance with the results of the present work.

Generally, the Al6061 alloy is used with a T6 treatment which induces stable strengthening phases inside the material. These phases enhance the mechanical properties of Al6061 alloy to considerable extent by impeding the dislocation movement. Also, it has been shown that particulate based Al6061 composites exhibit much better wear resistance when they are T6 treated [21,26,35]. Similarly, it has been shown that transition load for Al6061 composites sliding against 4140 steel can be enhanced by 30 percent if a suitable heat treatment is applied to the composites [39]. In the present work, however, the Al6061 alloy and its CNT based composite were used without any heat treatment. It is possible that the wear resistance of the Al6061-CNT composite becomes

much better if it is properly heat treated. However, the precipitation of strengthening phases in the presence of nanoparticles such as CNTs, must be first studied carefully.

It has been shown elsewhere [56] that wear resistance of extruded Al6061 composites is much better as compared to unextruded ones. Since extrusion causes strain hardening of the material and improves the reinforcement coherence with the matrix, it is understandable that why extrusion improves the wear resistance of the composite. In the present work, the pure Al6061 and its CNT based composed was tested in a sintered state without any post extrusion. Hence, the pure Al6061 and its CNT based composite may exhibit better wear resistance if extrusion is added after the sintering process. The extrusion is also expected to improve the alignment of CNTs inside the Al6061 matrix.

5.2.2 Friction Coefficient

Zhang et al. found very low friction coefficient, ranging between 0.11 and 0.15, for Al-CNT composites. These values are very small as compared to the values measured in the present work i.e. 0.35 to 0.45 under mild wear regimes. The possible reasons of such low value of friction coefficient may be most closely attributed to the fabrication technique used by Zhang et al. i.e. pressureless infiltration, which involved spontaneous infiltration of a molten Al alloy into CNTs–Mg–Al performs. Such method will result in high concentration of uniformly distributed CNTs on the specimen surface which caused stable lubricating action of CNTs during wear tests and hence low value of friction coefficient. Moreover, the CNT content used was considerably high as compared to the present work. As far as the work of Kim et al. [2] is concerned, the value of friction in case of 1 wt. % CNTs was found to be as high as 0.61 compared to only about 0.35 found

in the present work for the same CNT content and almost same applied load of 5 N. It is to be noted that the fabrication method of Kim et al. and the one used in the present work is exactly same i.e. SPS. However, the sliding speed used was only 0.02 m/s compared to 0.5 m/s used in the present work. Such low value of sliding speed possibly resulted in very high friction coefficient, even at very low load. Decrease in friction coefficient with increasing sliding speed is common due to various reasons and such trend has been reported elsewhere [44,51]. Choi et al. [3] observed extremely low coefficient of friction, in the range 0.025 to 0.1, for Al-CNT composite containing 4.5 vol. % CNTs. Although the sliding speed of 0.12 m/s was used, which is relatively low as compared to that used in the present work, the type of wear test used was very different i.e. ball-on-disk type, in which alumina balls acted as counterface. Also, the amount of CNTs used was considerably high as compared to the present work. However, the trend for the friction coefficient observed by Choi et al. is same as observed in the present study i.e. it increased linearly with applied load at constant sliding speed.

It has been shown that materials with high yield stress to elastic modulus ratio (Y/E) exhibit lower friction coefficient and wear rate as compared to those with lower Y/E value [3]. As presented earlier in Table 4.2, the composite has much lower value of Y/E as compared to pure Al6061. However, the friction coefficient and the wear rate for the composite were found to be higher than that of pure Al6061 only in case of higher loads. Whereas at lower load, reverse trend was observed.

5.2.3 Wear Mechanism

The SEM and EDS analyses of worn surfaces and the debris revealed mixed modes of wear mechanism. However, the intensity of each type of wear was found to be both material and load dependent. As far as monolithic Al6061 is concerned, significant proportion of Fe and O in both the pin as well as debris reveal that transfer of Fe from the counterface to the specimen occurred actively and then subsequent oxidation of specimen surface, especially at higher loads. The formation of thick mechanically mixed layer comprising of aluminum oxide and iron oxide on Al6061 specimens sliding against steel counterface has been shown elsewhere [44] and this layer is considered as a protective layer causing lower rate of the material. Also, adhesive wear was found to be equally dominant for pure Al6061 specimens. Yang [34] has also shown that adhesion is the main wear mechanism for Al6061 specimens sliding against steel counterface, especially at higher loads and speeds. Ramesh et al. [54] have also proposed the formation of a stable tribolayer comprising of different oxides in case of Al6061 specimens sliding against steel. They proposed that this tribolayer could develop on the specimen's as well as counterface surface which avoids direct contact of the specimen with the steel causing lower wear rate of the specimen. However, the mechanism and sequence of this Fe transfer, formation of tribolayer and adhesion are not well understood. As far as composite is concerned, transfer of Fe from the counterface is negligible, especially at higher loads. However, the debris contained noticeable amount of Fe which shows that increased hardness of the composite caused significant abrasive action on the counterface disk resulting in the removal of some Fe particles from the counterface. At lower loads, considerable amount of oxygen on the worn surfaces of the composite show formation of

stable oxide layer which might have contributed to better wear resistance of the composite at lower loads. However, at higher load, excessive fracturing and delamination in the composite due to porosity and increased brittleness, disabled the formation of any stable tribolayer and hence the worn surfaces were found to be mainly composed of aluminum whereas the debris was found to have significant proportion of Fe and O. Zhang et al. found oxidation as the main wear mechanism for Al-CNT composites. The formation of alumina layer on the composite and its subsequent delamination causing abrasion between the specimen and the counterface was proposed as the wear phenomenon for the composite. Zhang et al. performed all tests under a constant load and sliding speed with varying CNT content which could be the possible reason for one specific wear mechanism. However, Kim et al. observed mixed abrasive and adhesive wear for Al-CNT composites with varying CNT content and at fixed load and sliding speed. Oxidation wear was also observed, however it was minimal in case of 1 wt. % CNTs. Choi et al. observed microploughing and delamination as dominant wear modes for Al-CNT composites. At higher loads, more delamination was observed which resembles the results of the present work where delamination intensity sharply increased with increasing load for Al-CNT composites. The present results and the results presented in the literature are parallel to some extent, however, as already mentioned, due to vast difference in the CNT dispersion method, the composite fabrication method and the wear test parameters (speed and load), the comparison adds only a little value to the understanding of wear mechanisms in Al/CNT composites. The present work, however, clarifies that the friction and wear behavior of Al-CNT composites is largely influenced

by the applied load and there exists a critical stress value beyond which the CNTs could have a negative impact on the wear resistance of aluminum or its alloy.

CHAPTER 6

CONCLUSION AND FUTURE DIRECTIONS

Nearly uniform distribution of 0.5 to 2 wt. % Carbon Nanotubes (CNTs) inside Al6061 particulate matrix was achieved through 2-way dispersion method comprising of sonication followed by ball mixing. The powders consolidated by Spark Plasma Sintering (SPS) displayed good densification and hardness. However, the composite with 1 wt. % CNTs displayed best densification and hardness among all the CNT proportions used and was thus selected for subsequent characterization and wear tests.

The composite with 1 wt. % CNTs displayed fairly uniform distribution of CNTs with some porosity due to unavoidable CNT agglomeration at few locations. The XRD (X-Ray Diffraction) and DSC (Differential Scanning Calorimetry) analyses did not reveal any formation of Aluminum Carbide in the composite.

Wear tests conducted on the composite under pin on disk configuration at varying load and constant sliding speed showed that CNTs are effective reinforcements for Al6061 alloy at lower loads only as far as wear resistance is concerned. The composite displays better wear resistance at lower loads due to effective strengthening and lubricating action of CNTs. At higher loads, the porosity inside the composite, developed due to CNTs agglomeration, serves as a source of crack initiation and thus excessive surface fracturing and delamination results in poor wear resistance of composite as compared to the monolithic Al6061. Transition load for composite was found to be considerably lower as

compared to monolith revealing that CNTs have no advantage in terms of improving transition load. SEM and EDS analysis of worn out surfaces and debris revealed abrasion to be the main wear mode for both the monolith as well as composite at lower loads with the intensity being less in case of composite due to its better hardness. At higher loads, adhesion and oxidation were predominantly observed for monolith, whereas in composite, excessive subsurface damage in the form of fracturing and delamination was observed, resulting in poor wear resistance of composite as compared to monolith.

Although the present work adds some value regarding the understanding of friction and wear behavior of Al alloys reinforced with CNTs, there are plenty of other aspects which need to be addressed and analyzed in detail before the wear resistance of Al-CNT nanocomposites can be fully understood. We therefore highlight some of the beneficial future directions and work related to present research which may prove helpful in conceptualizing the wear behavior of Al-CNT nanocomposites:

- In the present work, ball milling was used only for improving the distribution of CNTs across the Al6061 matrix and that is why lower RPM and shorter duration was employed in ball milling. The intensity and duration of ball milling can be increased to study the effect of crystallite size and the contribution of CNTs on the wear behavior of Al6061 alloy.
- The present experimentation was carried out under dry conditions and also the literature available does not discuss the effect of any lubricant on wear resistance of Al-CNT composites. Therefore, it is suggested to use similar materials and test parameters under lubricated conditions by selecting any suitable lubricant.

- Wear tests could be done at higher temperatures, unlike the room temperature as used in the present work, to have an understanding of these composites at higher temperatures.
- Wear tests could be conducted at constant load and varying sliding speeds, as opposed to the present work, to see how the wear behavior is affected for the monolith and the composite under varying speeds.
- Relatively soft counterface material such as AISI 1010 steel, as opposed to very hard AISI 4140 steel used in the present work, can be employed to see how the wear resistance of Al-CNT nanocomposites is affected by the counterface properties.

REFERENCES

[1] S. Zhou, X. Zhang, Z. Ding, C. Min, G. Xu, and W. Zhu, "Fabrication and tribological properties of carbon nanotubes reinforced Al composites prepared by pressureless infiltration technique," *Compos Part A-Appl S*, vol. 38, Feb. 2007, pp. 301-306.

[2] I.-Y. Kim, J.-H. Lee, G.-S. Lee, S.-H. Baik, Y.-J. Kim, and Y.-Z. Lee, "Friction and wear characteristics of the carbon nanotube – aluminum composites with different manufacturing conditions," *Wear*, vol. 267, 2009, pp. 593-598.

[3] H.J. Choi, S.M. Lee, and D.H. Bae, "Wear characteristic of aluminum-based composites containing multi-walled carbon nanotubes," *Wear*, vol. 270, 2010, pp. 12-18.

[4] T. Noguchi, A. Magario, S. Fukazawa, S. Shimizu, J. Beppu, and M. Seki, "Carbon nanotube aluminium composites with uniform dispersion," *Materials Transactions*, vol. 45, 2004, pp. 602-604.

[5] C. Deng, X. Zhang, D. Wang, Q. Lin, and A. Li, "Preparation and characterization of carbon nanotubes/aluminum matrix composites," *Materials Letters*, vol. 61, Apr. 2007, pp. 1725-1728.

[6] C. Deng, D. Wang, X. Zhang, and A. Li, "Processing and properties of carbon nanotubes reinforced aluminum composites," *Materials Science and Engineering: A*, vol. 444, Jan. 2007, pp. 138-145.

[7] K. Morsi, a M.K. Esawi, P. Borah, S. Lanka, and a Sayed, "Characterization and Spark Plasma Sintering of Mechanically Milled Aluminum-Carbon Nanotube (CNT) Composite Powders," *Journal of Composite Materials*, vol. 44, Feb. 2010, pp. 1991-2003.

[8] T. Laha, Y. Chen, D. Lahiri, and A. Agarwal, "Tensile properties of carbon nanotube reinforced aluminum nanocomposite fabricated by plasma spray forming," *Composites Part A: Applied Science and Manufacturing*, vol. 40, May. 2009, pp. 589-594.

[9] H. Kwon, D. Hoon, J. François, and A. Kawasaki, "Investigation of carbon nanotube reinforced aluminum matrix composite materials," *Composites Science and Technology*, vol. 70, 2010, pp. 546-550.

[10] S. Iijima, "Helical microtubules of graphitic carbon," *Nature*, vol. 354, 1991, pp. 56-58.

[11] E.W. Wong, P.E. Sheehan, and C.M. Liebert, “Nanobeam mechanics: elasticity, strength, and toughness of nanorods and nanotubes,” *Science*, vol. 277, 1997, pp. 1971-1975.

[12] A. Esawi and M. Elborady, “Carbon nanotube-reinforced aluminium strips,” *Composites Science and Technology*, vol. 68, Feb. 2008, pp. 486-492.

[13] A.M.K. Esawi, K. Morsi, A. Sayed, M. Taher, and S. Lanka, “Effect of carbon nanotube (CNT) content on the mechanical properties of CNT-reinforced aluminium composites,” *Composites Science and Technology*, vol. 70, Dec. 2010, pp. 2237-2241.

[14] J.-zhi Liao, M.-J. Tan, and I. Sridhar, “Spark plasma sintered multi-wall carbon nanotube reinforced aluminum matrix composites,” *Materials & Design*, vol. 31, Jun. 2010, p. S96-S100.

[15] T. Kuzumaki, K. Miyazawa, H. Ichinose, and K. Ito, “Processing of Carbon Nanotube Reinforced Aluminum Composite,” *Journal of Materials Research*, vol. 13, Jan. 1998, pp. 2445-2449.

[16] H.-L. Lee, W.-H. Lu, and S.L.-I. Chan, “Abrasive wear of powder metallurgy Al alloy 6061-Sic composites,” *Wear*, vol. 159, 1992, pp. 223-231.

[17] S. Jacobson and N. Axen, “Transitions in the abrasive wear resistance of fibre- and particle- reinforced aluminium,” *Wear*, vol. 178, 1994, pp. 1-7.

[18] B. Venkataraman and G. Sundararajan, “Correlation between the characteristics of the mechanically mixed layer and wear behaviour of aluminium , Al-7075 alloy and Al-MMCs,” *Wear*, vol. 245, 2000, pp. 22-38.

[19] M. Takagi, H. Ohta, T. Imura, Y. Kawamura, and A. Inoue, “Wear Properties of nanocrystalline aluminum alloys and their composites,” *Wear*, vol. 44, 2001, pp. 2145-2148.

[20] E. Candan, H. Ahlatci, and H. Cimenoglu, “Abrasive wear behaviour of Al – SiC composites produced by pressure infiltration technique,” *Wear*, vol. 247, 2001, pp. 133-138.

[21] M.L.T. Guo and C.A. Tsao, “Tribological behavior of aluminum / SiC / nickel-coated graphite hybrid composites,” *Mater Sci Eng*, vol. A333, 2002, pp. 134- 145.

[22] Y. Sahin, “Wear behaviour of aluminium alloy and its composites reinforced by SiC particles using statistical analysis,” *Mater Des*, vol. 24, 2003, pp. 95-103.

[23] S. Won, U. Jong, S. Won, D. Keun, and K. Ogi, "Heat treatment and wear characteristics of Al / SiC p composites fabricated by duplex process," *Compos Part B-Eng*, vol. 34, 2003, pp. 737-745.

[24] M. Muratoglu and M. Izciler, "Wear behaviour of SiC reinforced 2124 Al alloy composite in RWAT system," *J Mater Process Tech*, vol. 132, 2003, pp. 67-72.

[25] S. Sawla and S. Das, "Combined effect of reinforcement and heat treatment on the two body abrasive wear of aluminum alloy and aluminum particle composites," *Wear*, vol. 257, 2004, pp. 555-561.

[26] J.M.G.D. Salazar and M.I. Barrena, "Influence of heat treatments on the wear behaviour of an AA6092 / SiC 25p composite," *Wear*, vol. 256, 2004, pp. 286-293.

[27] M. Murato and M. Aksoy, "Abrasive wear of 2124Al – SiC composites in the temperature range 20 – 200 ◦ C," *J Mater Process Tech*, vol. 174, 2006, pp. 272-276.

[28] D.P. Mondal and S. Das, "High stress abrasive wear behaviour of aluminium hard particle composites : Effect of experimental parameters , particle size and volume fraction," *Tribol Int*, vol. 39, 2006, pp. 470-478.

[29] R.N. Rao and S. Das, "Wear coefficient and reliability of sliding wear test procedure for high strength aluminium alloy and composite," *Mater Des*, vol. 31, 2010, pp. 3227-3233.

[30] R.N. Rao, S. Das, D.P. Mondal, and G. Dixit, "Effect of heat treatment on the sliding wear behaviour of aluminium alloy (Al – Zn – Mg) hard particle composite," *Tribol Int*, vol. 43, 2010, pp. 330-339.

[31] Y. Sahin, "Abrasive wear behaviour of SiC / 2014 aluminium composite," *Tribol Int*, vol. 43, 2010, pp. 939-943.

[32] S.K. Ghosh and P. Saha, "Crack and wear behavior of SiC particulate reinforced aluminium based metal matrix composite fabricated by direct metal laser sintering process," *Mater Des*, vol. 32, 2011, pp. 139-145.

[33] C.G. Cordovilla, J. Narciso, and E. Louis, "Abrasive wear resistance of aluminium alloy /ceramic particulate composites," *Wear*, vol. 192, 1996, pp. 170-177.

[34] L.J. Yang, "The transient and steady wear coefficients of A6061 aluminium alloy reinforced with alumina particles," *Compos Sci Technol*, vol. 63, 2003, pp. 575-583.

[35] L.J. Yang, "The effect of nominal specimen contact area on the wear coefficient of A6061 aluminium matrix composite reinforced with alumina particles," *Wear*, vol. 263, 2007, pp. 939-948.

[36] M.R. Rosenberger, E. Forlerer, and C.E. Schvezov, "Wear behavior of AA1060 reinforced with alumina under different loads," *Wear*, vol. 266, 2009, pp. 356-359.

[37] A.M. Al-Qutub, I.M. Allam, and T.W. Qureshi, "Effect of sub-micron A1203 concentration on dry wear properties of 6061 aluminum based composite," *Journal of Materials Processing Technology*, vol. 172, 2006, pp. 327-331.

[38] A.M.A. Qutub, I.M. Allam, and M.A.A. Samad, "Wear and friction of Al-A1203 composites at various sliding speeds," *Journal of Materials Science*, vol. 43, 2008, pp. 5797-5803.

[39] A.M. Al-Qutub, "Effect of heat treatment on friction and wear behavior of Al-6061 composite reinforced with 10 % submicron Al2O3 particles," *The Arabian Journal for Science and Engineering*, vol. 34, 2009, pp. 205-215.

[40] M.D. Bermúdez, G. Mart, I. Mart, and J.A. Rodr, "Dry and lubricated wear resistance of mechanically-alloyed aluminium-base sintered composites," *Wear*, vol. 248, 2001, pp. 178-186.

[41] A.R. Riahi and A.T. Alpas, "The role of tribo-layers on the sliding wear behavior of graphitic aluminum matrix composites," *Wear*, vol. 251, 2001, pp. 1396-1407.

[42] M. Singh, B.K. Prasad, D.P. Mondal, and A.K. Jha, "Dry sliding wear behaviour of an aluminium alloy – granite particle composite," *Tribol Int*, vol. 34, 2001, pp. 557-567.

[43] Y. Wang, W.M. Rainforth, H. Jones, and M. Lieblich, "Dry wear behaviour and its relation to microstructure of novel 6092 aluminium alloy – Ni 3 Al powder metallurgy composite," *Wear*, vol. 251, 2001, pp. 1421-1432.

[44] S.C. Sharma, "The sliding wear behavior of Al6061 – garnet particulate composites," *Wear*, vol. 249, 2001, pp. 1036-1045.

[45] J. Hemanth, "Wear behavior of chilled (metallic and non-metallic) aluminum alloy – glass particulate composite," *Mater Des*, vol. 23, 2002, pp. 479-487.

[46] J. Hemanth, "Fracture toughness and wear resistance of aluminum-boron particulate composites cast using metallic and non-metallic chills," *Materials and Design*, vol. 23, 2002, pp. 41-50.

[47] M.Y. Chen and M.C. Breslin, “Friction behavior of co-continuous alumina / aluminum composites with and without SiC reinforcement,” *Wear*, vol. 249, 2002, pp. 868-876.

[48] K.R. Suresh, H.B. Niranjan, P.M. Jebaraj, and M.P. Chowdiah, “Tensile and wear properties of aluminum composites,” *Wear*, vol. 255, 2003, pp. 638-642.

[49] M.H. Korkut, “Microstructure and wear behavior of Al2024 \ SiFe and Al2024\SiFe\Al2O3 composites,” *Tribol Int*, vol. 36, 2003, pp. 169-180.

[50] G. Abouelmagd, “Hot deformation and wear resistance of P / M aluminium metal matrix composites,” *Journal of Materials Processing Technology*, vol. 156, 2004, pp. 1395-1401.

[51] K.M. Shorowordi, A.S.M.A. Haseeb, and J.P. Celis, “Velocity effects on the wear , friction and tribochemistry of aluminum MMC sliding against phenolic brake pad,” *Wear*, vol. 256, 2004, pp. 1176-1181.

[52] V. Bhattacharya and K. Chattopadhyay, “Microstructure and wear behaviour of aluminium alloys containing embedded nanoscaled lead dispersoids,” *Acta Materialia*, vol. 52, 2004, pp. 2293-2304.

[53] S. Zhiqiang, Z. Di, and L. Guobin, “Evaluation of dry sliding wear behavior of silicon particles reinforced aluminum matrix composites,” *Materials and Design*, vol. 26, 2005, pp. 454-458.

[54] C.S. Ramesh, A.R.A. Khan, N. Ravikumar, and P. Savanprabhu, “Prediction of wear coefficient of Al6061 – TiO2 composites,” *Wear*, vol. 259, 2005, pp. 602-608.

[55] Z.H. Melgarejo and O.M. Sua, “Wear resistance of a functionally-graded aluminum matrix composite,” *Scr Mater*, vol. 55, 2006, pp. 95-98.

[56] C.S. Ramesh and M. Safiulla, “Wear behavior of hot extruded Al6061 based composites,” *Wear*, vol. 263, 2007, pp. 629-635.

[57] F. Tang, X. Wu, S. Ge, J. Ye, and H. Zhu, “Dry sliding friction and wear properties of B 4 C particulate-reinforced Al-5083 matrix composites,” *Wear*, vol. 264, 2008, pp. 555-561.

[58] M.K. Surappa, with Sudarshan, “Dry sliding wear of fly ash particle reinforced A356 Al composites,” *Wear*, vol. 265, 2008, pp. 349-360.

[59] A.E. Jiménez, M.D. Bermúdez, J. Cintas, and E.J. Herrera, “Dry wear of NiAl 3 - reinforced mechanically alloyed aluminium with different microstructure,” *Wear*, vol. 266, 2009, pp. 255-265.

[60] S.R. Bakshi, V. Singh, S. Seal, and A. Agarwal, "Aluminum composite reinforced with multiwalled carbon nanotubes from plasma spraying of spray dried powders," *Surface & Coatings Technology*, vol. 203, 2009, pp. 1544-1554.

[61] K. Morsi, A.M.K. Esawi, S. Lanka, A. Sayed, and M. Taher, "Spark plasma extrusion (SPE) of ball-milled aluminum and carbon nanotube reinforced aluminum composite powders," *Composites: Part A*, vol. 41, 2010, pp. 322-326.

[62] M. Gupta and E.W.W. Leong, "Microwaves and Metals," *Microwaves and Metals, John Wiley & Sons*, 2008.

[63] M.M.A. Baig, "Friction and wear of 20% volume fraction submicron A12O3/6061 aluminum alloy composite for brake system application," *MSc Thesis, Mechanical Engg. Dept., KFUPM*, 2009, pp. 51-52.

[64] A. Esawi and K. Morsi, "Dispersion of carbon nanotubes (CNTs) in aluminum powder," *Composites Part A: Applied Science and Manufacturing*, vol. 38, Feb. 2007, pp. 646-650.

[65] W. Salas, N.G. Alba-Baena, and L.E. Murr, "Explosive Shock-Wave Consolidation of Aluminum Powder/Carbon Nanotube Aggregate Mixtures: Optical and Electron Metallography," *Metallurgical and Materials Transactions A*, vol. 38, Oct. 2007, pp. 2928-2935.

[66] K. Morsi, M.K. Esawi, P. Borah, S. Lanka, and A. Sayed, "Characterization and Spark Plasma Sintering of Mechanically Milled Aluminum-Carbon Nanotube (CNT) Composite Powders," *Journal of Composite Materials*, vol. 44, 2010, pp. 1991-2003.

VITA

Name: ABDULLAH KHALIL

Year and Place of Birth: 1987, Riyadh, Saudi Arabia

Email: newton_1987@hotmail.com

EDUCATION

- **Master of Science in Mechanical Engineering**
  Sep 2010 - May 2012
  King Fahd University of Petroleum and Minerals
  Dhahran, Saudi Arabia

- **Bachelor of Industrial and Manufacturing Engineering**
  Jan 2006 - Dec 2009
  NED University of Engineering and Technology
  Karachi, Pakistan

PROFESSIONAL EXPERIENCE

- **Sep 2010 – May 2012:** Research Assistant, *Mechanical Engineering Department, King Fahd University of Petroleum and Minerals,* Dhahran, Saudi Arabia

- **Jan 2010 – Aug 2010:** Quality Control Engineer, *Dawlance Pvt. Ltd*, Karachi, Pakistan